The Effects of Recycled Media on Culture Growth and Hormone Profiles in Heterotrophic *Euglena gracilis*

A Thesis Submitted to the Committee of Graduate Studies

In Partial Fulfilment of the Requirements

for the Degree of

Master of Science

In the Faculty of Arts and Science

TRENT UNIVERSITY

Peterborough, Ontario, Canada

Environmental and Life Sciences M. Sc. Graduate Program

May 2020

Abstract

The Effects of Recycled Media on Culture Growth and Hormone Profiles in Heterotrophic *Euglena gracilis*

Alexandra Margaret Kuhne

The rapid expansion of the worldwide population has caused an urgent need for the development of new, more environment-conscious, food sources. In this context, algae, such as Euglena, are of interest thanks to their capacity to naturally produce essential nutrients such as proteins and oils commonly found in animals and plant sources. While these processes are currently being investigated, underlying measures affecting growth of *Euglena gracilis* like hormonal influences and growth stress like nutrient deprivation are poorly understood. From this vantage point, this thesis seeks to understand the role of phytohormones cytokinin (CKs) and abscisic acid (ABA) in complex mechanisms underlying heterotrophic growth of *Euglena gracilis* under recycled, organic media conditions with no supplementation. Hormone profiles were quantified by HPLC-ESI-MS/MS and compared to culture growth dynamics of pH, weight accumulation, glucose content, cell count and morphology. It was expected that ABA acted as an inhibitory hormone and this was confirmed by its higher levels when CKs where low and vice versa. Contrastingly, it was expected that CKs stimulated growth, in which this was shown not to be the case. Interestingly, it was revealed that both hormone groups increase with increasing recycling. Other key findings include: *E. gracilis* synthesizes CKs via the tRNA-degradation pathway and is cZ and iP dominated, recycling *E. gracilis* medium is viable for growth, however, the percentage (25% or less) is crucial to cell viability and markedly

no ABA was detected in *E. gracilis* pellet fractions from recycled media. Therefore, this data revealed that recycled media has a striking influence on physiological aspects of growth and illustrated unique changes in hormone profiles of which could be manipulated to help the food industry.

Keywords: *Euglena gracilis*, recycled medium, heterotrophic, endogenous hormones, cytokinin, large scale microalgae cultivation.

Acknowledgments

"In the middle of difficulty lies opportunity". - Albert Einstein

I would first like to thank my thesis advisor **Dr. Neil Emery**. His door was always open whenever I ran into a trouble spot or had a question about my research or writing. He consistently allowed this paper to be my own work but steered me in the right direction whenever he thought I needed it. To him and his family, the kindness shared, and lasting memories will be cherished. To be noted, Ocean (and Babou) have open rights to any-time watching.

I would like to acknowledge **Dr. Gordon Balch** as the second reader of this thesis, and the 'Big Picture' mentor throughout my journey with this project. With all the support and determined curiosity for my research, Gordon constantly reminded me to stay committed and seek the full story.

To **Dr. Celine Gueguen**, as a committee member, I am gratefully indebted to her very valuable comments on this thesis. Her support from the beginning idea to the final story was surely a main factor in my success.

This project would not be possible without the foundation and constant support, both academically and financially, from **Noblegen Inc.** As model 'algaepreneurs' to you both, **Andressa Lacerda** and **Adam Noble**, the opportunity to work with such a successful start-up will always be something I am proud of. Thank you also to **Philip Siambi** for your algae "guru" wisdoms and always being a huge supporter. I look forward to the growing impact that Noblegen Inc will have on the future and sustainability of food using algae.

Thank you to all the **Administration Staff** from both the Environmental and Life Sciences Program and Graduate Studies office; Linda Cardwell, Mary-Lynn Scriver, Erin Davidson, and Jane Rennie, for all of your advice and encouragement.

To **Katie Horlock-Roberts**, a dear friend, colleague and a main source of my encouragement, I could not have done any of this without you from day one. You kept me on track, interested and focused on the end goal. Your involvement with my experiments and later Noblegen related items has ensured my success. You are such a generous, kind friend that I am extremely lucky to know.

To **Dr. Anna Kisiala** you constantly pushed me to make my work the best it could be, undoubtedly enabled the science workings of my project (chiefly the whole mass spec system) and was always there to go for lunch or go on adventures with me. You never failed to make me smile. I am incredibly fortunate to call you my friend.

To **Dr. Erin Morrison** (friend and recently discovered related family member), thank you for your constant positivity and direction with this piece of work and in my day to day life. Thank you for being such a wonderful human, I appreciate you so much!

To **Megan Aoki**, we traveled the world and became better scientists together. Without your constant shenanigans, insight, and kindness, I am sure my last two years would not have been as much fun or memorable! Thank you for always being someone I could count on. See you at the Skybar.

Emery Lab. You are my science family! Mark Seegobin (travel buddy), Thien Nguyen, Tamzida Rahman, Natasha Trzaskalski, Nourhene Grich, Cody Butler, Ibraheem Alimi, Peter Andreas, Shaojun Li and Zhiyong Zhang and to the undergraduates that make our lives so much easier (Adele Davis) thank you all for being an incredible source of support.

Friends. Where would I be without them? B109'ers, 'GIFChat' members, Trail Intermural team members, thank you for keeping me sane and giving me too many reasons to celebrate! Special thank you to Michael McKenzie as my office partner in crime and a heck of a friend. Additionally, thank you to my friends Katie Brasenell, Julie Hoekstra, Samantha Stahn and Guillem Dayer for always being a huge foundation of support and making everything better. Thank you to Damien Shields for all your encouragement and steadfast admiration for this work, you kept me grounded trying to make you proud. I am so incredibly lucky to have you all by my side.

Family. I could not have done this without my family. Each and every one of you has helped shape me to become the person I am today. Driving my curiosity, kindness and encouraging me to pursue more education. Thank you for always being a foundation of love and support.

I must express my very profound gratitude to my partner, **Taylor**, for providing me with unfailing support and continuous encouragement throughout my studies and process of researching and writing this thesis. You changed my life without even trying. This accomplishment would not have been possible without you.

Trent University. For taking me in as a young and confused undergrad and spitting me back out older and more confused. Thank you for being exactly what I needed.

Table of Contents

List of Figures

List of Tables

List of Abbreviations

ACN	Acetonitrile
AU	absorbance units
ABA	abscisic acid
AGC	automatic gain control
AMP	adenine monophosphate
ADP	adenine diphosphate
ATP	adenine triphosphate
BA	benzyladenine
BAR	benzylaminopurine riboside
CHASE	cyclases/histidine kinases associated sensory extracellular domain
*c*Z	*cis*-zeatin CKs
*c*ZNT	*cis*-zeatin nucleotide
*c*ZR	*cis*-zeatin riboside
*c*ZOG	*cis*-zeatin-o-glucoside
*c*ZROG	*cis*-zeatin-o-glucoside riboside
*c*Z9G	*cis*-zeatin-9-glucoside
CKs	cytokinins
CKX	cytokinin oxidase
DPI	days post inoculation
DHZ	dihydrozeatin
DHZR	dihydrozeatin 9-riboside
DW	dry weight
DZ	dihydrozeatin
DZNT	dihydrozeatin nucleotide
DZOG	dihydrozeatin-o-glucoside
FB	Freebase CKs (DHZ + *t*Z + *c*Z + iP)
FPP	farnesyl diphosphate

GLUC	Glucosides (DZOG + *t*ZOG + *c*ZOG + DZROG + *t*ZROG + *c*ZROG + DZ9G + *t*Z9G + *c*Z9G)
HESI	heated electron spray ionization
HMBDP	hydroxy-methylbutenyl diphosphate
HPLC	high performance liquid chromatography
IP	N^6-isopentenyladenine
IPNT	N^6-isopentenyladenine nucleotide
IPP	Isopentenyl pyrophosphate
IPR	N^6-isopentenyladenosine
IPT	Isopentenyl-transferase
IT	injection time
LC-(ESI) MS/MS	liquid chromatography - electrospray ionization-tandem mass spectrometry
LOG	lonely guy gene
MEP	methylerythritol phosphate (pathway)
MeSiP	2-methylthio-N^6-isopentenyladenine
MeSiPR	2-methylthio-N^6-isopentenyladenosine
MeSZ	2-methylthio-N^6-zeatin
MeSZR	2-methylthio-N^6-zeatin riboside
MET	methyl-thiol CKs (2MeSZ + 2MeSiP + 2MeSZR + 2MeSiPA)
MVA	mevalonate (pathway)
NCE	normalized collision energies
NIR	near infrared reflectance
NOM	Noble Organic Media
NT	nucleotide CKs (DHZNT + *t*ZNT + *c*ZNT + iPNT)
PDCK	protist derived cytokinins
PRM	parallel reaction monitoring
RB	riboside CKs (DHZR + *t*ZR + *c*ZR + iPR)
RPM	revolutions per minute
S/N	signal-to-noise threshold

SPE	solid phase extraction
*trans*Z (tZ)	*trans*-zeatin CKs
tRNA	transfer ribonucleic acid
tZNT	*trans*-zeatin nucleotide
tZOG	*trans*-zeatin-o-glucoside
tZR	*trans*-zeatin riboside
tZROG	*trans*-zeatin-o-glucoside riboside
tZ9G	*trans*-zeatin-9-glucoside

1. Introduction

Microalgae are used as candidate species for academic research and technological applications, and more recently, they have gained popularity in food industries (Figure 1) (Vigani et al, 2015). Microalgae are a rich source of micronutrients, lipids, and proteins and can be produced in ways that do not compete with traditional food crops for space and resources. Microalgae are an encouraging environmental solution, especially for farming,

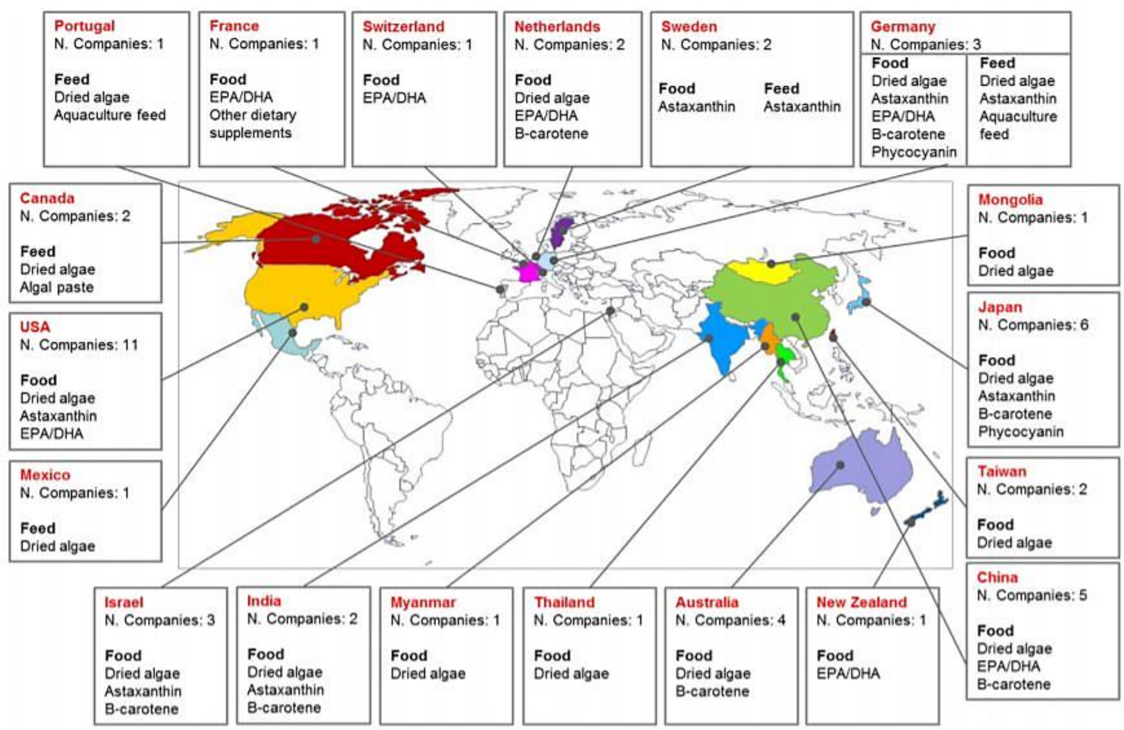

Figure 1: Global distribution of private companies producing commercial food and feed products derived from micro-algae (Vigani, *et al*, 2015).

because they can prosper with so little. Grown year-round, they consume only about one percent of the water as soybean, all while producing 38 times more protein per acre per year (Bleakly and Hayes, 2017 & Flachowsky, Meyer, and Sudekum, 2017). Repurposed old buildings ca be used to industrially grow, thus, allowing the gain of these precious essential nutrients like proteins and fatty acids with minimal damage to our planet or disrupting the current space used by traditional farming. Additionally, with the demand for dietary oils already outstripping supply and projected to double over the next 30 years, algae are taking the lead as the primary replacement from current agricultural practices ahead of even fish farming (Flachowsky, Meyer, and Sudekum, 2017). This key switch from traditional plant and animal farming is critical to disrupting current production and environmental impacts.

Phytohormones (growth signaling molecules in plants), have been investigated with emphasis on both growth and yield studies in agriculture for many years. Many of the same endogenous hormones are found in microalgae and can be used to optimize or adjust target compound outputs (Yandu & Jian, 2015). The presence of these hormones in microalgae may suggest similar important regulatory roles as in higher plants as potential targets for growth strategies (Yandu & Jian, 2015). By exploiting a naturally robust range of nutraceutical products, profiling endogenous hormones will help to understand how to optimize conditions that enable efficient growth and production of critical compounds like proteins and oils.

Using a targeted method for cultivation, microalgal species can be used for sustainable and environmentally conscious large-scale production of essential nutrients. However, the growth conditions must be specific for the candidate microalgae species. By highlighting growth parameters associated with targeted product yield, industries could use different ways to cultivate algae that produce less waste and more re-use of secreted algal compounds through recycled fermentation. An industry collaborator, Noblegen Inc., has begun the investigation into this type of algae cultivation, with waste stream recycling to mitigate losses of extra nutrients and post-cultivation waste. Further research to highlight the ability of nutrient recycling and the complexity of associated hormones driving growth under recycled conditions, are essential to the balance of sustained large-scale cultivation of microalgae.

1.1 Microalgae

Algae are classified into more than a dozen significant groups, predominantly based on pigment composition, use of energy, and cell morphology (Gualtieri, 2001). It is estimated that there are more than 50,000 species of algae worldwide, among which about 30,000 have been studied (Bacellar & Vermelho, 2013). The largest group, the green lineage (Viridiplantae), comprises the green algae and their descendants, the land plants. The green algae then diverged into two discrete clades, Chlorophyta and Streptophyta, which include the charophyte green algae from which land plants evolved (Schmidt & Wilhelm, 2014) (Figure 2). Through secondary endosymbiosis, three eukaryotic lineages of the green algae diverged and acquired fully integrated secondary plastids giving rise to photosynthetic properties. These are categorized as: euglenids, chlorarachniophytes and the "green" dinoflagellates (Keeling & Inagaki, 2004, Archibald, 2009 & Leliaert et al., 2009). Currently, euglenoids are garnering much attention as model organisms for study; however, it should be noted that Euglena has a taxonomy that is somewhat contentious, as the genus is arguably placed in either the protist phylum, Euglenozoa, or the algal phylum, Euglenophyta. As a diverse genus of unicellular protists (microalgae) composed of both photosynthetic and non-photosynthetic members, this particular genus is of valuable interest for commercial interest as industry could exploit either light and dark modes of growth to better repurpose building space – horizontal versus vertical farming (Keeling &

Inagaki, 2004). These microalgae are found worldwide in both freshwater and marine habitats and are distributed across a broad range of environments from high salinity,

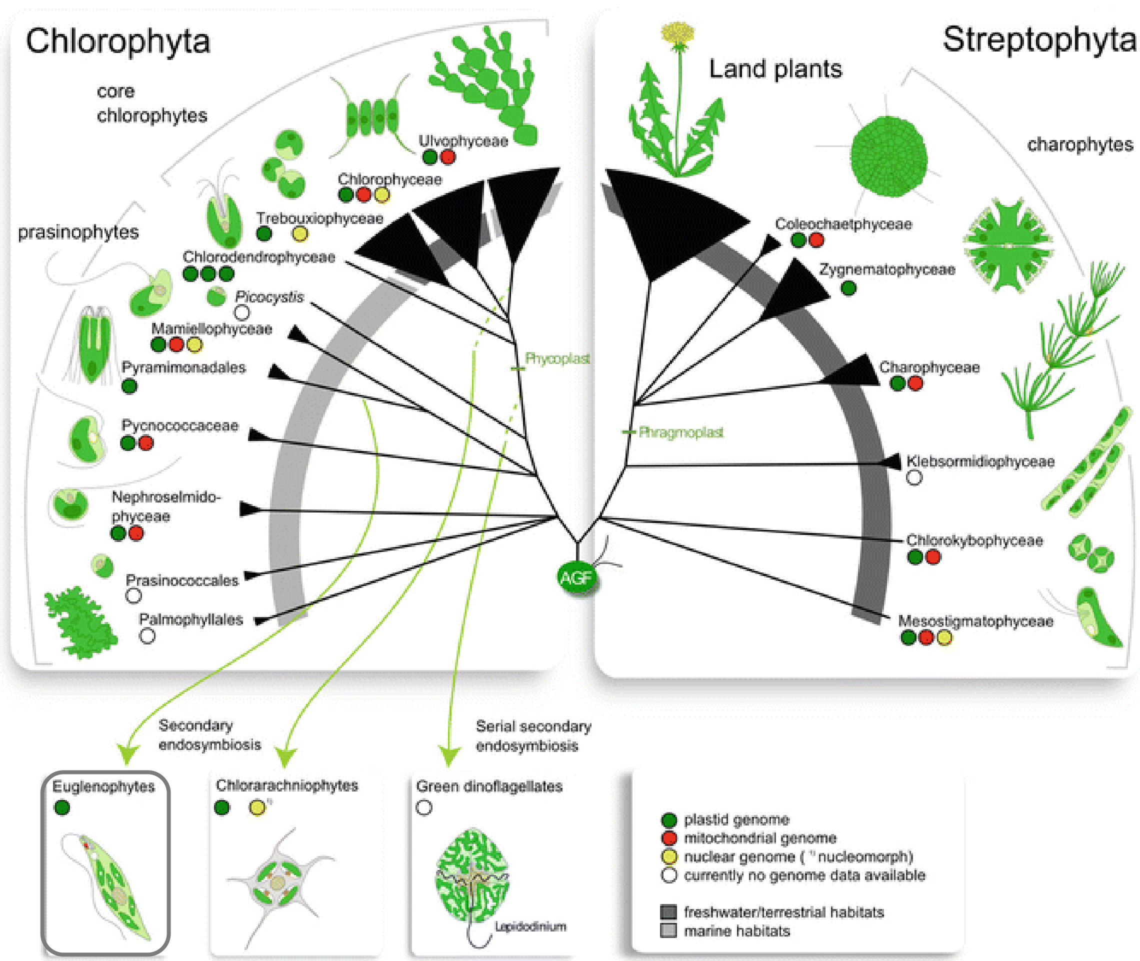

Figure 2: Phylogenetic relationships of major clades of the green lineage, including primary (Chlorophyta and Streptophyta) and complex (chlorarachniophytes, euglenophytes, green dinoflagellates) plastid-bearing taxa (Schmidt & Wilhelm, 2014).

extreme temperatures to soil or even the fur of mammals (Singh, & Saxena, 2015). Thus, they play a crucial role in the global ecosystem. Microalgae can exploit varied media components (organic or inorganic), use different methods of cultivation (fed-batch or continuous) and modes of nutrition (heterotrophic, autotrophic, or mixotrophic). Like plants, the majority of algae use photosynthesis to capture light energy to convert inorganic substances into simple sugars for energy (Ogbonna, & Tanaka, 2000). Alternatively, some

Euglena species like *Euglena gracilis* can also use heterotrophic metabolism whereby they can exploit exogenous organic materials as a source of energy. Explicitly, this metabolic pathway nutritional mode can give industry a key advantage for cultivating these microalgae in closed, dark systems, for efficient production for the market.

1.1.1 *Euglena gracilis*

Euglena gracilis (*E. gracilis*) is a photosynthetic flagellate protist. *E. gracilis* varies in size from about 10 to 100 µm (Figure 3) with a general lifespan of up to three weeks, depending on conditions (Leedale, 1964). Predominately facultative mixotrophs in aquatic environments, they have a green secondary plastid, which allows them to be photosynthetic (autotrophic) or not (heterotrophic) (Keeling and Inagaki, 2004). *E. gracilis* possess typical features of eukaryotic cell anatomy whereby both the cell surface and flagellum are

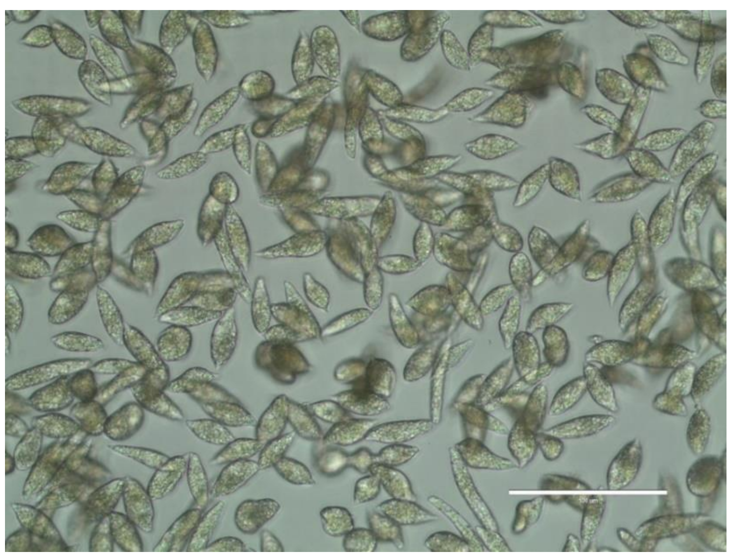

Figure 3: Micrograph of *Euglena gracilis* grown in Noble Organic Media (500 ml), 5 hours after inoculation, at 60x magnification, scale bar standing for 200 µm.

significant to life cycle progression, and interactions with the environment (Gomez, Harris, Walne, 1974, and Langousis and Hill, 2014 & Kings et al., 2017). They have a large red eyespot usually composed of astaxanthin used for phototaxis, aiding in the detection of light. (Passarelli, et al., 2003 & Kings et al., 2017).

E. gracilis has a life cycle with free-swimming and non-motile stages (Tannreuther, 1922). In the free-swimming stage, *E. gracilis* reproduces rapidly by a type of asexual reproduction method known as binary fission. When environmental conditions become unfavourable, they enter the palmelloid stage during which *E. gracilis* gather and encyst themselves within a thick protective layer called the pellicle, which is comprised of protein that provides both strength and flexibility during the non-motile stage. When environmental conditions once again become favourable, these new daughter cells become flagellated and are released to begin the cycle over again (Tannreuther, 1922, Cook, 1968 & Buetow, Gottfried, & Van, 2011). *E. gracilis* is a vital organism because of its evolutionary history and different cellular architecture; together, its multifaceted biology has considerable potential for exploitation, making it a candidate species to obtain nutritional ingredients of interest for industry (O'Neill, et al., 2015).

1.1.2 Growth Characteristics of *Euglena gracilis*

Cell growth for microorganisms is typically characterized by a five-stage growth curve composed of lag, exponential, decline, stationary and death stages (Figure 4) (Price & Farag, 2014). Each of these growth stages can impact the overall health of cell culture as each stage denotes a change in growth associated with cell viability, reproductive strength and excretion of intracellular material. The lag phase is dictated by the initial cell density and growth rate when culture is first transferred to liquid culture and is essential to shorten the lag phase for industrial applications. The exponential phase is characterized by the most rapid rates of increase in cell density. In the third phase, decline, the growth rate diminishes as culture parameters begin to limit growth, leading to the stationary phase when no growth occurs as the limiting factors and growth rate are balanced. For the last stage, death, cell density decreases rapidly leading to culture collapse. The key to the success of algal production is maintaining the culture(s) in the exponential phase of growth, enabling the highest growth rate and maximum cell density. Moreover, once the cells have reached the third stage of the growth curve, the nutritional value of the algae begins to deteriorate due to the deficient composition of nutrients, and possible production of toxic metabolites (Bumbak et al., 2011 and Doucha and Livansky, 2012).

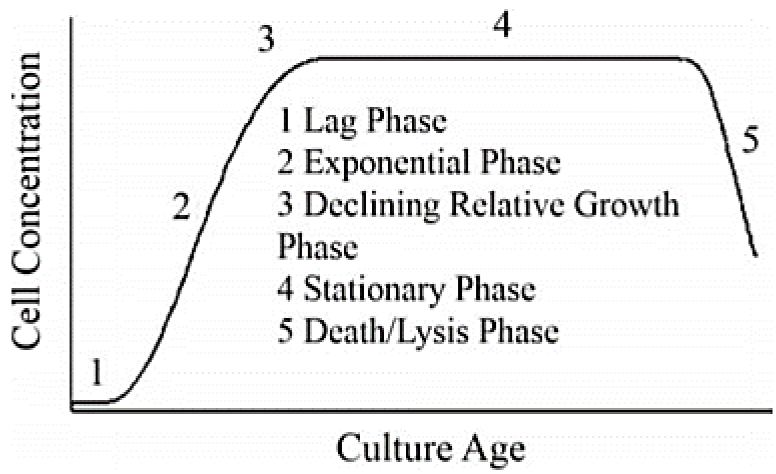

Figure 4: Graphical representation of typical five-phase growth curve of microalgae for a fed-batch culture system (Price & Farag, 2014)

While cell growth for microorganisms is best evaluated using the five-phase growth curve, surrounding conditions may cause variations to the growth curve. These changes could be attributed to nutrient availability, pH, temperature, or possible contamination with bacteria (Lowrey, Armenta, & Brooks, 2016). Compared to phototrophic growth, heterotrophic cultivation of microalgae drastically increases growth rates, cell mass, protein and lipid content likely due to the changes in nutrients sources and metabolic pathway use (Chen, 1996, and Perez-Garcia, *et al.*, 2011). Many microalgae species have been identified for optimized heterotrophic production of commercially attractive products ranging from whole biomass for nutritional supplements both for humans and animals, to high-value products like fatty acids or lipids for biofuels (Bumbak *et al.*, 2011). Heterotrophic microalgae cultures, therefore, have a place in current sustainability efforts to employ organisms that make favourable products for industry (Gissibl et al., 2019).

1.2. Industrial Application of Recycling Media in Algae

Microalgae can improve the nutritional and functional quality of foods, act as feed for animals and even produce biofuels (Hlavova, Turoczy, and Bisova, 2015) (Figure 5). However, current microalgal mass culture technologies have failed to produce bulk

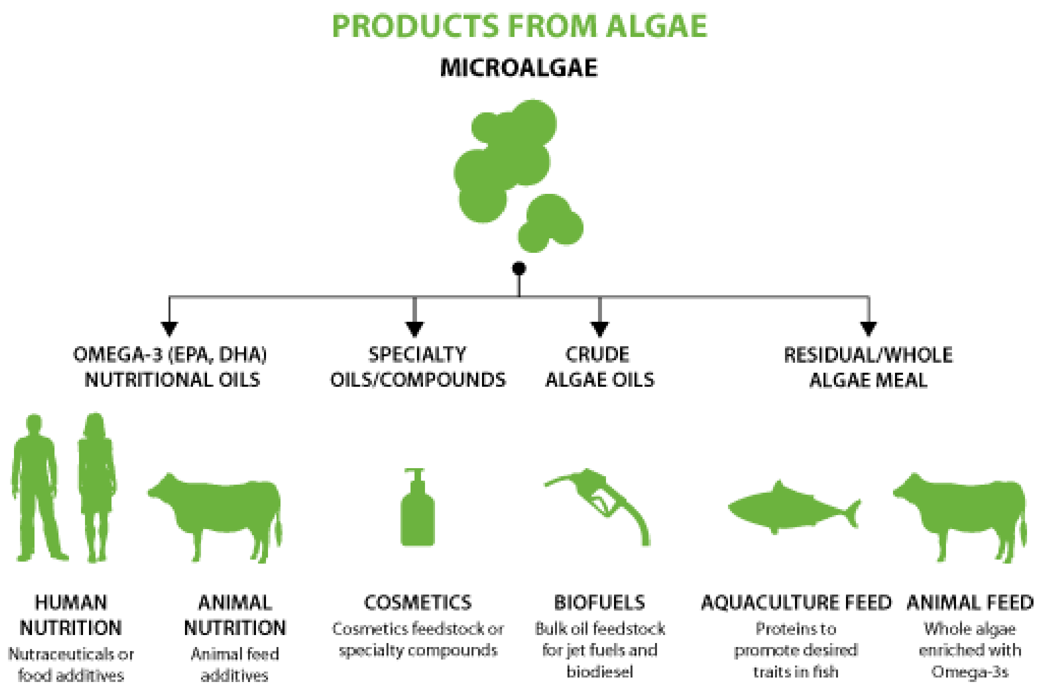

Figure 5: Products from Algae. Sourced from the Algencal Bioenergy Project <*http://www.algencal.it/microalgae/?lang=en*>.

volumes of microalgal biomass at low cost due to inefficient harvesting techniques and large waste streams.

Nutrient recycling technologies, in the algae production industry, can mitigate these economic barriers by making use of the recycled media, and thereby harvesting nutrients for re-use, and alleviating the incurred waste streams by recirculating portions of it back into the system. That liquid waste from algae cultivation, as the residual components of the original fermentation medium (spent media), can, therefore, be re-used in secondary and subsequent fermentations after that (Rodolfi et al., 2003 & Rösch et al., 2012). These residual nutrients could include varying concentrations of organic carbon (sugars and carbohydrates), nitrogen (inorganic and complex organic nitrogen), essential minerals and extracellular metabolites not wholly depleted during the primary fermentation (Rösch et al., 2012, Discart et al., 2014, Liu, Pohnert, and Wei, 2016).

1.3 Use of Recycled Medium for Microalgae Growth

While there are significant economic and environmental benefits, there are some underlying challenges that must be overcome before the adoption of nutrient recycling is viable at a commercial scale. The feasibility of nutrient recycling largely depends on operating scale and techniques like fortifying, filter sterilizing or autoclaving the spent media as well as characteristics of the selected microalgae species (Willems et al., 2016, & Kozlova, et al., 2017). Both these aspects are foci of this thesis. Proper nutrient recycling regimes, if the considerations mentioned above are accounted for, can translate to significant savings of raw material inputs and avoided material loss (Lin, 2005).

The importance of recycling the growth medium in the large-scale production of microalgae is not new. The potential was first recognized in "Algal Culture: From Laboratory to Pilot Plant", by J.S. Burlew in 1953. As microalgal biomass production has been estimated to consume around one metric ton of water alone, per kg of microalgal biomass produced (Farooq, 2014), there is a significant need for alternatives, to lessen the ecological impact in scale-up measures and associated costs (Yang et al., 2011).

As important as the operation scale, choice in microalgal species is essential for successful nutrient recycling. An ideal microalga should demonstrate reasonable growth rates, high product yields, and capability for consistent growth in industrial settings that are optimized for heterotrophic production of commercially attractive products (Hnain, Cockburn, and Lefebvre, 2011). While effects of the recycled medium on algae growth are often situation-specific, and dependent on differences in environmental variables or harvesting methods, some particular species appear to be more suitable for medium recycling (Loftus, and Johnson, 2017). A survey of research to date has shown decreased biomass productivity or decline in growth rates observed for several species including *Nannochloropsis* sp., *Arthrospira platensis* and *Chlorella zofingiensis* (Fret et al., 2017) suggesting there are limitations for using medium recirculation. On the other hand, *Tetraselmis* sp. and *Chlorella* vulgaris were cultivated with medium recycling without significant impact on growth (Lowery, Armenta, and Brooks, 2016). It becomes clear that results are variable and species-dependent (Rodolfi et al., 2017). In this thesis, a microalgae species, from the *Euglena* genus, *Euglena gracilis*, was assessed for its potential for mass cultivation by making use of its organic, recycled medium for sustained growth.

1.4 Undefined Media

Arguably the most critical aspect of microalgae cultivation is nutrition use and its influence on growth and composition (Bumbak et al., 2011 & Singh and Saxena, 2015). To further the importance of nutrient utilization, the re-use of such - containing many organic compounds and unutilized substrates, is of high interest as it represents an under-explored opportunity for economical and sustained microalgae cultivation as well as academic pursuits in knowledge (Ilavarasi et al., 2011 & Pachapur et al., 2017).

Media with ingredients that are known chemical compounds are referred to as "defined". By contrast, "undefined" media such as yeast extract contain complex ingredients as a mixture of many chemical species in varied or unknown proportions per quantity isolated and produced (Schwartzbach, 2014). Thus, there are different types of media suitable for growth and selection of media type is critical to growth. In this thesis, liquid, undefined, Noble Organic Media (NOM) that contained molasses, yeast extract, ammonium phosphate, ethanol and vegetable oil, was used for growing *E. gracilis* culture.

1.5 Phytohormones

Phytohormones are chemical messengers involved in a broad spectrum of physiological and biochemical processes in higher plants, even when present at very low concentrations. Although documented first in plants, phytohormones have been found in many other organisms like bacteria, fungi, algae and humans (Stirk and Van Staden 2010, Spichal, 2012, Noble et al., 2014, Morrison et al., 2017 & Seegobin et al., 2018). Conventionally, phytohormones consist of five classic classes—auxins, abscisic acid, cytokinins, gibberellins, and ethylene—as well as their precursors and synthesized analogs (Allaf, 2013). Other phytohormone classes exist and include brassinosteroids, jasmonates, salicylic acid, and polyamines. Plant hormones have many roles in regulatory processes, including: reproduction, defence responses, differentiation and development, and cell division (Stirk, 2003, Santner, Calderon-Yillalobos and Estelle, 2009). This thesis will focus on displacing the previously narrowly focused and plant-centered knowledge base of cytokinins - with specific emphasis on a microorganism, *Euglena gracilis*, to better understand the diversity of cytokinins. Because of the evolutionarily close relationship between plants and algae, phytohormones are expected to play roles that are similar between plants and algae. (Tsavkelova et al., 2006, Yanda, et al., 2014 & Noble et al., 2014).

1.5.1 Cytokinin (CK)

Currently, there are many natural and synthetic cytokinins known and identified as adenine derivatives with a nitrogen-6 (N^6) side chain with alternating substituents that differentiate the forms (some are shown in Kamada-Nobusada and Sakakibara, 2009) (Figure 6). CKs are found in living organisms as various forms such as: free bases, ribosides, nucleotides, and glucosides (Fig 7). When isoprenoid CKs and their derivatives are modified at the second carbon (C-2) within the adenine ring with a methyl-thiol group, they are considered as Methyl-thiol CKs (METs) (Zürcher, & Müller, 2016). CKs and their modified forms can act over long distances or in the direct vicinity (paracrine) of the CK producing cells (Schmulling, 2004). Therefore, many aspects of growth and development are coordinated by these phytohormones, at incredibly low concentrations (fM to pM). As these aspects are important for all living organisms, it is important to define the mechanisms involved in their production. Interestingly, CKs are generated using two main pathways which can influence the CK type produced.

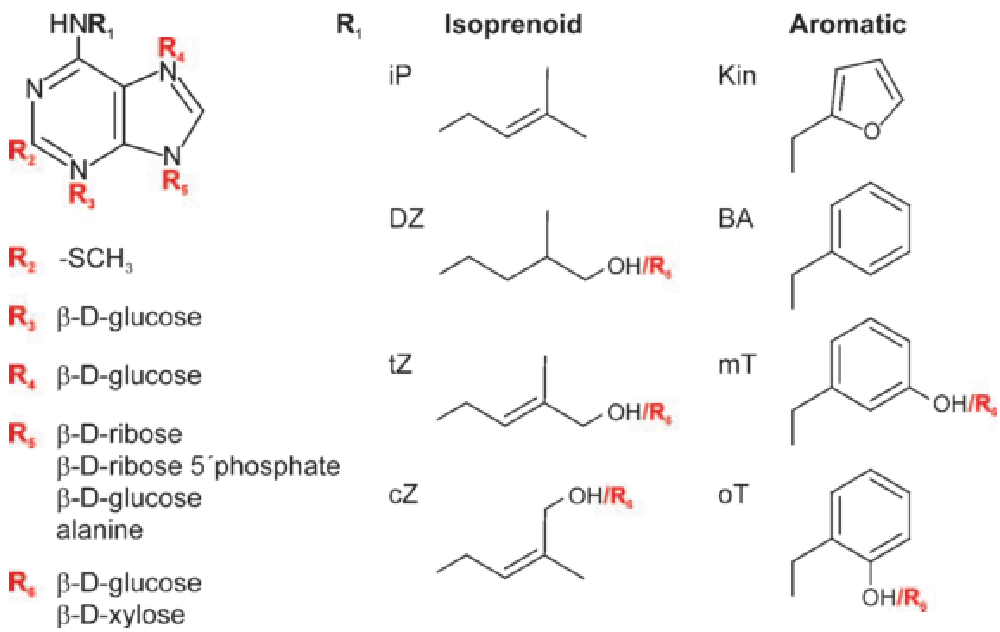

Figure 6: Structure of Adenine-type CKs. Black R_1 represents the determinant side chain, R2 to R6 (in red) indicate the type of CK conjugate resulting; iP, N^6-isopentenyladenine; DZ, dihydrozeatin; tZ, trans-zeatin; cZ, cis-zeatin; Kin, kinetin; BA, N^6-benzyladenine; mT, meta-topolin; oT, ortho- topolin modified from Morrison *et al.*, 2017.

CKs are classified according to their side-chain substituents as either isoprenoid or aromatic cytokinins. Isoprenoid cytokinins include: N^6-(2-isopentenyl) adenine (iP), trans-zeatin (tZ), cis-zeatin (cZ) and dihydrozeatin (DHZ) forms. The aromatic cytokinins include N^6-benzyladenine (BA) and topolin forms (Stirk and Van Staden, 2010 & Spichal, 2012). As addressed in this thesis, CK forms are denoted as follows: free-base (FB), riboside (RB), nucleotide (NUC), glucoside (GLUC) and Methyl-thiol (MET) and CK Types according to fraction as: FBs (DHZ + tZ + cZ + iP), RBs (DZR, tZR, cisZR, IPR), NUCs (DHZNT + tZNT + cZNT + iPNT), GLUCs (DZOG + tZOG + cZOG + DZROG + tZROG + cZROG + DZ9G + tZ9G + cZ9G), and METs (2MeSZ + 2MeSiP + 2MeSZR + 2MeSiPA).

Cytokinin Biosynthesis

It has been proposed that CK production occurs by two biosynthetic pathways for the isoprenoid CKs. (1) the methylerythritol phosphate pathway (MEP) more commonly known as the *de novo* pathway within the chloroplasts and (2) the mevalonate pathway (MVA) or more frequently termed as the transfer ribonucleic acid degradation (tRNA-degradation) pathway within the cytosol (Hirose et al., 2008, Kamada-nobusada & Sakakibara, 2009).

Derived from tRNA, modifications of the RNA molecule at the C1 or C6 positions (Figure 8), cause a separation that leads to cis-zeatin from the MVA pathway, with iP production via either pathway (Kim, Filtz & Proteau, 2004). In the MEP pathway (Figure 8), catalysis of isopentenyl side-chain forms the initial substrates – iP types. Followed by hydroxylation of the same side-chain, trans-zeatin (tZ) type compounds are formed. Further side-chain desaturation to dihydrozeatin (DZ) type or the oxidation of a carbon-carbon bond to form tZ types finishes this pathway (Kakimoto, 2001, Sakakibara, 2006, Kieber & Schaller, 2014, Jarchow-choy, Koppisch, & Fox, 2014). Alternatively, within the MVA pathway, it is indirect whereby the turnover of tRNA releases cis-zeatin (cZ) CK types and methyl-thiol (MET) CK forms (Figure 9) (Mok, Martin, & Mok, 2000, Kasahara, et al., 2004, Morrison, et al., 2015).

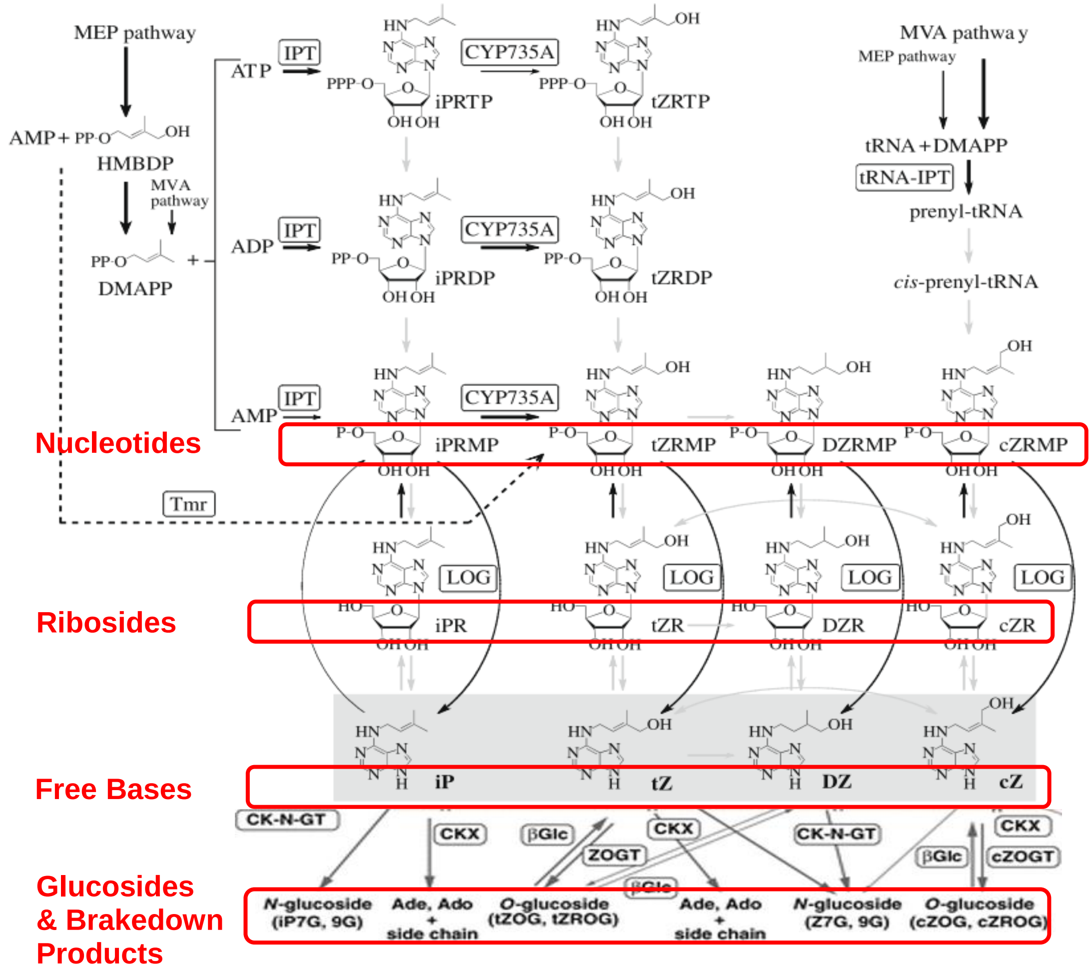

Figure 7: Current model of isoprenoid cytokinin (CK) biosynthesis pathways in Arabidopsis. Isoprenoid side chains are produced via the methylerythritol phosphate (MEP) pathway and the mevalonate (MVA) pathway (black arrows) including interconversion and degradation schemes of CK types and enzymes. Modified from Takei, Yamaya, Sakakibara, 2004, Sakakibara, 2006, and Kamada-Nobusada & Sakakibara, 2009.

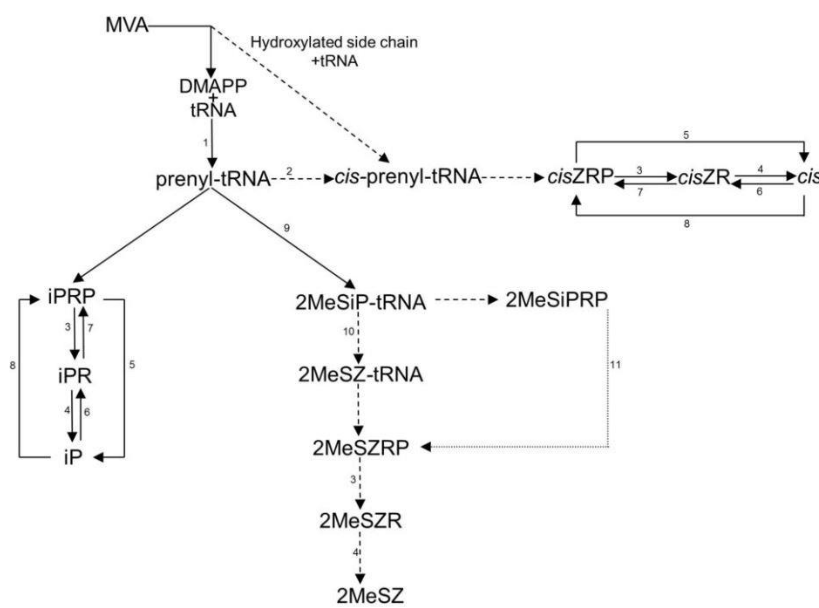

Figure 8: Proposed tRNA degradation pathway where numbers represent inferred enzymes see Morrison et al., 2015.

The *de novo* CK pathway begins with the NT form that are precursors to the active FBs. This follows either a 1-step conversion if the Lonely Guy enzyme is present, or by two steps via ribosylated intermediates (Lomin et al., 2015). If deactivated through glycosylation of the FBs or RB forms, either O- or N-GLUCs are produced as non-active CKs. O-GLUCs can be reversed back into the active CK forms, whereas N-GLUCs were considered irreversibly inactivated by N-glycosylation, however, recent research demonstrated this may not be the case as they can be reversed (Hosek, *et al.*, 2019). METs are thought to originate through the MVA pathway, but their activity remains unknown (Morrison et al., 2015). Destructive degradation occurs to RBs, NTs, and FBs by the protein Cytokinin Oxidase/Dehydrogenase (CKX) (Sakakibara, 2006 & Morrison et al., 2015). The interconversion between the different cytokinin metabolites highlights the importance of the transition between active, inactive, storage and transport forms to control various process in growth and development (Tomaz & Marina, 2010).

Cytokinins in Microalgae

Recent research has shown that cytokinins (CKs) can be found in all algal groups. Compared to the Charaphyceae lineage and land plants, algae from the Chlorophyta lineage, exclusively express enzymes of the methylerythritol phosphate pathway (MEP) and use the path for isoprenoid CK biosynthesis (Schwender, Gemunden, and Lichtenthaler, 2001, & Stirk, 2003). Definitive roles, however, have not been determined (Bradley, 1991; Evan and Trewavas, 1991; Jameson, 1993 & Yanda, et al., 2014). In *Euglena gracilis*, both cytokinin pathways are known to occur; however, the mevalonate pathway (MVA) is predominant whereas the MEP pathway only contributes to carotenoid biosynthesis (O'Neill *et al.*, 2015). To date, much of the exploration of CKs in algae comes from environmental sampling and, therefore, it has been suggested that CKs may be an artefact of bacterial associations rather than the algae themselves (Jameson, 1993). To investigate this potential CK relationship, various studies have used exogenous application of CKs and observed varied effects on algal development ranging from increased growth rate to decreased cell sizes (Mooney and Van Staden, 1986, Georgianna & Stephen, 2012). Phytohormones have further been shown to impact both lipid and protein profiles such that understanding these roles would be influential to industry to help control the suite of lipids or protein generation (Trinh, Tran and Bui, 2017, Han, Zeng and Bartocci, 2018).

Both endogenous and exogenous work using the *de novo* CK biosynthesis pathway showed that the MEP pathway forms (FB tZ and its metabolites) are the most prevalent found in some vascular plants whereas, in non-vascular plants, the free-base form isopentyladenine (iP) dominates (Rolc, Hradecka, and Skirk, 2009). Since plant hormones are thought to have evolved from pre-existing elements of the primary metabolism in algae (Pils et al., 2018), it is worth investigating cytokinin roles outside of the plant kingdom. Genes discovered in plants that regulate physiological responses to CK levels like CK oxidase/dehydrogenase (CKX) and isopentenyl transferase (IPT) genes, while present, do not behave in the same ways in algae as their characterized homologs in plants (Lu and Xu, 2015). Divergent from land plants with new stresses, algae had the primary mechanics of a Cyclases/Histidine kinases Associated Sensory Extracellular (CHASE) domain, however, did not use it as a “functional CHASE domain” (Pils, et al., 2018). As documented in more elaborate and complex regulation systems like in higher-order plants, the CHASE domain helps bind diverse low-molecular weight (Kendrick and Crane, 1997 & Pils, et al., 2018). This may be the case, due to the early evolution of CK signaling in algae, causing an adaptation that does not require CHASE domain functionality.

Cytokinins are complex signaling molecules, and their balance is critical for growth and development. From enzymes that control these processes to metabolic conversions between the multiple types, knowledge about regulatory networks is crucial (Kieber, & Schaller, 2018). Liaising between plant-centered research and research outside of plants, it is now vital to establish a more species-specific vocabulary relating these hormones across kingdoms. In this thesis, cytokinins that are found within the model species, *Euglena gracilis*, will be termed Protist Derived Cytokinins (PDCKs).

1.5.2 Abscisic Acid

The Abscisic acid (ABA) molecule is classified as a terpenoid and, while found universally in plants, it can also be found across kingdoms, in protists, fungi, and bacteria (Takezawa & Komstsu, 2011). ABA was thought to be associated with abscission and dormancy; however, it can act more like a promoter of growth when applied exogenously (Davies, 2014 & Hussain *et al.*, 2014). This hormone helps the plant adapt to stress, playing a key role in survival in adverse conditions – where its levels increase to counteract the environmental stressors. Abscisic acid is also pivotal to roles in the development of seed dormancy, stomatal closure, and senescence (Zhu, 2002, Takezawa and Komstsu, 2011, & Gururani, Mohanta, and Bae, 2015). ABA biosynthesis occurs via the terpenoid pathway. ABA production starts with isopentenyl pyrophosphate (IPP), the key to the biosynthesis of isoprenoids in the MEP pathway and after a series of reactions that give rise to the carotenoid pathway lead to the eventual creation of the ABA molecule (Figure 10) (Srivastave, 2002, Wasilewska *et al.*, 2008, Waadt, & Schroeder, 2011).

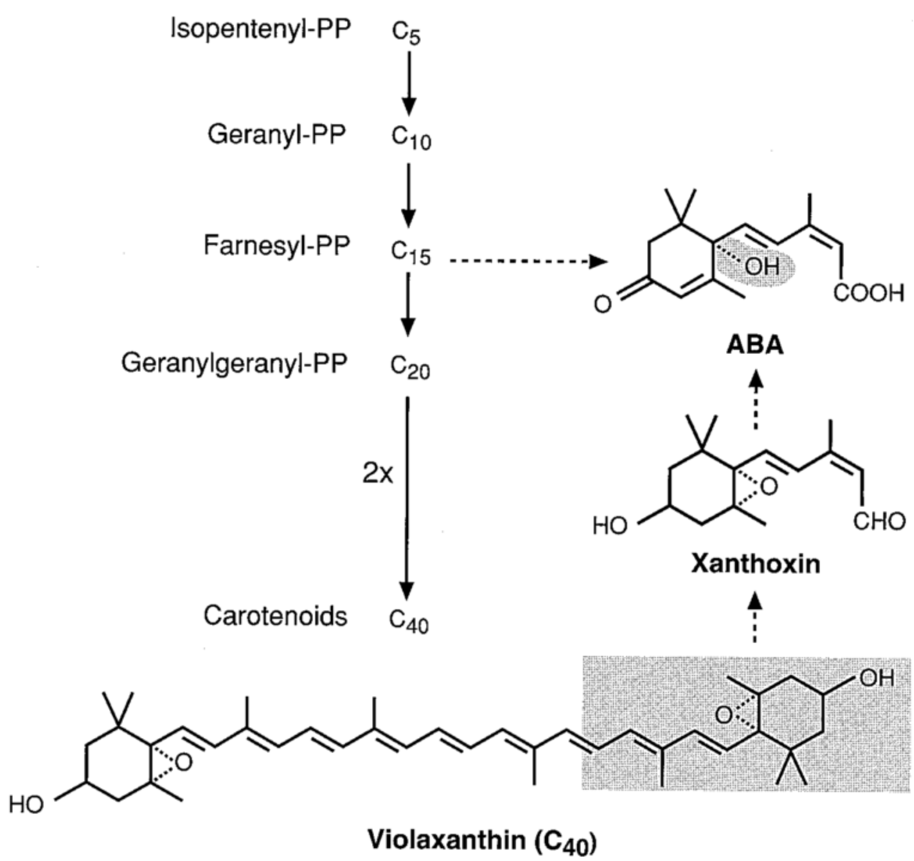

Figure 9: Two possible pathways for the synthesis of ABA in higher plants are shown by dashed lines, one directly from farnesyl diphosphate and the other an indirect pathway via carotenoids (Srivastave, 2002).

Abscisic Acid (ABA) in Microalgae

Although best known and studied in higher plants, in particular in *Arabidopsis thaliana*, there is evidence that ABA is synthesized in algae (Hartung, 2010). Though first discovered by bioassays in the 1960s as ABA or ABA-like substances, the physiological functions of ABA in algae have yet to be clearly defined. GC-MS tested early identification and detection of ABA in many species of algae including some algal divisions like Euglenophyta, Chlorophyta and Streptophyta (Hirsch, Hartung & Gimmler, 1989, & Tietz, et al., 1989). ABA production in algae is triggered in part by stressful conditions like salinity, nitrogen deficiency, heat, drought, acidity, oxidation, light, and alkalinity which lead to increased levels of ABA (Cowan & Rose, 1991, Tominaga, Takahata & Tominaga, 1993, Hartung, 2010, & Noble et al., 2014). Further research has shown that ABA concentration affects several aspects of cellular function. For example, in membrane permeability of solutes, ABA has been revealed as both stimulatory (Ord et al., 1997) and inhibitory (Hirsch, Hartung & Gimmler, 1989). ABA increases ion uptake (Wanless et al. 1973) but it is inhibitory (Hirsch, Hartung & Gimmler in 1989) in the algae species *Nitella flexilis*. Other parameters, like respiration and differentiation, have also shown contradictory responses. ABA can promote growth within the cyanobacteria families but conversely it inhibits the growth of diatom species, which suggests the effect of ABA is species-dependent (Hirsch, Hartung & Gimmler, 1989). Research surrounding ABA function and content remains a challenge to interpret. With both potential inhibitory or stimulatory-like effects, this thesis will determine the role of ABA as either a stimulatory or inhibitory signal in heterotrophically grown microalgae under stress, as manifested by nutrient recycling.

1.6 Research Objectives

Euglena is a promising algal species for sustainable and environmentally conscious, large-scale production, and it is of high interest to the food sector. *E. gracilis* possesses the potential for mass cultivation in a manner that is crucial for reducing costs to industry. One way of doing this is by making use of its recycled materials via the efficient conversion of input components to maximize the yield of target output products. Growth optimization of *E. gracilis* for large-scale production of essential nutrients, framed in an environmental context, would help to limit waste and maximize efficiency through algal medium recycling. In application, it is crucial to understand the growth characteristics such that growth parameters can be manipulated (facilitated expression) to generate targeted bioproducts for a company like Noblegen Inc.

Microalgae species are capable of growth using different modes of nutrient and energy acquisition. For this thesis, *E. gracilis* was grown heterotrophically to assess exploitation of organic media components as the primary energy source. Heterotrophic modes of nutrition require an alternate metabolic pathway than phototrophic mechanisms (Bumbak et al., 2011). Whereas phototrophic growth requires, the sole uptake of carbon dioxide (inorganic carbon) and light for energy, heterotrophic growth depends on organic sources of carbon (Lowery, Armenta, and Brooks, 2016). Heterotrophic microalgae are of interest to industry as they enable flexible situations for production and fermentation vessels and use less horizontal space than photobioreactors (Bumbak et al., 2011).

To further take advantage of the algal sector, investigation of the underlying mechanisms that positively influence microalgae growth was investigated. The hormone profiles of *E. gracilis*, specifically ABA and CK, will be elucidated as both of these hormone groups are known to be pervasive in many different life forms, including algae, bacteria, fungi, and even humans. As *Euglena* sits at a unique evolutionary position, at the juncture between plants and protists, this is an excellent nexus to explore and reveal the potential of hormones to impact cells and organization, which is of interest to industry. It will also reveal evolutionary aspects of cytokinins beyond plants as CKs are associated with growth promotion of algae and highlight the action of the antagonist hormone ABA. The overall focus of my research is to optimize growth parameters for growth in recycled media and determine the roles of CK and ABA within this system with future application to sustained large-scale microalgal cultivation using *E. gracilis.*

1.7 Hypothesis and Predictions

Parameters related to optimizing the growth of *Euglena gracilis* include harvest rate, growth characteristics, and growth hormone profiles. The length of time of a single growth cycle for sufficient harvest of the biomass and supernatant can be defined as the harvest rate. Growth characteristics can be grouped as macro and micro-growth metrics/phenotypes of *E. gracilis* under recycled conditions. These macro-growth parameters include: morphology, cell counts, growth curves, biomass and supernatant levels, glucose content, pH levels, and the micro-growth characteristic of pigment content. Of primary interest, are the micro-growth characteristics of hormone profiling endogenous hormones associated with expected phenotypes. In this thesis, it will be the cytokinins (CKs) and the antagonist stress-related hormone abscisic acid (ABA).

For industry, continued re-use of microalgae growth medium for commercial production of microalgae biomass is possible; however, the culture must be grown rapidly and harvested quickly to generate target biomass levels within a shorter time to meet high production demands (Khan, Shin, & Kim, 2018). To determine the capacity of *E. gracilis* culture medium for industry continued re-use, it was hypothesized that a quick harvest rate, three-day as opposed to a four-day growth cycle, would not adversely affect cell growth and product recovery (Tables 1 & 2, Appendix I).

Related to the recycling capacity of *E. gracilis* for industry use, an industry collaboration partner, Noblegen Inc., has shown that recycling media may be actually be beneficial to *E. gracilis* culture growth and product recovery. Current literature suggests that recycling medium is possible within many microalgae cultures; however, it is specific to the microalgae strain, its growth conditions, and media recycle ratio (Rodolfi et al., 2003, Xinyi, Crofcheck & Crocker, 2016, Lowery, Armenta, and Brooks, 2016, Fret, J. et al., 2017 & Loftus and Johnson, 2017). It was therefore hypothesized that a higher recycled rate would negatively affect cell growth. It was predicted that cells would be the most adversely affected by 75% recycled medium, followed by 50% and 25% respectively when compared to 0% of recycled medium. It was further predicted that *E. gracilis* algae growth (Figure 5) would change according to nutrient availability via different recycled rates of used medium to the fresh medium, thus negatively altering growth curves. Accordingly, a higher recycled rate of used supernatant would lead cells to reach exponential and stationary phases quicker, ultimately entering the death phase earlier (Figure 10).

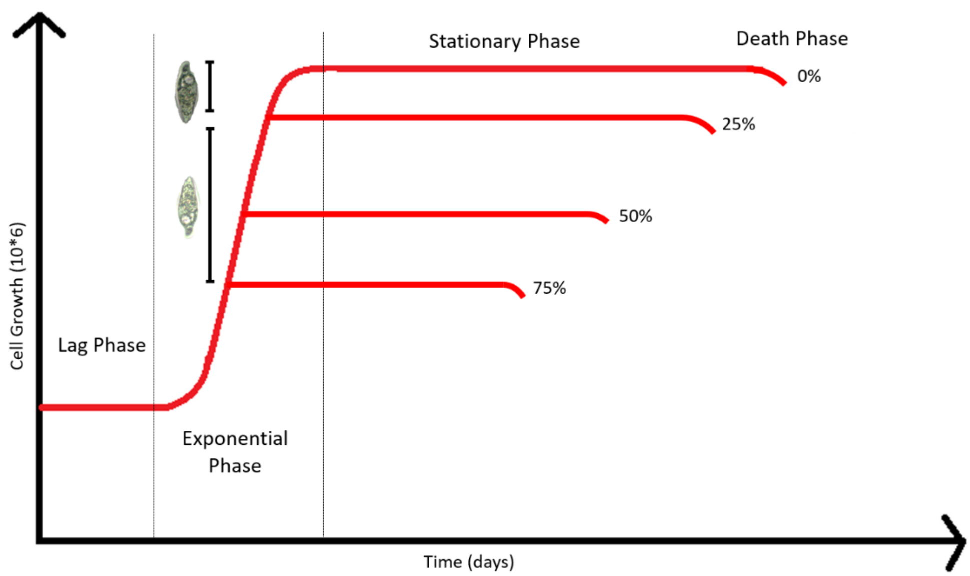

Figure 10: Expected growth curves of *E. gracilis* under varied recycled supernatant rates, 0, 25, 50, 75% along the classical microorganism growth curve with lag, exponential, stationary, and death phases marked as a function of cell growth (10^6) versus time (days).

In an academic sense, there is interest to investigate the potential use of recycled medium, as a means of imposing a culture stress for the elucidating the function of – cell growth modifying phytohormones, the CKs, and their influence on biomass accumulation and ABA – an environmental stress indicator hormone (Brien & Benkova, 2013, & Rashid, Rehman, and Han, 2013, & Noble et al., 2014). It is also of high interest to industry, which may be able to exploit results by modulating cultures through their hormones and hormone response pathways. Previous work with microalgae indicates that CKs act as growth regulators; however, little is known about their specific roles in *E. gracilis.* When using recycled media, trying to reduce cost and potential re-use of beneficial substrates for growth promotion is key, however, often at higher concentrations, recycled media result in growth inhibition (Lowery, Armenta, and Brooks, 2016). This research investigated the influence of endogenously produced and exogenously imposed CKs and ABA. It was shown how these endogenous CK and ABA are impacted and how responses to exogenous treatment changed at different recycling rates. All this was done in the context of influencing cell productivity.

Any identification of how hormone profiles change and whether those changes can be connected to growth parameters variation would be novel in *E. gracilis*. It was hypothesized that higher recycle rates would negatively affect culture growth resulting in (1) lower activity profiles of CK (lower abundance or a preponderance of less active CKs), and/or (2) higher ABA levels. It was therefore predicted that 25%, 50% and 75% recycled medium rates would, in a dose-response manner, decrease CK activity profiles and increase ABA levels.

2. Materials and Methods

2.1 Organism Description and Culture Parameters

Euglena gracilis (*E. gracilis*), was obtained from UTEX Culture Collection of Algae (Ca no: UTEX 753; University of Texas, Houston, TX, USA). Axenic liquid cultures of *E. gracilis* were maintained heterotrophically in sterile, optimized organic Noble Organic Medium (NOM) containing: Black Pearl Select molasses (3g/L; International Molasses Corporation, Ltd., Malt Products Corporation, Saddle Brook, NJ, USA), yeast extract (5g/L; Bioshop; Burlington, ON, Canada), ammonium phosphate monobasic, 2g/L; Bioshop; Burlington, ON, Canada), generic brand of vegetable oil (2g/L), ethanol (2g/L; Commercial Alcohols; Brampton, ON, Canada) (Noblegen Inc, Peterborough, ON, Canada). *E. gracilis* stock was cultured using culture flasks with ajar solid caps, in an incubator set at 120 rpm/min at 27.0°C. These preliminary cultures were harvested as a cell concentrate (over 5 mL) made via centrifugation (Thermo Scientific Sorvall ST 16 centrifuge; 2400 x g, 5 min) to propagate all future experiments. Each series of tests used the same optimized organic, autoclaved media described above. Recycled supernatant was recirculated from the initial culture in prepared dilutions and compared to the control using a fed-batch technique.

2.2 Experimental Procedure

Preliminary experiments were performed to establish optimal experimental conditions which included appropriate culture medium volume, air exchange metrics, instrumental settings, materials and to provide proof-of-concept for recycling culture medium (Table 3, Appendix I). It was determined that baffled bottom 1L culture flasks (Fisherbrand; Fisher Scientific Company, Ottawa, ON, Canada) with volumes of 500 mL, vented closure caps with a PTFE membrane, 0.22µm pore size for sterile air exchange, and incubator shaker plate (Adolf Kuhner Shaker Tray Carrier 008) set at 120 rpm/min and 27.0°C (Adolf Kuhner AG, Model, ISF-4-V) using a three-day harvest rate model worked best. These conditions validated an effective combination between current literature support for heterotrophic, fed-batch culturing techniques of microalgae and preliminary experimental findings with an industry collaboration partner, Noblegen. The main experiment, (Experiment 4), tested dilutions of recycled 0%, 25%, 50%, and 75% medium to fresh medium fractions, per culture volume, to determine the dilution rate that best supports cell viability (Figure 1, Appendix I). For example, a 500 mL cycle 1 test 1 flask with a 25% recycle rate contained 125 mL of recycled supernatant from the previously cultured 25% test flask and 375 mL fresh organic media. Four, 2 L culture flasks were filled with 1 L of media volume and inoculated with $2 \cdot 10^6$cells/mL and left to grow concurrently with Experiment 4 flasks to supply cells for inoculation the beginning of each cycle, every three days. Twelve, 1 L flasks filled with 500 mL of culture were used as experimental test cultures, each recycled rate having three replicate flasks. All experimental cultures were inoculated with $2 \cdot 10^6$cells/mL. Culture flasks were contained in the incubators (Adolf Kuhner AG, Model ISF-4-V) and Max Q 6000 (Model 4359; Thermo Scientific, Massachusetts, United States) and set at 29°C with shaking speed of 120 rpm.

During this experiment, set-up and take-down of the cultures were performed at the same time through all five, three-day-long cycling periods (9:00 h and 14:00 h respectively), to ensure consistent sampling times. 23 mL of culture was sampled daily for further analysis. Breakdown of analysis included:

- 10 mL sample for cytokinin and abscisic acid extraction,
- 10 mL sample centrifuged for 5 minutes, 2400 x *g*, and fractioned for supernatant and pellet for supernatant depletion and biomass accumulation analysis,
- 2 mL sample for biochemical analysis of glucose content,
- 1 mL sample for pH testing. The 1 mL sample for pH testing was first used for morphological assessment of the culture using a microscope.

2.3 Growth Parameters

Throughout experiments, the following macro-characteristics were recorded as they are typical parameters used to assess cell health: cell morphology, cell density, biomass accumulation, supernatant depletion, pH, and glucose content, both qualitatively and quantitatively (Lin, 2005). Cell counts were used to determine culture density. Morphological assessment of cells were conducted using light microscopy to assess the size, shape, and appearance of cells in culture. In addition to these parameters, pigmentation measurements acted as qualitative support to cell state.

Cell morphology was assessed using a microscope (Life Technologies EVOS FL Auto AMAFD1000) from 2 mL samples per triplicate and recycle rate (0, 25, 50 and 75%) tested. 10 μL was used for viewing the cells under 20x objective with a 200 μm field of view. Cells were qualitatively assessed for cell size, shape, and structural appearance as per morphological assessment qualities according to Noble *et al.*, 2014.

Cell density was measured using a Cell Counter (Life Technologies, Countess II FL, Model AMOAF1000) and a Countess II FL double-well slide. Parameters were set so that each cell count used the same settings (Auto Final Count threshold size of 6 μm to 60 µm, Auto Lighting 0 – 147 brightness units, and a maximum threshold of shape –oval to circular per 10 µL sample). Cell counts were performed in duplicate as number of cells per mL.

Biomass accumulation and supernatant depletion were measured by collecting 10 mL of culture in pre-weighed 15 mL tubes and centrifuged at 2,400 x g, 5 min (Thermo Scientific Sorvall Legend XF). Upon centrifugation, the sample was separated into supernatant and pellet. The resultant supernatant was filtered using glass fibre filter circles, 4.25 cm, with 22 µm pore size (Fisherbrand, Fisher Scientific Company, Ottawa, ON, Canada), weighed and freeze-dried (Labconco, Model 7806021) for 24 hours. The resultant pellet was rinsed with 5 mL deionized water and centrifuged twice (2,400 x g, 5 min), water was removed, and the remaining pellet weighed and freeze-dried for 24 hours. Wet and dry weights were recorded for collected supernatant and pellets.

pH was measured in 2 mL aliquots of culture media (containing cells) comprised of 0, 25, 50, and 75% recycled media per culture volume, twice per cycle (zero days post-inoculation (DPI 0) and two days post-inoculation (DPI 2)) over a three-day growth course, for four cycles (Sevenmulti Mettler Toledo AG, Model 8603 pH meter).

Glucose content was measured in 2.5 mL of culture using a Biochemical Analyzer (YSI 2700 Select). Before sampling, the biochemical analyzer was calibrated using YSI 1531 D-Glucose Standard 9.00 g/L and re-calibrated after five samples or after a 15-minute standby period. A YSI 2357 Buffer Concentrate Kit and YSI 2776 D-Glucose Standard 2.50 g/L, L-lactate 0.50 g/L concentrations were used to measure against each sample. Linearity checks with a 9.0 g/L linearity check solution (2.25 g glucose/250 mL water), were examined alongside the standard and fell between +/- 5% of labelled glucose. Triplicate samples were analyzed for one minute. It was found that the samples needed an

8-fold dilution per sample, such that the substrate concentration was within the linear range of the glucose curve (between 8.55 g/L and 9.45 g/L).

2.3.1 Cytokinin Extraction and Hormone Quantification by High-Pressure Liquid Chromatography-High Resolution Tandem Mass Spectrometry (HPLC-MS/MS)

A modified protocol described by Quesnelle and Emery (2007), Farrow and Emery (2012) and Kisiala et al. (2013) was used for CK and ABA extraction of *E. gracilis*. Collected samples of *E. gracilis* pellet and supernatant – as per the biomass accumulation and supernatant depletion protocol, was freeze-dried, and supernatant samples were stored at -80°C until CK extraction was performed. Upon CK extraction, samples were re-suspended in extraction buffer Bieleski #2 (Methanol: Water: Formic Acid; CH_4O:H_20:CH_2O_2 [15:4:1, v/v/v]), spiked with 144 nanograms (ng) of [$2H_4$] Abscisic Acid (ABA) (PBI, Saskatchewan, Canada) and 10 ng of each of the deuterated internal standard CKs, (OlChemim Ltd., Olomouc, Czech Republic; Table 1), and homogenized using a ball mill and stainless steel cylinders (RetschMM300; 5 min, 25 Hz) at 4^{o}C with zirconium oxide grinding beads (Comeau Technique Ltd., Vaudreuil-Dorion, Canada). The samples were allowed to extract passively overnight (approximately 12 hours) at -20^{o}C. Pellets were removed by centrifugation (Thermo Scientific; Model Sorvall ST16, Ottawa, Canada; 10 min at 10000 Revolutions Per Minute (RPM), the collected extracts and samples were re-extracted with 1 mL Bieleski #2 extraction buffer at -20^{o}C for 30 minutes. The pooled supernatants were dried in a speed vacuum concentrator at 35^{o}C (UVS400, Thermo Fisher Scientific, Waltham, Massachusetts, USA).

Extraction residues were reconstituted in 1 mL of 1M formic acid (pH 1.4) to ensure complete protonation of all CKs. Each extract was purified on a mixed-mode, reversephase, cation-exchange cartridge (Canadian Life Sciences; IRIS MCX 6 mL; 25-35 μ 200 mg, Peterborough, ON, Canada). Cartridges were activated with 5 mL of High-Performance Liquid Chromatography (HPLC) grade methanol and equilibrated using 5 mL of 1M formic acid (pH 1.4). After equilibration, each sample was loaded and washed with 5 mL of 1M formic acid (pH 1.4). ABA and CKs were eluted based on their chemical properties. ABA was eluted first with 5 mL of HPLC grade methanol (MeOH), next the nucleotide (NTs) fraction was eluted using 5 mL of 0.35 M ammonium hydroxide, Free Bases (FBs), Ribosides (RB), Glucosides (GLUCs) and Methyl-thiols (METs) retain on the column based on charge and hydrophobic properties and, thus, these were eluted last using 5 mL of 0.35M ammonium hydroxide in 60% methanol. All samples were evaporated to dryness in a speed vacuum concentrator at 35^{o}C and stored at -20°C.

NTs were dephosphorylated using three units of bacterial alkaline phosphatase (12 μL) in 1 mL of 0.1M ethanolamine-hydrochloric acid (pH 10.4) for 12 hours at 37°C (Emery et al., 2000). The resulting RBs were brought to dryness in a speed vacuum concentrator at 35°C. Samples were reconstituted in 1.5 mL double distilled water for further purification on a reversed-phase C18 column (Canadian Life Sciences; C18/14%, 6 mL, 500 mg; Peterborough, ON, Canada). Columns were activated using 3 mL HPLC grade methanol and equilibrated with 6 mL double distilled water. The samples were loaded onto the C18 cartridge and allowed to pass through the column by gravity. The sorbent was washed with 3 mL of double distilled water and analytes were eluted using 1.25 mL HPLC grade methanol. All sample eluents were dried in a speed vacuum concentrator at 35°C and stored at -20°C until further processing. Before HPLC-MS/MS analysis, all dried samples were reconstituted in 1.5 mL of starting conditions buffer (CH_3COOH:CH_3CN:ddH_2O [0.08:5.0:94.92, vol/vol/vol]).

Hormones were identified and quantified by LC-MS analysis. A 25 µL sample volume was injected into a Dionex Ultimate 3000 HPLC coupled to a QExactive Orbitrap mass spectrometer (Thermo Scientific). Compounds were resolved using a reversed-phase C18 column (Kinetex 2.6µ C18 100 A, 2.1 × 50 mm; Phenomenex, Torrance, CA, USA). All hormone fractions were eluted with a multistep gradient of component A: Water (H_2O) with 0.08% Acetic Acid (CH_3COOH) mixed with component B: Acetonitrile (CH_3CN) with 0.08% CH_3CO_2H at a flow rate of 0.3 mL per minute for ABA and 0.4 mL per minute for CKs. The initial conditions were 5% B increasing linearly to 10% B over two minutes followed by an increase to 95% B over 6.5 minutes; 95% B was held constant for one and a half minutes before returning to starting conditions for five minutes.

CK samples were analyzed using a Thermo Fisher Scientific QExactive Orbitrap (Santa Clara, CA, USA) equipped with a heated electrospray ionization (HESI) source and operated in a positive ion mode. To determine scanning start and end times in parallel reaction monitoring mode, the mass range in full scan mode was m/z 150-550 and resolution was set at 35,000. Temperatures of the HESI probe and capillary were 450°C and 250°C, respectively, and the spray voltage was 3.9 kV. Sheath, auxiliary and spare gases were operated at 30, 8 and 0 arbitrary units, respectively, and the S-lens RF level was 60. PRM parameters included an automatic gain control (AGC) of 1×10^6 and a maximum injection time (IT) of 128 msec. The precursor isolation window width was m/z 1.2 and normalized collision energies (NCE), individually optimized for each compound, ranged from 28 to 40 eV depending on the compound.

Raw data files collected during LC-MS/MS analysis were processed using the Thermo Fisher Scientific Xcalibur software (v. 3.0.63; Santa Clara, CA, USA). Peaks were extracted using the accurate mass of the two most intense fragment ions and a mass tolerance of three ppm. Peak integration employed five smoothing points and a signal-to-noise (S/N) threshold of 0.5. Quantification was achieved through isotope dilution analysis based on the recovery of 2H-labelled internal standards.

Endogenous CK analysis was normalized by subtracting the average background levels of existing endogenous hormones in the organic Noble Organic Media (NOM) media (media blank) (Table 4, Appendix I), and CK concentrations were calculated using Xcalibur software package as per cell dry pellet weight. Deuterated CK internal standards purchased from OlChemim Ltd. (Olomouc, Czech Republic) were used for the analysis. Deuterated ABA was obtained from the National Research Council Canada (Saskatoon, SK, Canada).

Table 1: Phytohormones (Cytokinins (CKs), and Abscisic Acid (ABA)) scanned for by high-performance liquid chromatography-tandem mass spectrometry (HPLC-MS/MS).

Isoprenoid Cytokinins	Labelled CK Standard
Nucleotides (NT)	
1. Trans-zeatin riboside-5′-monophosphate (tZNT)	
2. Cis-zeatin riboside-5′-monophosphate (cZNT)	$^{2}H_{3}$[9RMP]DHZ
3. Dihydrozeatin riboside -5′-monophosphate (DHZNT)	
4. N6 -isopentenyladenosine-5′monophosphate (iPNT)	$^{2}H_{6}$[9RMP]iP
Ribosides (RB)	
5. *Trans*-zeatin riboside (tZR)	$^{2}H_{5}$[9R]Z
6. *Cis*-zeatin riboside (cZR)	
7. Dihydrozeatin riboside (DHZR)	$^{2}H_{3}$[9R]DHZ
8. N6 -isopentenyladenosine (iPR)	$^{2}H_{6}$[9R]iP
Free bases (FB)	
9. Trans-zeatin (tZ)	$^{2}H_{5}$Z
10. Cis-zeatin (cZ)	
11. Dihydrozeatin (DHZ)	$^{2}H_{3}$DHZ
12. N6 -isopentenyladenine (iP) 2 H6iP	
Glucosides (GLUC)	
13. Trans-zeatin-O-glucoside (tZOG)	$^{2}H_{5}$ZOG
14. Cis-zeatin-O-glucoside (cZOG)	
15. Dihydrozeatin-O-glucoside (DHZOG)	$^{2}H_{7}$DHZOG
16. Trans-zeatin-O-glucoside riboside (tZROG)	$^{2}H_{5}$ZROG
17. Cis-zeatin-O-glucoside riboside (cZROG)	
18. Dihydrozeatin-O-glucoside riboside (DHZROG)	$^{2}H_{7}$DHZROG
19. Trans-zeatin-9-glucoside (tZ9G)	$^{2}H_{5}$Z9G
20. Cis-zeatin-9-glucoside (cZ9G)	
21. Dihydrozeatin-9-glucoside (DHZ9G)	$^{2}H_{3}$DHZ9G
Methylthiols (MET)	
22. 2-Methylthio-trans-zeatin (2MeSZ)	$^{2}H_{5}$MeSZ
23. 2-Methylthio-trans-zeatin riboside (2MeSZR)	$^{2}H_{5}$MeSZR
24. 2-Methylthio-N6 -isopentenyladenine (2MeSiP)	$^{2}H_{6}$MeSiP
25. 2-Methylthio-N6 -isopentenyladenosine (2MeSiPA)	$^{2}H_{6}$MeSiPA
Aromatic cytokinins	
26. Benzylaminopurine (BA)	$^{2}H_{7}$BA
27. Benzylaminopurine riboside (BAR)	$^{2}H_{7}$BAR
Abscisic Acid (ABA)	
28. Abscisic Acid (ABA)	$^{2}H_{4}$ABA

2.3.2 Pigment Analysis

Pigment analysis was conducted on *Euglena gracilis* cultures at two-, three-, four-, six-, and nine-day long growth periods without recycling. Pigment analysis was investigated using a visible spectrophotometer (ThermoScientific Genesys 20) to evaluate pigment content based on the absorbance wavelength values of A_{470}, A_{480}, A_{537}, A_{647}, A_{649}, and A_{664}. This experiment was completed in tandem with the same cell line as a deviation from the normal three-day harvest time to address pigment changes over a longer growth period and to further report if pigment could be used as an indicator of algal health status. Three technical replicates from samples were measured per 100 mg cell biomass/12 mL vial volume. Seven mL of dimethyl sulfoxide (DMSO) was added and incubated at 65°C for 30 minutes in a water bath, shaken periodically and brought up to a total of 10 mL DMSO, transferred to a 1 mL cuvette and measured as per Hiscox and Israelstam (1978). The spectrophotometer was calibrated against DMSO at absorbance levels listed above. The absorbance readings were used to calculate 1) Chlorophyll a, 2) Chlorophyll b, 3) total chlorophyll, 4) anthocyanin and 5) carotenoid content using the following equations and average values per growth period was calculated (Hiscox and Israelstam, 1978, and Sims and Gamon 2002):

1) Chlorophyll A = $(2(12.19*A_{664}-3.45*A_{649}) * (100/\text{weight(mg)})$

2) Chlorophyll B = $(2(21.99*A_{649}-5.32*A_{664}) * (100/\text{weight(mg)})$

3) Chlorophyll Total = $(2(17.76*A_{649}+7.34*A_{664}) * (100/\text{weight(mg)})$

4) Anthocyanin = $(0.8173*A_{537}-0.00697*A_{647}-0.002228*A_{664})$

5) Carotenoid = $((2*1000*A_{480}-2.14*\text{Chl A}-70.16*\text{Chl B})/(220*(100/\text{weight(mg)})))$

2.3.3 Statistical Analysis

Statistical analysis of CK levels was conducted using Statistica 8.0 software. Measurements were compared within each recycle rate and cycle with a two-way ANOVA (Table 5, Appendix I) for significant values: $*p < 0.05$; $**p < 0.01$; $***p < 0.001$. This was followed by Duncan's multiple range test for post-hoc analysis with statistical differences ($P \leq 0.5$) for cycle versus day per recycling rate, and the significance between cycle versus recycling rate. The resultant data from endogenous CK hormone profiling was therefore analyzed for these significant differences against the control of zero percent recycled media with raw data in Tables 8 & 9, Appendix I.

3. Results

3.1 Macro-level Growth Analytics

3.1.1 Morphology

Cell morphology is influenced by many factors including the cell cycle, each phase of its growth, the aging or individual properties per cell, and the environmental impacts or stressors it experiences (Marba-Ardebol, 2018). Cell morphology, therefore, can be used as a suitable parameter to assess changes during growth as dynamic morphological changes are often related to cell physiology and viability (Zachler, Bisova, & Vitova, 2016). Moreover, the constituents in a given media can also affect the cell size, as well as the circularity and phase homogeneity of the algae cells (Albertin et al., 2011; Timoumi, 2017). To assess the morphological changes, *Euglena gracilis* cells were viewed using light microscopy (Noble, *et al.,* 2014). As shown in Figure 11, control cells experiencing no recycled supernatant, showed "classical" *E. gracilis* growth (as defined by Noble et al., 2014, Al-ashra, Abiad, & Allahem, 2014) which was cylindrical or spindle-shaped, sized between 40-80 μm long and 18-25 μm wide, and had a slight attenuated and rounded anteriorly body shape. Cells under a 25% recycled rate, showed morphology that was similar to the control except for having more cells of smaller size and smaller proportions of cell component release as a waste product and analyzed by POS Bio-Sciences (Appendix II) (Figure 11B). Cells treated with 50% recycled supernatant were irregularly shaped, and some were encysted – as shown by cells of a darker colour and of circular shape - also of note, this media complex had high oil content (Figure 11C). Figure 11D, cells under 75% recycled supernatant (25% fresh media) displayed a dominant eye spot – characterized by carotenoid accumulation (James et al., 1992), and had a lower occurrence of intracellular components and cellular motility seemed to be reduced (Figure 11D).

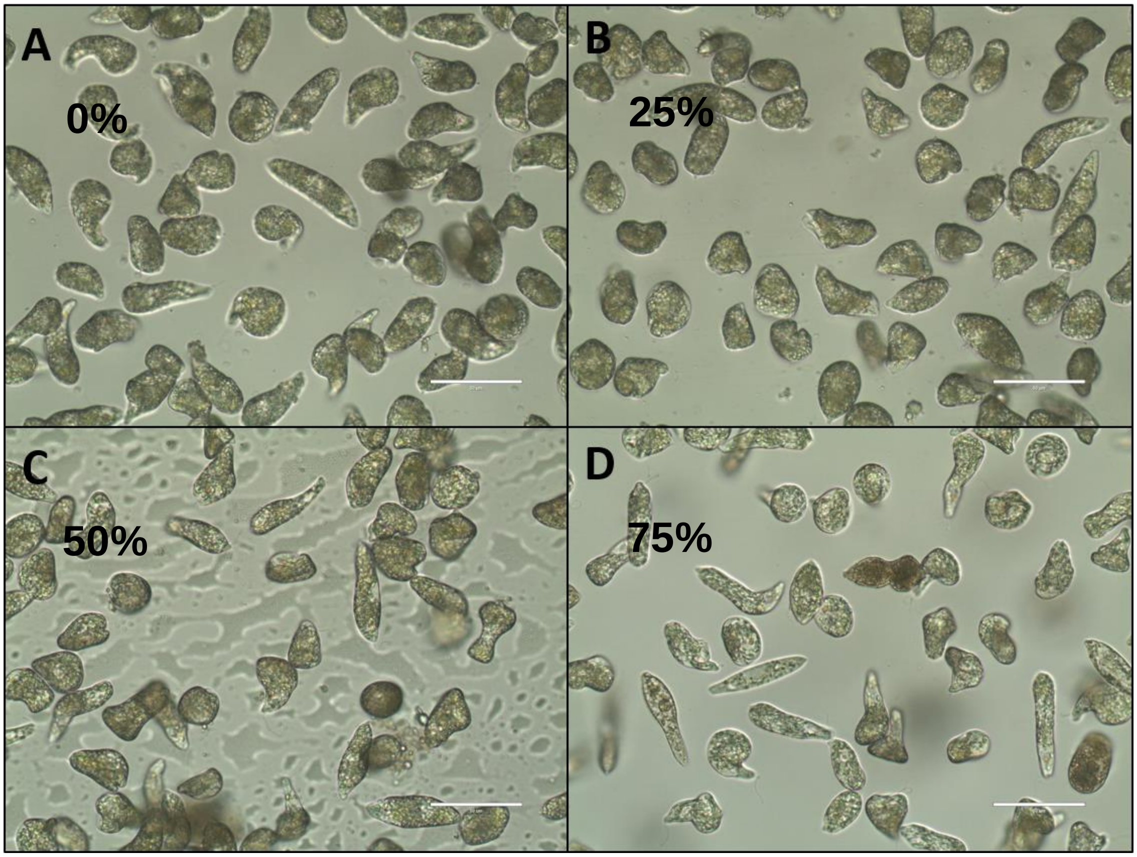

Figure 11: Morphological assessment of *E. gracilis* under varied recycled conditions at the 40x magnification with scale bar standing for 200 µm using a Life Technologies EVOS FL Auto AMAFD1000 microscope. A, represents control cells under no recycled conditions, B, 25% recycled rate, C, 50% recycled rate, and D, 75% recycled rate of used medium to fresh medium per 500 mLs.

3.1.2 Growth Curves, Biomass Accumulation and Resultant Supernatant

The growth of microorganisms is assessed against a generalized microorganism growth curve that marks the four main stages of growth – lag, exponential growth, stationary and death (Price & Farag, 2014). These stages of growth are inherently affected by a variety of factors, chiefly nutrient availability when under heterotrophic, axenic, anaerobic fermentation conditions (Lee, Jalalizadeh, & Zhang, 2015). Growth was further influenced when nutrient availability was augmented or limited by the addition of fresh medium or re-use of exhaust medium from preceding growth periods.

Actual growth curves of *E. gracilis* under mixed fractions of recycled medium to fresh medium were plotted in by first and last days of the growth cycle, Figure 12. As a function of days post-inoculation (DPI) at the beginning of the three-day-long growth cycle (0) to the end of the cycle (2), A, B, C and D, represent growth curves for cycles 1-4 (Table 9, Appendix I).

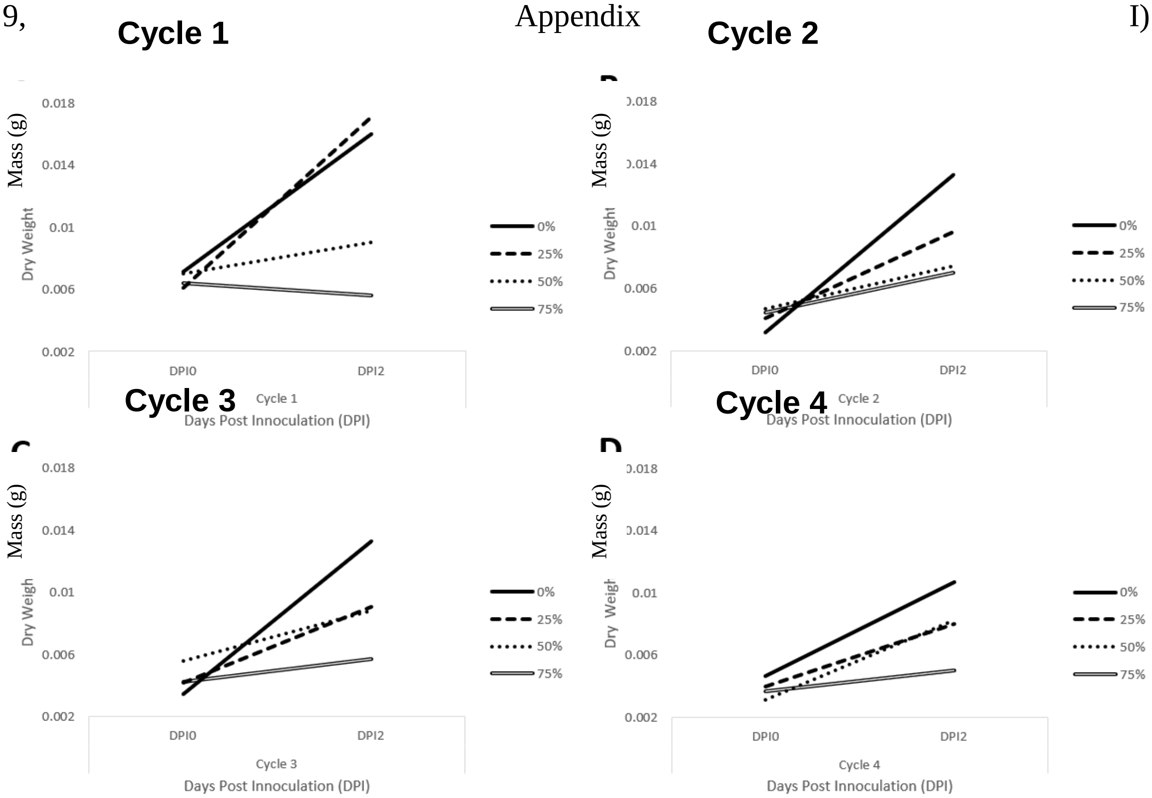

Figure 12: Growth curves as measured by accumulation of dry mass of *E. gracilis* as a function of Days Post Inoculation (DPI) 0, start, and 2, end, for cycles 1 (A), 2(B), 3(C), and 4(D), verses Dry mass (g/L) per recycled rates 0, 25, 50, and 75%.

Dry biomass weights for recycled rates of 0% and 25% were closely matched, where the 50% rate showed a slight increase in growth oppositely to the 75% recycled rate as it decreased growth by about 40% less cell biomass (Figure 12A). This trend of the higher output of biomass from start to finish was echoed for 0% and 25% in all cycles (A, B, C, D). 50% and 75% recycled rates showed nearly identical growth in cycle 2 (Figure 12B). During the third recycle period, the growth of 25% recycled medium and above, generated less biomass, however, 25% and 50% ended with similar biomass generation. In the last cycle (Figure 12D), 0% had less overall starting biomass compared to cycle 3, however, was greater than 25, 50 and 75% which had similar biomass recovery between cycles 3 and 4. Interestingly, while all recycled rates showed a similar degree of starting biomass as regulated by the same inoculation density, each recycling rate demonstrated that by the third day of growth, the end dry product recovery varied. Additionally, the time it took to reach the end product recovery slowed from the beginning to the end. These results showed that recycled medium rates negatively affected *E. gracilis* growth in terms of biomass recovery and time to generate biomass to varying degrees – it took three days to reach 0.01 g in cycle 1 and by cycle 3 it took six days to reach 0.01 g.

Comparing biomass accumulation and supernatant residue, Figure 13 showed the proportional percent of dry biomass weight (g/L) and dry supernatant residue (g/L) from the total mass collected for each recycling rate. This was measured for each 0, 25, 50, and 75% (used medium to unused medium) per cycle 1 and 4. Generally, used medium had higher residue in higher recycling rates and extended recycling cycles which indicated more nutrients remain in solution compared to ratios with alternatively high fresh medium (0% and 25% recycled rates). For example, supernatant residue total weight increased from cycle 1 to 4 within both 50 and 75% as opposed to a decrease in total weight of supernatant reside within both 0 and 25% rates. These trends signify that recycling medium, in varied ratios, altered the final growth profiles of *E. gracilis* cells. Comparing cycle 1 to cycle 4 more specifically, a 0% recycled rate was similar in cellular biomass by about 5% (20.02% to 25.17%) with the corresponding supernatant change, similarly to the 25% recycled rate, which indicated a steady recovery or increase of biomass weight between each of these recycled fractions (Figure 13). The 50% recycled rate showed a similar trend of increase in biomass and decrease in supernatant residue; however, it was less than 2% (16.36% to 18.06 %). By contrast, the 75% recycled rate showed a 3% (13.92 % to 10.62%) decrease in biomass from cycle 1 to 4. In all cases, approximately 80% of the dry mass collected from both biomass weight and supernatant was held in the supernatant fraction with the 75% recycled fraction having the highest levels of supernatant present in both respective cycles followed by 25%, 50% then 0% in which the 0% recycled rate maintained the highest level of dried biomass per respective cycles. Therefore, the dried supernatant analysis

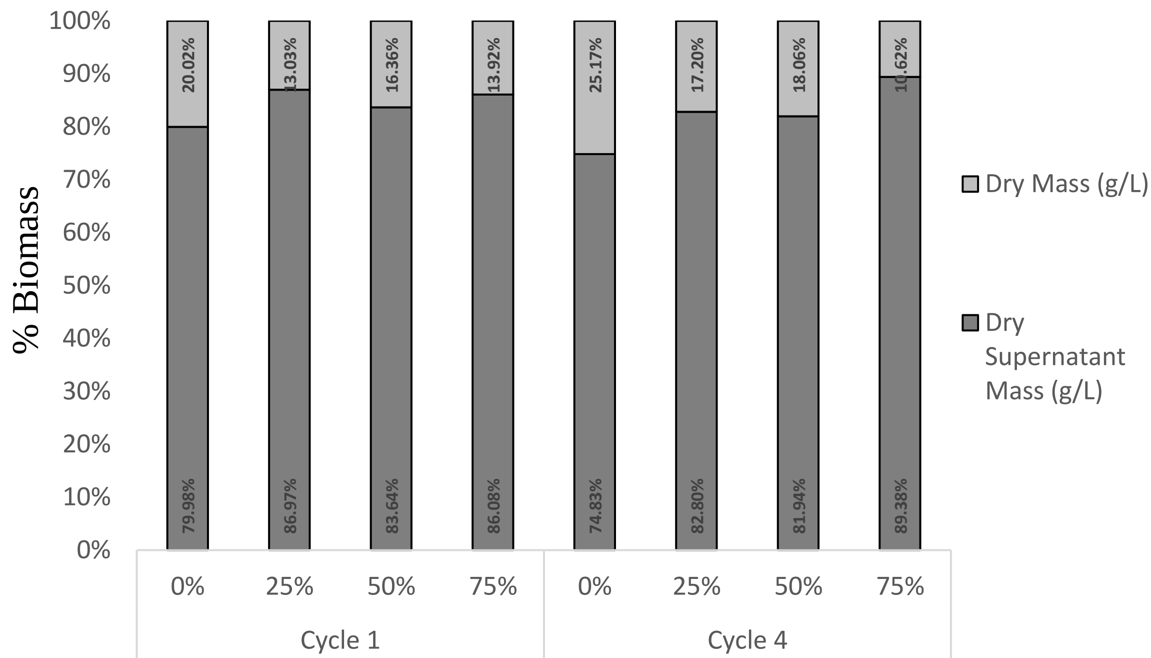

Figure 13: Biomass distribution as Dry Mass (g/L) compared to resultant supernatant as Dry Supernatant Mass (g/L) of *Euglena gracilis* for cycle 1 and 4,under all recycled media fractions, 0, 25, 50 and 75% of recycled medium to fresh medium as a total percent of dry weight collected (g/L).

showed that the 0, 25, and 50% recycled fractions contained less recycled media nutrients over time, compared to the 75% recycled fraction. These results show that varied recycle rates of 0, 25, 50, and 75% affect biomass generation and supernatant nutrient consumption.

3.1.3 Glucose Content and pH Levels

Glucose content and pH are critical features that strongly affect cell growth therefore, these measurements can be used as quantitative measurements to detail the changes within the recycled medium conditions (González-lópez *et al.,* 2013, & Rodolfi, *et al.*, 2003). Therefore, both these parameters were tracked during four cycles (1-4) of 3-day long growth periods of *E. gracilis* cells under varied recycled conditions (0, 25, 50, and 75%). Glucose content was analyzed at the beginning and end of each cycle, DPI0 and DPI2 respectively Figure 14 & Table 9, Appendix I. Data collected from the glucose content showed trends of decreasing glucose concentrations during cycles 1 and 4 for all recycle rates. Interestingly decreases of glucose concentrations were also found during cycle 2 for only the 50 and 75% recycled fractions and during cycle 3 for only the 75% recycled fraction. Trends of increasing sugar content within the media was observed in only cycles 2 and 3 for both 0 and 25% recycled fractions and 50% during cycle 3 only. Steepest declines in media sugar content were most pronounced in 0% followed by 25% recycled fractions, whereas 50 and 75% did not decrease as dramatically. Interestingly, in cycles 2 and 3, all recycled fractions had similar sugar content at the beginning of the cycle between 0.5 and 1 g. By the end of the cycle, sugar varied by 0.5 g in cycle 2 and by 0.5 to 1.5 g in cycle 3. Early cycle cells (0 and 25%) had greater uptake of glucose except for 75% in cycle 1 as shown by Figure 14. Glucose content analysis, therefore, indicated that under heavy recycled conditions, glucose uptake/consumption was less pronounced.

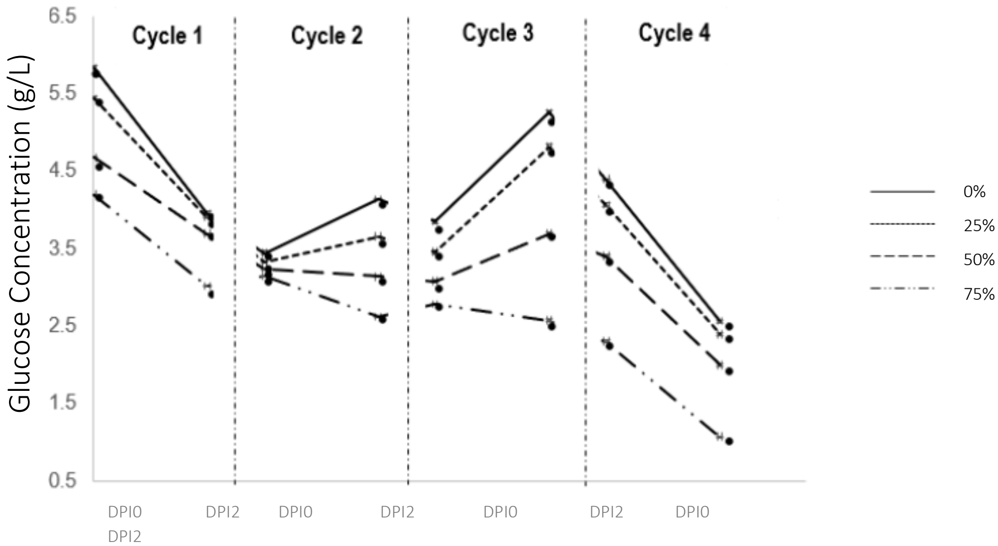

Figure 14: Change in Glucose Content as g/L was measured from *Euglena gracilis* cultures grown for 3-days and measured on the first and last day of growth (DPI0 and DPI2) for four cycles under four recycled fractions of 0, 25, 50, and 75% to fresh medium. Analysis was performed using Biochemical Analyzer YSI 2700 Select using YSI 1531. D-Glucose Standard 9.00g/L [900 mg/dL].

pH measures were taken of *E. gracilis* cultures per day (DPI 0-2) for all cycles (1-4) under all recycled rates (0, 25, 50, and 75%) shown in Figure 15. These data show clear trends of increasing pH from DPI 0 to DPI 2 in all cases of recycled fractions and cycles, except for the 0% recycled fraction as it was pH-stable at 3.2. The higher the recycling rate, the greater the pH increase. While 25% induced moderate pH increase of 0.2 even by cycle 4 when it was only 3.5 pH units, 50% showed great pH shifts to 3.3 at cycle 1 to as high as 3.7 by cycle 4. The 75% impacted the pH very strongly by about 0.4 at cycle 1 to 4.2 (cycle 2) and as high as 4.6 by DPI2 of cycle 4. This data showed that extended recycling of medium and ratio of recycled medium to fresh media, strongly impacted pH.

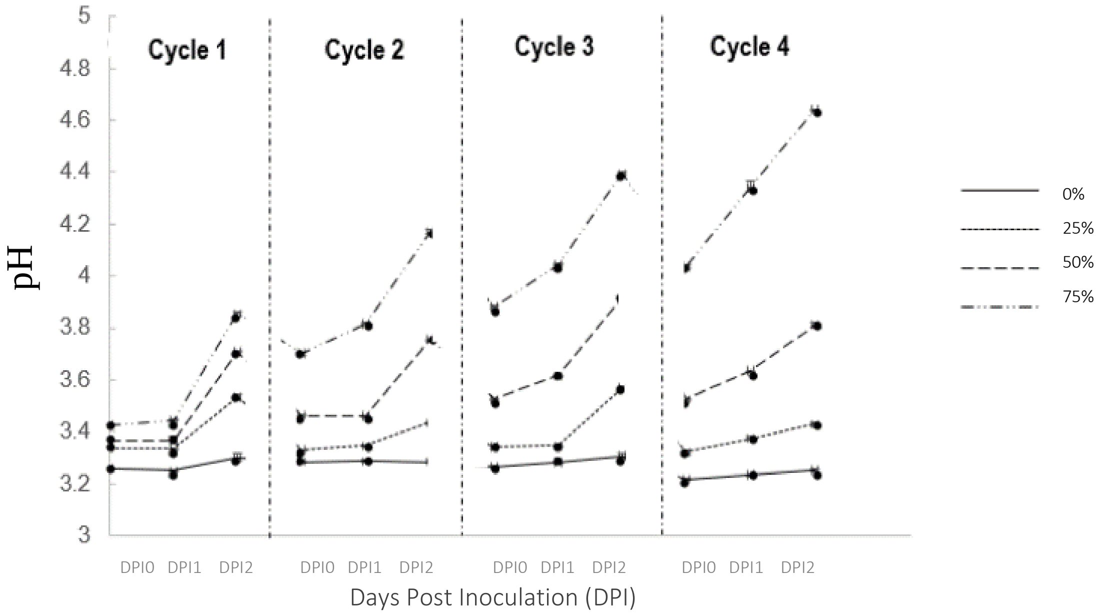

Figure 15: pH levels from *Euglena gracilis* cultures grown for 3-days and measured per day post-inoculation until the cycle was completed (DPI 0-3), cycled through four rounds under recycled conditions of 0, 25, 50, and 75% to fresh medium.

3.1.4 Pigment Analysis

Microalgae are gaining attention as a source of high value products such as carotenoid pigments, vitamins, and proteins (Filomena *et al.*, 2013). In some cases, development of pigments from the carotenoid family and interconversions of these molecules can be used as an indicator of healthy cells based on their accumulation levels (Kuczynska, Jemiola-rzeminska, & Strzalka, 2015 & Kass *et al.*, 2017). As such, cultures of *Euglena gracilis* were grown for various growth periods of two-, three-, four-, six- and nine-days to assess chlorophyll a and b, carotenoids, and anthocyanin content (Figure 16). These results show that between, two-, three-, and four-day long growth periods, there were similar trends for all chlorophyll and carotenoids. Except for anthocyanin content, pigment levels in *E. gracilis* cells grown for six days showed a level response from two to four days of growth and thereafter a gradual decline progressing from four to nine days. Chlorophyll *b* and total chlorophyll content was the highest for all growth periods followed by carotenoids, chlorophyll *a*, then anthocyanin pigment. Anthocyanin levels were not impacted by growth period/culture growth duration. Collectively, these findings show that pigment content generally decreases as days of growth increase and that chlorophyll content is the highest level of pigment found in heterotrophically grown *E. gracilis* cultures grown for various growth cycles.

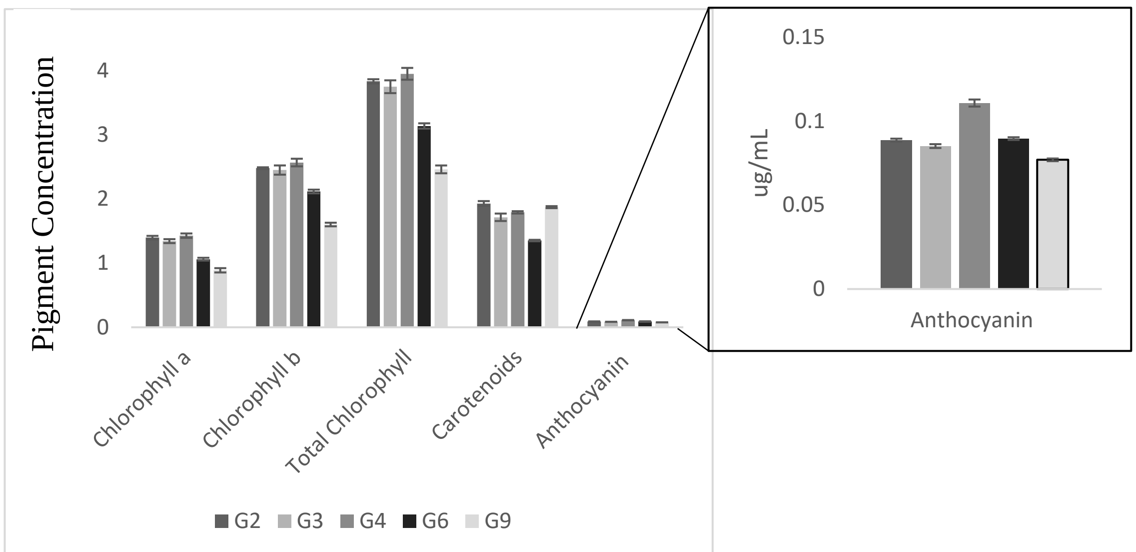

Figure 16: Chlorophyll, Carotenoid, and Anthocyanin pigment content in *Euglena gracilis* cultures grown for 2, 3, 4, 6, and 9-days. Evaluation of pigment content in µg/mL was analyzed using a visible spectrophotometer ThermoScientific Genesys 20 using absorbance values of A^{470}, A^{480}, A^{537}, A^{647}, A^{649}, and A^{664}.

3.2 Hormone Profiles

Phytohormones can function as endogenous components of microalgae affecting growth ptocess and when added exogenously can increase cell counts in *E. gracilis* as shown in Noble *et al.*, 2014. Other hormonal effects relate to the biosynthesis of compounds like pigment and lipids (Priyadarshani & Rath, 2012). It is therefore novel to investigate these changes in the levels and types present, of endogenous cytokinins (CKs) and abscisic acid (ABA) in heterotrophically grown microalgae *Euglena gracilis* in response to the use of recycled media for industrial use. Specifically, the reuse of an organic medium was tested for three-day-long growth cycles for four consecutive cycles to assess the hormone profiles, fractions were split for analysis between supernatant and pellet samples for both cycles 1 and 4.

Samples were further subdivided by recycled fraction and cycle parameters and measured for CK levels using five CK groups: Free Bases (FBs), Ribosides (RBs), Nucleotides (NTs), Glucosides (GLUCs), and Methyl-thiols (METs). Per the five CK groups, there are corresponding CK types, dihydrozeatin (DZ), trans-zeatin (tZ), isopentenyl adenine (iP), and cis-zeatin (cZ). Along with CK level measurements, the CK antagonist hormone ABA was also measured. CK and ABA analysis was performed for both the pellet and supernatant fractions. The analysis was grouped as follows: Total CK Levels, CK Types Total Levels (tZ, cZ, DZ, and iP) and CK Form Total Levels (FBs, RBs, NTs, METs, and GLUCs).

All hormone data were corrected for the level of CKs and ABA present in fresh media used in culturing of *E. gracilis*. This was done by taking experimental media-only blanks, analyzing the phytohormone levels and then subtracting average levels bases on the dilution rate in the recycled media. It is therefore possible that reported hormone levels would be representative of hormones synthesized or processed by the Euglena cells above and beyond that found in the medium. The exogenous presence of hormones in the media could impact the overall endogenous profile of the Euglena cell pellet and or the hormones excreted into the media and the cell-free spent media used in subsequent cycling rounds.

Figure 17 and 18 show the total cytokinin levels, CK types and CK fractions between cycles 1 and 4 for both supernatant and pellet. Figure 19 displays the level of ABA found within the supernatant fraction for both cycles 1 and 4. A heat map developed to visualize the hormone data analysis is shown in Figure 20 with raw data included as Table 8, Appendix I. In Figures 17 and 18, DZ9G was omitted for the simplicity of describing the active types of CKs present where DZ9G represents a type of glucoside that is an irreversible conjugate without the potential for being active.

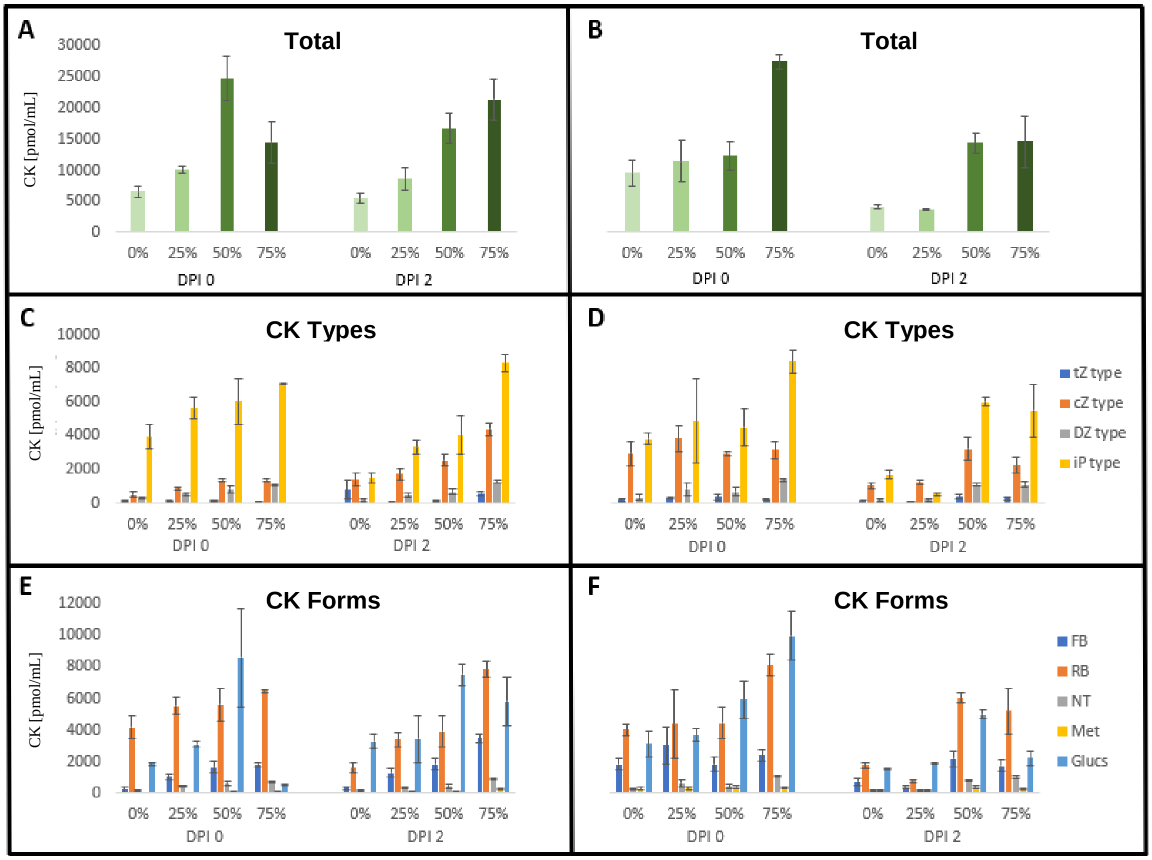

Figure 17: Cytokinin (CK) levels of *Euglena gracilis* in the supernatant fraction for the first-day post-inoculation (DPI0) and the final day (DPI2) for cycles 1 and 4 under all recycled conditions 0, 25, 50 and 75% (recycled medium to fresh medium) in 500 mL culture flasks. Panels A, C, E for Cycle 1, and Panels B, D, F for cycle 4. Panels A and B show total cytokinin (CK) levels in the supernatant in all recycled rates (0, 25, 50, and 75%). Error bars represent the standard error for each sample. Concentration for each CK is given on the y-axis in pmol/mL. Panels C and D show CK types detected in the supernatant in all recycled rates. Panels E and F show CK forms detected in the supernatant within the specified recycle rates. CK types: tZ represents *trans*-zeatin type, cZ *cis*-zeatin type, DZ dihydrozeatin type, and iP N^6-isopentenyladenine type. CK forms: FB represents Free Bases, RB as Ribosides, NT as Nucleotides, MET as Methyl-thiols, and GLUCs as Glucosides.

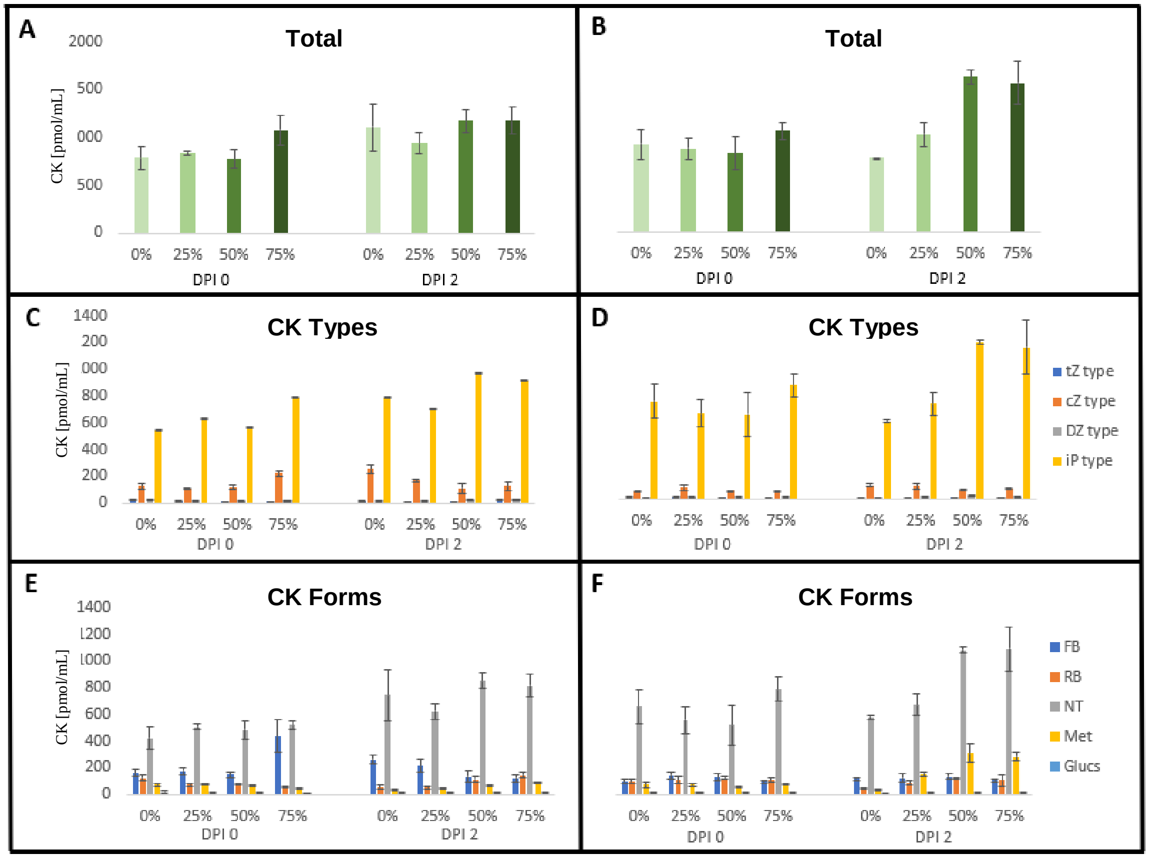

Figure 18: Cytokinin (CK) levels of *Euglena gracilis* in the pellet fraction for the first-day post-inoculation (DPI0) and the final day (DPI2) for cycles 1 and 4 under all recycled conditions 0, 25, 50 and 75% (recycled medium to fresh medium) in 500 mL culture flasks. Panels A, C, E for Cycle 1, and Panels B, D, F for cycle 4. Panels A and B show total cytokinin (CK) levels in the supernatant in all recycled rates (0, 25, 50, and 75%). Error bars represent the standard error for each sample. Concentration for each CK is given on the y-axis in pmol/mL. Panels C and D show CK types detected in the supernatant in all recycled rates. Panels E and F show CK forms detected in the supernatant within the specified recycle rates. CK types: tZ represents *trans*-zeatin type, cZ *cis*-zeatin type, DZ dihydrozeatin type, and iP N^6-isopentenyladenine type. CK forms: FB represents Free Bases, RB as Ribosides, NT as Nucleotides, METs as Methyl-thiols, and GLUCs as Glucosides.

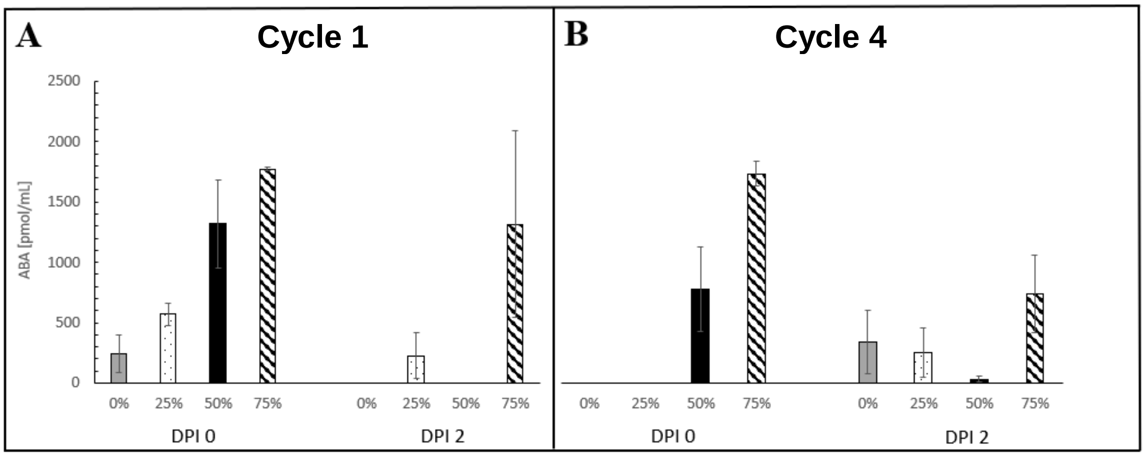

Figure 19: Abscisic Acid (ABA) hormone levels. A, level of ABA in cycle1 and B, levels of ABA in cycle 4. All recycle rates 0, 25, 50 and 75% (recycled medium to fresh medium) were tested with the media blank subtracted from the total level.

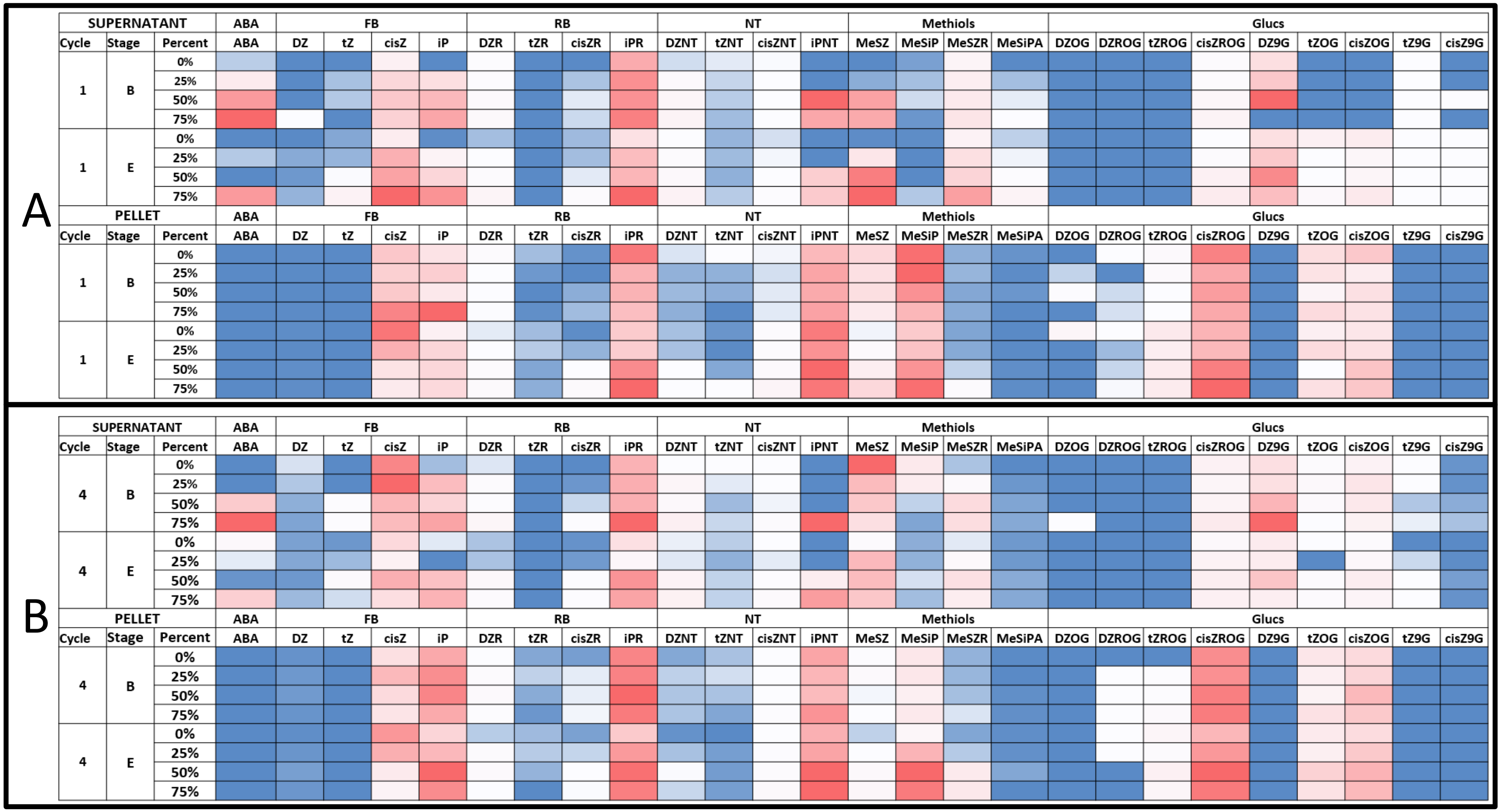

Figure 20: Abscisic Acid (ABA) and Cytokinin (CK) levels of *Euglena gracilis* in both supernatant and pellet fractions for the beginning (B) and end (E) cycle 1 under recycled conditions 0, 25, 50 and 75% of recycled medium to fresh medium in 500 mL culture flasks represented in a heat map. Colours were assigned as blue (lowest), red (highest) and white (not detected). All remaining values were assigned a colour per value with three different shades of both blue and red. Panel A displays the supernatant fraction and B, the pellet fraction. CK forms as Free Bases (FBs), Ribosides (RBs), Nucleotide (NUCs), Methyl-thiol (METs), and Glucosides (GLUCs) and CK Types as transCKs, cisCKs, FBs (DHZ + tZ + cisZ + iP), RBs (DZR, tZR, cisZR, IPR), NUCs (DZNT + tZNT + cisZNT + iPNT), METs (MeSZ + MeSiP + MeSZR + MeSiPA) and GLUCs (DZOG + DZROG + tZROG + cisZROG + DZ9G tZOG + cisZOG + tZ9G + cZ9G).

3.2.1 Supernatant Fraction

The majority of the CKs present were ~ 50% RB form followed by ~30% GLUC and ~10% FB forms. The dominant CK types included iP and cZ. In general, higher RBs are observed at the beginning of the cycle, with the GLUC form (storage form) accumulating towards the end of each cycle. Analysis of the changes in CK profiles highlights conserved trends in the varying culture conditions towards increasing RB and GLUC forms, including iP and cZ types with increased culturing time. ABA hormone levels were only detected within the supernatant fraction and levels increased with increased recycling rate.

Total cytokinin level for supernatant

Total CK levels increase with increased recycling rate (4000 pmol/mL 0% to 20,000 pmol/mL 75%) as shown in Figure 17A & B and Figure 20. In the control (0% recycled media), between the beginning and end of the cycle, total CK levels remained consistent (Figure 17A). This trend was also observed for the 25% recycling rate. Interestingly, at the beginning of the cycle the 50% recycling rate was at least 2x the total levels of both the 0 and 25% rates at over 20,000 pmol/mL and higher than the 75% (15,000 pmol/mL) by ~5000 pmol/mL. Markedly, the 50% recycled rate is the only rate to decrease by the end of the first cycle. The 75% recycling showed increased total levels between the beginning and end of the cycle, while also demonstrating the greatest CK change by the end of the first cycle. By cycle 4, Figure 17B displays a distinct profile. Among the recycling rates, at the beginning of the cycle, 0, 25, and 50% rates were comparable with just over 10,000 pmol/mL detected, while the 75% rate nearly tripled in total detected CKs. By the end of cycle 4, total CK levels decreased for all, except 50%. It was noteworthy that both the 0 and 25% recycled rates were detected at the lowest levels and were comparable at ~3000 pmol/mL as both the 50 and 75% rates distinctly increased by a factor of 5x comparatively. From this data, one recycled period had a higher total CK profile within the higher recycling rates, which suggested that CKs increased within the supernatant because of extensive recycling.

CK types within the supernatant

iP was the dominant CK type followed by cZ type (Figure 17C & D and Figure 20). This was also reflected in Figure 18. While both DZ and tZ were detected, levels ranged from two to seven times less than iP and cZ, with DZ type being the least detected type found. Increasing levels of iP from beginning to the end of cycle 1 to cycle 4 across all recycled rates was evident (Figure 17C & D). Although there was an increasing trend of iP type with increased recycling rate in cycle 1, by cycle 4 (Figure 17, D), levels showed an overall reduction in the dominant iP CK type (with the exception of 75% which increased by ~1000 pmol/mL in levels detected), comprised solely of the riboside conjugate of iP (Figure 17C & Tables 10 & 11, Appendix I). iP had the highest level in the maximum recycled rate, 75%, and decreased with reduced recycling rate in both cycles (Figure 17C & D). This trend was mirrored in cycle 1 by cZ type CK, particularly with increases in cZR however, with levels far less at ~2000 pmol/mL compared to ~6000 pmol/mL (Figure 17, C). During cycle 4 (Figure 17D), cZ dropped in the lower recycling rates at the beginning of the cycle and increased towards the end of the cycle in the 50 and 75% rates (1000pmol/mL to ~2500pmol/mL). The DZ type followed a similar increasing trend with increased recycling rate from the start and end of cycle 4. Approaching cycle 4, the tZ type was reduced from cycle 1 to cycle 4 (Figure 17C & D). During the recycling of supernatant, it was clear that *E. gracilis* recycled culture medium highlights an external environment rich with active type CKs and key CKs change depending on recycling rate and number of cycles.

CK forms within the supernatant

At the beginning of cycle 1, RBs were the predominant form. In contrast, at the end of cycle 1, RBs had decreased, and an increased proportion of GLUCs was present due to a reduction in DZR and iPR and an increase in tZOG and cZOG (Figure 17E, Figure 20, Tables 10 & 11, Appendix I). Overall CK RBs were reduced from the start to end of cycle 1 (~6000 pmol/mL to ~4000 pmol/mL) except for the 75% recycled rate, due to the overall reduction of iP CK types (Figure 17C & Tables 10 & 11, Appendix I). By cycle 4, while RBs continued to increase with increasing culturing time and increased recycling rate, by the end of the cycle, the RB profile drastically reduced for the 0 and 25% rates by ~four fold (~4000 pmol/mL to ~1000 pmol/mL) (Figure 17F). This trend was paralleled by changes in the GLUCs profile (Figure 17F). As there is an increase in GLUC forms at the end of the cycle, at the beginning of the next cycle, interestingly, at the higher the recycled rate ($P \leq 0.5$), more GLUCs were present at the start of the cycle (Figure 17E & F). Comparatively in cycle 4, GLUCs increased at the beginning of the cycle, however, decreased by the end (Figure 17F). In terms of FBs, during cycle 1, all recycled rates increased levels of FB CKs with the highest levels found at the end of cycle 1 (Figure 17E). Starting at higher levels during the beginning of cycle 4, FBs, sharply decreased from ~1000 pmol/mL within 0 and 25% ($P \leq 0.5$) rates to ~100pmol/mL; however, they remained consistent between the start and end for both 50 and 75% rates at ~2000 pmol/mL (Figure 17F). While RB, GLUC and FB forms were variable, METs were extremely low until cycle 4, where levels begin to appear and increase with increased recycling rates this trend is also found in the NT forms (~20x less then RBs). Notably, the recycled medium retained high levels of RB forms.

ABA levels within the supernatant

The ABA data from the supernatant of cultures grown under different recycling rates showed that in the beginning of cycle 1, levels in the culture media increased with higher recycling rates: 0% - 200 pmol/mL, 25% - 600 pmol/mL, 50% - 1300 pmol/mL, and 75% - 1800 pmol/mL (Figure 19A). At the end of cycle 1, ABA levels reduced in all recycle rates by >25% of their starting values (Figure 19B). Relative to the other recycled rates, 75% had the highest level of ABA at the beginning and end of cycle 1 and the beginning and end of cycle 4 ($P \leq 0.5$) (Figure 19A & B). The highest concentration of ABA was found at the beginning of cycle 1, with the 75% recycling rate more than 7x higher than the 0% recycling rate. Towards the end of cycle 1, ABA levels decreased in all recycled rates with highest levels detected in the 75% rate (Figure 20). It appeared at the start of cycle 4 that both 50 and 75% had the highest detected levels of ABA, whereby the end, detected levels dropped by over half, 800 pmol/mL to 100 pmol/mL and 1800 pmol/mL to 900pmol/mL respectively. In all cases, the 75% recycle rate maintained the highest concentration detected. Between cycles 1 and 4, the start of 25% was significant as was between the beginning and end of cycle 1, 50% and cycle 4, 75% ($P \leq 0.5$).

3.2.2 Pellet Fraction Hormone levels

In terms of the total CKs for the pellet, greater levels of increase towards the end of the cycle were observed in higher recycling rates (50% and 75%). From both Figures 18 and 20, it is clear that increasing the recycling rate and recycling duration, all forms of iP were highly detected along with an increase in NT as well as MET forms. Interestingly, in this fraction, there was a slight decrease in cZ types. Within the pellet fraction, total detected CK levels averaged ~1000 as opposed to ~10,000 pmol/mL in the supernatant.

Total cytokinin level for pellet

Total CK levels vary between recycling rates as shown in Figure 18A & B. Between the beginning and end of cycle 1, CK total levels increased with increased recycling rate (Figure 18, Panel A). Within the start of cycle 1, 0, 25, and 50% recycling rates were comparable at ~800 pmol/mL. The 75% rate showed the highest levels of CKs of just over 1000 pmol/mL. Finishing cycle 1, while all levels increased, the increases were highest for the 0 and 50% rates. From the beginning to the end of cycle 1, there was little change between total CK levels found in the 75% recycling rate. By cycle 4, Figure 18B, levels begin with a similar trend to cycle 1 with similar CK levels detected for all rates. By the end, the 25, 50, and 75% rates increased, with 50% having the highest total levels detected followed closely by 75% (Figure 20). Overall, total CKs, levels increased from the beginning to end in higher recycled rates such that higher recycled rates accrued more CKs under longer culturing times.

CK types within the pellet

The iP type highly dominated the pellet fraction in both cycles 1 and 4 and all recycled rates (Figure 18C & D and Figure 20). Although levels did not consistently increase with increased recycled rate, levels of iP were higher in the later recycled rates 50% and 75% by the end of each cycle (cycle 1, ~900 pmol/mL and cycle 4, 1200 pmol/mL) due to the abundance of iPNT ($P \leq 0.5$) counterbalanced with an overall reduction in iPR ($P \leq 0.5$) (Figure 18C and D & Tables 10 & 11, Appendix I). Overall, cZ types decreased subtly due to decreased cZ ($P \leq 0.5$) across all recycled rates ~100 pm/mL in cycle 4 (Figure 18C & D). The 50% recycle rate showed the most dramatic increase in detected levels followed by 75% due to the increase in iP types (Figure 18C, & D). The main iP CK type was iPNT followed by iPR. While there was a decrease in cZ, there was a distinct increase in cZNT.

CK forms within the pellet

In contrast to the supernatant fraction, the majority of the CKs present in the pellet were NT (~600 pmol/mL) followed by FB (~200 pmol/mL) and RBs (~100 pmol/mL) forms (Figure 18, E & F). Although higher levels of METs (~200 pmol/mL) were detected within the higher recycling rates 50 ($P \leq 0.5$) and 75% ($P \leq 0.5$), this was strictly due to later cycle abundance of 2MeSiP at the end of cycle 4 as at the beginning of the cycle; levels are ~30 pmol/mL (Figure 18, E & F). Within the pellet fraction, all forms were detected with similar profiles with a few exceptions. Levels were heavily dominated by NTs as they increased by the end of both cycles 1 and 4 and was closely followed by FB forms (Figure 18, E & F). While at the end of cycle 1, this trend was also observed, but, by cycle 4 end, METs became the highest form detected then FB and RB respectively (Figure 18, E & F). Of the MET CKs, 2MeSiP was reduced between the beginning and end of cycle 1, whereas it increased between the beginning and end of cycle 4 for 25, 50 ($P \leq 0.5$) and 75% ($P \leq 0.5$) recycled rates (Figure 18, C and D & Tables 10 & 11, Appendix I).

4. Discussion

Creation of sustainable biofuels, biofertilizers, waste conversion metrics, and providing alternative nutrient sources for both humans and animals are all direct applications of the commercial algal industry (Huntley *et al.*, 2015, Hnain, Cockburn, & Lefebvre and 2011, Borowitzka, 2013). This interest in finding new alternative microorganism sources to fulfill our current global food issues, invites opportunities to adjust current industrial practices with vested interest in sustainability and product development. Modernizing the algae industry, with focus on food product development in environmentally conscious ways, is one solution to address current nutritional demands. *E. gracilis* is a robust microalga able to adapt to survive varied growth-related conditions like pH and light conditions making it a candidate species to explore other further growth-related stressors. Re-purposing spent media as a growth media is poorly understood, however, it is a potential factor in financial savings and industrial scalability. Research to define the underlying growth characteristics and hormone network involved during used nutrient conditions, would further substantiate its use in many industrial applications and uncover the biological responses underlying the ability of Euglena to acclimate in suboptimal growth conditions

Illustrating a complex profile of hormone balance between CKs and ABA, this study presents a unique lens to uncover the roles of CKs outside of the plant taxa. This is in support of current literature that finds the dominance of the tRNA degradation pathway with main production of cZ and iP CKs followed by low levels of both tZ and DZ (Stirk *et al.*, 2003, Ördög *et al.,* 2004, Jirásková *et al*., 2009 & Stirk *et al*., 2013). The presence of active CK types like cZ and iP, and their rapid utilization and conversion from NT forms suggests that CKs are involved in maintaining cell growth. The full role of CKs and corresponding enzymes involved in hormone signaling, however, have yet to be established. Perhaps their role as inter-kingdom signaling molecules (Spíchal, 2012) is more inclusive of different roles they may play in other organisms. Therefore in this thesis, cytokinins are posed to be redefined as protist-derived cytokinins (PDCKs) to lead to a better understanding of their role in microalgae physiology and the cross-functionality of cis-zeatin CKs.

This research was the first assessment of *E. gracilis* hormone profiles under varied recycled organic media conditions with no supplementation. Under these conditions, it was expected that ABA was inhibitory to growth and CKs promoted growth. This research showed that ABA was inhibitory and further revealed that CKs do not promote growth. These results showed the CKs rather play a role in slowing and delaying growth under these suboptimal conditions, contrary to Noble *et al*, (2014), that CKs promote growth in *E. gracilis.* While not optimal for growth as shown by macro- characteristic effects like cell physiology, recycling *E. gracilis* medium is a viable means for overall growth, however, the degree of recycling should be carefully considered (25% or less) to maintain cell viability. Interestingly, while cell physiology seemed to decline as recycling rate increased, it was revealed that both CK and ABA hormone levels increase with increased recycling, indicating that hormones are important under extreme recycling regimes.

4.1 CK biosynthesis, forms and potential activity

4.1.1 *E. gracilis* synthesizes CKs via the tRNA-degradation pathway

CK types can vary based on environmental conditions, tissue type or developmental stage (Schafer *et al*., 2016)). A dominance of a particular CK type can also indicate the activation of a particular biosynthetic pathway. For example, systems are typically more active in the MEP pathway (*de novo*) when dominated by tZ types whereas those dominated by the MVA (tRNA degradation) pathway often have more cZ CKs. cZ CK types and related conjugates were the abundant types found among all experiments including varied organic media recirculation of heterotrophically grown *E. gracilis.* This was followed by iP and DZ types which were next most abundant. Methyl-thiol CKs were also detected, and these are also proposed to be synthesized by the MVA pathway which demonstrates the significance of CK methyl-thiol derivative production and the use of the tRNA degradation pathway (Morrison *et al.,* 2015 & Zi, *et al.,* 2017). Though the tRNA degradation pathway is the only widely accepted source of cZ, *E. gracilis* is capable of also synthesizing CKs using the MEP pathway to produce tZ and its conjugates. This prevalence of cZ over tZ types suggested by the hormone data corresponds well with findings within other microalgae which have higher reported cZ levels (Emery *et al.,* 1998, Jirásková *et al*., 2009, Stirk et al., 2003, 2010, Yonekura-Sakakibara, 2004, Kiseleva, Tarachovskaya and Shishova, 2012 & Noble *et al.*, 2014).

4.1.2 cZ and iP CK type activity profile balance

The quantities, forms and types of CKs present are controlled by the biosynthesis pathways. In the case of *E. gracilis*, this involves tRNA degradation along with possible conjugation and deconjugation between active and inactive CK forms. There is also degradation to inactive forms, as well as potential transportation or translocation out of the cell (Auer, 1997, Kim, Filtz & Proteau, 2004 & Sakakibara, 2006). With heavy production of iP and cZ type CKs, this study highlighted that these types of CKs fluctuate and thereby may adjust hormone activity that is connected to increased culturing time. Overall, there was a trend towards decreased iP types and an increase in cZ types throughout culturing time in the supernatant fraction. Among the pellet fraction, it went the opposite way and there was a reduction of cZ types and increase in iP types. The balance of cZ and iP CKs between supernatant and pellet environments in *E. gracilis* agrees with results of other microalgae, which indicates active biosynthesis and implies there is a capability to synthesize and excrete or retain particular CKs into the surrounding environment to control growth (Ördög et al. 2004, Jirásková *et al*., 2009 & Xinyi, Crofcheck, and Crocker, 2016). Gajdos *et al.,* (2011) showed that proportions of isomers differ greatly during the lifespan of *Arabidopsis,* Maize, annual rye grass and chickpea associated with growth-limiting conditions resulting from internal and/or external cues. Perhaps cZ CKs are responsible for the maintenance of CK activity necessary for survival and recovery from restrictive conditions. Therefore, the balance of cZ with other CK types like iP, is likely important in response to stress conditions. It may be also via nutrient recycling that cZ was found to be higher in growth deficient environments. The cZ and iP CK type balance is also indicative of a tRNA dominant system. As biomass increased, cZ and iP may induce more long-term effects. For example, iP may be taken up by the cells and converted to iPR and iPNT to be further utilized later, rather than being involved in a short-term effect (Stirk *et al.,* 2013).

4.1.3 Recycling nutrients causes switches in CK Forms and activity profile

In general, within the supernatant fraction, there were higher RBs observed at the beginning of the cycle, with the GLUC form becoming abundant at the end of the cycles. The accumulation of GLUCs indicates that *E. gracilis* is able to deactivate CKs into GLUC forms. As RBs are thought to be an intermediate form to making the most active FBs, the increase at the beginning of growth coincides with the potential of converting to active CKs under favorable growth conditions (Stirk *et al.*, 2013). The high amounts of GLUCs within the supernatant fraction could be due to many reasons. First, as GLUCs are the largest form of CKs found, the presence of these molecules outside of the cell indicates a potential for an unknown secretory pathway via a vesicle exocytosis pathway – which may selectively and actively secrete the glucoside conjugates (Satiat-Jeunemaitre and Hawes, 1993 & Bajguz and Piotrowska, 2009). An alternative to detection outside of the cells would occur through an uncharacterized transporter to move the metabolites into the external environment. Or, there may be an exogenous enzyme allowing conjugation such that when FB ribosides are secreted they are conjugated for use later in the growth cycle, but this is currently not validated.

In the pellet fraction, there was a buildup of NT matched by a decrease in FB. As NTs are abundant and first produced in the pellet (where biosynthesis occurs), extremely low detected levels of NTs in the supernatant corresponds to active biosynthesis within the pellet fractions. Also, with the increase of NTs and decrease in other forms, it suggests that NTs are selectively retained (unable to be transported) by whatever unknown carriers may be transporting smaller CKs. FBs were detected throughout the entirety of recycling; these forms are typically the most biologically active forms that are used quickly or conjugated to an alternative form. Interestingly, within the pellet fraction there was later cycle inclusion of METs which were higher in heavy recycling conditions. This later incorporation of METs may indicate that these forms of CK are useful to *E. gracilis*, however, the function or purpose of METs in *E. gracilis* is unknown. While documented in prokaryotes in high levels along with iP derivatives, this system accumulated METs within the pellet, a result that was similar to a study of *Rhizobium* bacteria (Kisiala et al., 2013); however, functional relevance of METs in bacteria remains unclear. METs have been discovered in other organisms like mammalian canine samples, however their roles remain obscure regardless of the organism (Seegobin *et al.*, 2018).

Early accumulation in both the supernatant and pellet may also be a factor of CK activity profile detection in *E. gracilis*. This surge of CKs at the beginning of the cycle may point towards a growth-defense trade-off as higher levels at the beginning and lower levels at the end to reduce cell division under nutrient limiting conditions. This could explain why RBs and NTs are high at the beginning for conversion to active FBs and there is a subsequent buildup of storage form CKs near the end. As nutrition and CK content are closely related (Kuiper et al., 1989), perhaps under recycled conditions, *E. gracilis* regulates a switch of CK forms to best adapt to the changing stressful nutrient conditions via a complicated network of hormone signaling like quorum sensing in bacteria.

4.1.4 High levels of hormones correspond with high recycling rates

Hormone analyses show changes in CK profiles in culture supernatant and pellet that indicate microalgae can process different CK types in either fraction. It was hypothesized that a higher recycle rate would negatively affect culture growth, such that in higher recycling rates there would be a decrease in CK activity profiles (growth promotion) and increase in ABA levels (stress regulation). In this thesis, higher recycling of media showed increased levels of both CK and ABA– particularly in the 75% fraction. Altogether, the strong impact of stress on cell growth under recycled conditions might result from the necessity of the combined activities of both hormone pathways; ABA and CKs. Therefore, it may be apt to hypothesize that under recycled conditions, *E. gracilis* cells may use quorum sensing – a series of chemical signals coordinated as a response to population density to regulate hormonal balance under these conditions (Zhou *et al.,* 2016).

In the microbial world, quorum sensing is a common means of cell-to-cell communication. Much like CK hormones, quorum sensing is mediated by low molecular weight molecules that can move across membranes and accumulate in targeted places. CKs often create a nutrient sink to perform their action, where quorum sensing molecules amass in a dense environment where they are produced to regulate growth at high densities once a threshold is met, thereby causing a coordinated response (Proust, *et al.,* 2011). As identified by Chi, *et al*., 2017, cross-kingdom quorum sensing signaling between bacteria and host confer indirect biological functions like slowed growth and other physiological functions (Gambello and Iglewski, 1991), production of secondary metabolites and were involved in defense responses (Chi, *et al*., 2017). Perhaps then, ABA and CKs levels increased within the supernatant with higher recycling rates to signal other cells in defense to poor conditions and to slow growth, or that CKs may be secreted since *E. gracilis* is a single-celled organism that no longer requires the excess metabolites. Likely it is a combination of the two. Cooperatively through a complex – and not well understood process, CK and ABA stimulation, inhibition or absence of activity is important improve the ability of *E. gracilis* to cope with constantly changing environments, chiefly nutrient recycling.

4.2 Cell health

4.2.1 Absence and impact of ABA

ABA is thought to act as an inhibitory hormone. It is present often when nutrients are low (Nambara and Marion-poll, 2005 & Hauser, Waadt, and Schroeder, 2011) oppositely to CKs however, can also be present when cells are actively dividing during active biosynthesis, like CKs (Takezawa and Komatsu, 2011 & Noble *et al.,* 2014). As a hormone studied predominantly in plants and its affects during drought and saline stress, the model of *E. gracilis* offers a convenient unicellular model system for elucidating the potential role of ABA and the interrelationship of ABA to CK signaling and influence on growth under nutrient stress.

In this study, compared to the media blank, ABA concentrations were only detected in the supernatant fraction indicating these molecules are produced and secreted such that they are not held within the pellet fractions. In accordance with initial hypotheses – that ABA is inhibitory to CK, ABA was confirmed to be inhibitory to *E. gracilis* cells, as the levels increased with increasing recycling rates. It was further shown that ABA and CKs did not show an opposite trend as typically seen in higher plants; ABA levels reduce, CK levels increase, suggesting that *E. gracilis* may differ from regulatory hormonal communication in higher order plants (Hirsch, Hartung and Gimmler, 1989, Yokoya *et. al.*, 2010). This mechanism is indicative of a quorum-sensing which may also suggest that Euglena have the ability to secrete ABA into the surrounding environment and does so preferentially. Cells therefore may respond to nutrient stress by excreting the ABA into the media to initiate signaling events to surrounding cells (Romanenko, Kosakovskaya, and Romanenko, 2015, Lu and Xu, 2015, Chi, *et al.,* 2017 & Han, Zeng and Bartocci, 2018).

Considering the reported antagonistic relationship between CKs and ABA in microalgae (Lu *et al.*, 2014) it is also possible that CK production caused inhibition or the slowing of the cell cycle because of a potential quorum sensing like mechanism to balance the stressful conditions. By entering a “survival” mode, the cells could accumulate storage products like glucosides and potentially lipids to survive longer (Yanda *et al*, 2014).

4.2.2 Macro-characteristic effects

The influence of endogenously produced CKs and ABA and how these are impacted by recycled rate can lend to a better understanding of cell productivity and viability in *E. gracilis*. The identification of how these hormone profiles change and if the changes can be connected to growth parameters changes is novel for *E. gracilis*. Monitoring the growth and viability of these cells, therefore would be key to elucidate associated parameters linked to cell preservation. In this thesis, pH, morphology, glucose content and weight were analyzed as measures of cell viability.

pH reflects the acidity or alkalinity within a sample. This acts as a good determinant to see if, under recycled conditions, pH levels shift and correlate with changes in cell viability. Within this research, it was shown that 0 and 25% recycle rates maintain buffering capacity, while the higher recycled rates, 50 and 75% lost buffering capacity. With more recycling of nutrients, the surrounding environment became increasingly basic. pH changes could be caused by several reasons, temperature, CO_2, waste product accumulation, contamination etc. In this case, the medium became more basic suggesting maybe due to nutrient loss or buildup of hydroxide ions (Ratzke and Gore, 2018).

Morphology is a critical aspect of assessing cell health. Observing the cells directly affords the opportunity to detail cellular changes under varied conditions. In Table 2, cell stage and morphological description were used to assess health of *E. gracilis*. It was shown that higher recycle rates, particularly the 75% rate, negatively impacted cell health causing cells to cyst, burst, shrink and become non-motile. This type of change in morphology can be correlated to other changes like damaging effects of increasing pH, changes in hormone levels affecting cell survival, or recovery of biomass.

As glucose content can be a measure of metabolically active cells, it was important to track the use of glucose under recycled conditions. Cells under higher recycled rates (50 and 75%) and late cycle (cycle 4) cells use more sugar. This suggests that these cells are metabolically active and therefore need glucose for energy. Given the poor nutrient conditions of the heavy recycling, these conditions may also reflect that *E. gracil*is cells rely on increased levels of hormone molecules to cope with the changing environment.

Recovered supernatant residue and biomass was vital to compare nutrient recycling differences between treatments and to quantify hormone profiles. These results show that levels of biomass were fairly consistent also in agreeance with consistent cell counts. This was unexpected due to the distinct adverse morphological changes observed between the recycling regimes. Recovery of supernatant residues showed that the highest recycled rate, 75%, used less recycled media nutrients over time. It is possible to imply that medium recycling not only decreases nutrients available, but disrupts cell organization, metabolism and biosynthesis to adapt to conditions in alternative ways.

pH, morphology, glucose content and weight are parameters that are commonly monitored in cell culturing (Lowrey, Armenta and Brooks, 2016). While these parameters were monitored, this research looked at the unregulated effects of these parameters to track changes caused by fluctuating conditions. Using minimal processing during growth, these parameters further highlighted intricate variations caused by nutrient deprivation and altered nutrient profiles. These growth parameter changes reflect the dynamic work of hormone regulation, illuminating the potential use of these parameters to help detect hormone profile changes.

4.3 Conclusions

There is an emerging market for *E. gracilis*-derived products, reflected by the recent surge in microalgal cultivation for food products with emphasis on new companies specialized in the cultivation and commercialization of microalgae including *E. gracilis*. Profiling endogenous hormones and characterizing micro- and macro-characteristics ultimately will help, enhance, and guide industrial production. This thesis has illustrated results that both supported and refuted that hormones act solely as growth promoting agents. Under recycled conditions using an organic medium it was shown that:

1. Recycling *E. gracilis* culture medium can be used as a growth medium. Recycling medium however, is best under a 25% recycled to fresh medium ratio;
2. *E. gracilis* synthesizes CKs via the tRNA-degradation pathway;
3. *E. gracilis* cells increase in iP, iPR, iPNT under media recycling; upregulation of the iP pathway;
4. *E. gracilis* has high levels of hormones in higher recycling rates; and
5. *E. gracilis* cells do not retain Abscisic Acid – though they appear to make and export it.

Noble *et al.*, 2014, showed that CKs promoted culture growth of Euglena, this research showed that endogenous CKs do not promote growth and could not be used to overcome recycling media limitations. Industrial applications of this research, however, could lead to matching hormone data and modifying *E. gracilis* output to match the most productive hormone profile, ultimately garnering a heavy influence on the future of culturing conditions and techniques. In this thesis, it is notable to industry to adjust parameters to reduce glucoside abundance and to highlight the importance of iP and cZ types CKs during the growth process. This thesis also confirmed that under these conditions, a shorter harvest time of 3-day long cycles were as efficient as 4-day long cycles, increasing turnaround for industry scalability. To address effectively current bottlenecks associated with microalgal cultivation, a leap in both fundamental knowledge and technological applicability is necessary.

Adding to the research field of hormone profiling, this body of work was the first to scan 27 different types of CKs in addition to ABA, in *E. gracilis* cells and supernatants. Further fundamental knowledge of cZ hormone functions as a potential inter-kingdom molecule is needed.

4.4 Future Directions

Accordingly, it will be necessary to conduct life cycle assessments of a nutrient recycling regime to determine if the experimental outcomes translate to a viable method for commercial applications. Even more, the experimental data must be sourced from an optimized culture that is representative of outcomes expected at commercial-scale rather than simply flask-scale experiments. As it was shown that extreme recycling is not useful, experiments that investigate recycling at lower rates is essential for industrial viability. As a viable alternative to high percentage of recycling, direct supplementation to the recycled media could help target nutrient deprivation and alleviate culture growth challenges. It is also possible to use exogenous applications of hormones as a means in increase production with careful consideration to levels of dosing and forms or types used. Furthermore, co-culturing or genetic modification of *E. gracilis* with bacteria, or strict genetic modification of *E. gracilis* may be useful to also generate valuable products for industry use and should be considered.

5. References

Acién Fernández, F. G., García Camacho, F. & Chisti, Y. Photobioreactors: light regime, mass transfer, and scaleup. *Progress in Industrial Microbiology* **35,** (1999).

Albrecht, T. & Argueso, C. T. Should I fight or should I grow now? The role of cytokinins in plant growth and immunity and in the growth-defence trade-off. *Ann. Bot.* **119,** 1–11 (2017).

Allaf, M. M. Effect of plant hormones on the production of biomass and lipid in microalgae. *N/a* 109 (2013).

Archibald, J.M. The puzzle of plastid evolution. *Current Biology*. **19**(2), 81-88 (2009).

Auer, C. A. Cytokinin conjugation: recent advances and patterns in plant evolution. *Plant Growth Regul.* 17–32 (1997).

Bajguz, A. & Piotrowska, A. Phytochemistry Conjugates of auxin and cytokinin. *Phytochemistry* **70,** 957–969 (2009).

Beacham, T. A., Sweet, J. B. & Allen, M. J. Large scale cultivation of genetically modified microalgae: A new era for environmental risk assessment. *Algal Res.* **25,** 90–100 (2017).

Benson, A. A. & Calvin, M. The Path of Carbon in Photosynthesis. *Oxford Journals* **I,** 63–68 (1949).

Blanc, G. *et al.* The Chlorella variabilis NC64A Genome Reveals Adaptation to Photosymbiosis, Coevolution with Viruses, and Cryptic Sex. *Plant Cell* 22, 2943–2955 (2010).

Bleakly, Stephen and Hayes, M. Algal Proteins: Extraction, Application, and Challenges Concerning Production Stephen. *J. Foods* 1–34 (2017).

Bradley, P.M. Plant hormones do have a role in controlling growth and development of algae. *J Phycol*. **27,** 317–32 (1991).

Brantes, L., Mendes, B. & Vermelho, A. B. Allelopathy as a potential strategy to improve microalgae cultivation. *Biotechnol. Biofuels* **6,** 1 (2013).

Brien, J. A. O. & Benková, E. Cytokinin cross-talking during biotic and abiotic stress responses. **4,** 1–11 (2013).

Bumbak, F., Cook, S., Zachleder, V., Hauser, S. & Kovar, K. Best practices in heterotrophic high-cell-density microalgal processes: Achievements, potential and possible limitations. *Applied Microbiology and Biotechnology* **91,** 31–46 (2011).

Buetow, D. E., Gottfried, C. & Van, A. Euglena. *Encycl. Life Sci.* 1–5 (2011).

Burlew, J.S. Algal Culture: From Laboratory to Pilot Plant (Publication No. 600). Washington DC: Carnegie Institution of Washington. (1953).

Butler, C. cis-Cytokinins from the tRNA-degradation pathway impact the phenotype and metabolome of Arabidopsis thaliana: evidence from AtIPT2 and AtIPT9 null mutants. (2019).

Chen, F. High cell density culture of microalgae in heterotrophic growth. *Trends in Biotechnology* 14, 421–426 (1996).

Chi, W. *et al.* Quorum sensing of microalgae associated marine Ponticoccus sp. PD - 2 and its algicidal function regulation. *AMB Express* **7**, 1–10 (2017).

Cook, J.R. The Cultivation and Growth of Euglena. *The Biology of Euglena*, **1,** 243–314. (1968).

Cowan, A.K., & Rose, P.D. Abscisic Acid Metabolism in Salt-Stressed Cells of Dunaliella salina: Possible Interrelationship with β-Carotene Accumulation. *Plant Physiol*. 97, 798–803 (1991).

Davies, P. J. The Plant Hormones : Their Nature, Occurrence, and Functions. (2014).

Discart, V., Bilad, M. R., Marbelia, L. & Vankelecom, I. F. J. Bioresource Technology Impact of changes in broth composition on Chlorella vulgaris cultivation in a membrane photobioreactor (MPBR) with permeate recycle. *Bioresour. Technol.* 152, 321–328 (2014).

Doucha, J. & Lívanský, K. Production of high-density Chlorella culture grown in fermenters. *J. Appl. Phycol.* 24, 35–43 (2012).

Emery, R. J. N., Ma, Q. & Atkins, C. A. The Forms and Sources of Cytokinins in Developing White Lupine Seeds and Fruits. Plant Physiol. 123, 1593–1604 (2000).

Emery, R. J. N., Leport, L., Barton, J. E., Turner, N. C. & Atkins, C. A. cis-Isomers of Cytokinins Predominate in Chickpea Seeds throughout Their Development 1. *Plant Physiol.* 117, 1515–1523 (1998).

Evans, L.V., & Trewavas, A.J. Is Algal Development Controlled by Plant Growth Substances? *J Phycol.* **27**, 322– 326 (1991).

Farooq, W., Suh, W. I., Park, M. S. & Yang, J. Water use and its recycling in microalgae cultivation for biofuel application. *Bioresour. Technol.* 184, 73–81 (2014).

Farrow, S. C. & Emery, R. J. N. Concurrent profiling of indole-3-acetic acid, abscisic acid, and cytokinins and structurally related purines by high-performance-liquid-chromatography-tandem electrospray mass spectrometry. *Plant Methods* **8,** 1–17 (2012).

Feng Jian, Shi Yiting, Yang Shuhau, Z. J. *Hormone Metabolism and Signaling in Plants - Cytokinins*. (2017).

Flachowsky, G., Meyer, U. & Südekum, K. Land Use for Edible Protein of Animal Origin — A Review. *Animals* **7,** 1–19 (2017).

Fret, J. *et al.* Reuse of rejuvenated media during laboratory and pilot-scale cultivation of Nannochloropsis sp. *Algal Res.* **27,** 265–273 (2017).

Gajdos, S. *et al.* Distribution, biological activities, metabolism, and the conceivable function of cis -zeatin-type cytokinins in plants. *J. Exp. Bot.* **62,** 2827–2840 (2011).

Gambello, M. J. & Iglewski, B. H. Cloning and Characterization of the Pseudomonas aeruginosa lasR Gene, a Transcriptional Activator of Elastase Expression. *J. Bacteriol.* 3000–3009 (1991).

Gissibl, A., Sun, A., Care, A., Nevalainen, H. & Sunna, A. Bioproducts From Euglena gracilis: Synthesis and Applications. *Front. Bioeng. Biotechnol. Rev.* **7,** 1–16 (2019).

Graham, L.E. (1993) Origin of Land Plants. pp 287. New York: John Wiley and Sons

Gomez, M. P., Harris, J. B. & Walne, P. L. Studies of *Euglena gracilis* in aging cultures. I. light microscopy and cytochemistry. *Br. Phycol. J.* **9,** 163–174 (1974).

Georgianna, D. R. & Stephen, P. Exploiting diversity and synthetic biology for the production of algal biofuels. *Nature* **488,** 329–335 (2012).

Gualtieri, P. Morphology of photoreceptor systems in microalgae. *Micron* **32,** 411–426 (2001).

Gururani, M. A., Mohanta, T. K. & Bae, H. Current Understanding of the Interplay between Phytohormones and Photosynthesis under Environmental Stress. 19055–19085 (2015).

Hadj-Romdhane, F., et al. Development and validation of a minimal growth medium for recycling Chlorella vulgaris culture. *Bioresour. Technol.* **123,** (2012).

Hadj-Romdhane, F., et al. The culture of Chlorella vulgaris in a recycled supernatant: Effects on biomass production and medium quality. *Bioresour. Technol.* **132,** 285–292 (2013).

Han, X., Zeng, H. & Bartocci, P. Phytohormones and Effects on Growth and Metabolites of Microalgae: A Review. *Fermentation* **4,** 1–15 (2018).

Hartung, W., & Gimmler, H. A stress physiological role for abscisic acid (ABA) in lower plants. *Progress in Botany*. 55, 157–173 (1994).

Hussain, S., *et al*. Exogenous application of abscisic acid may improve the growth and yield of sunflower hybrids under Drought. *Pak. J. Agri. Sci.* 51, 49–58 (2014).

Hauser, F., Waadt, R. & Schroeder, J. I. Evolution of Abscisic Acid Synthesis and Signaling Mechanisms Review. *Curr. Biol.* 21, 346–355 (2011).

Hirose, N., Takei, K., Kuroha, T., Kamada-nobusada, T. & Hayashi, H. Regulation of cytokinin biosynthesis, compartmentalization and translocation. 59, 75–83 (2008).

Hirsch, R., Hartung, W. & Gimmler, H. Abscisic Acid Content of Algae under Stress. *Bot. Acta* 102, 326–334 (1989).

Hiscox, J.D., & Israelstam, G. F. A method for the extraction of chlorophyll from leaf tissue without maceration. *Can. J. Bot* **57,** 1332–1334 (1979).
Hlavova, M., Turoczy, Z. & Bisova, K. Improving microalgae for biotechnology — From genetics to synthetic biology. *Biotechnol. Adv.* 33, 1194–1203 (2015).

Hnain, A. K., Cockburn, L. M. & Lefebvre, D. D. Microbiological processes for waste conversion to bioenergy products: Approaches and directions. *Environ. Rev.* 19, 214–237 (2011).

Hosek, P., Hoyerova, K., Nagavalli, K. S., Dobrev, P. I, Zahajska, L., Filepova, R., Motyka, V., Muller, K., and Kaminek, M. Distinct metabolism of *N-glucosides* of isopentenyladenine and *trans*-zeatin determines Cytokinin metabolic spectrum in Arabidopsis. *New Phytologist.* **225**, 2423-2438 (2019).

Hyams, J. S. The Euglena paraflagellar rod: structure, relationship to other flagellar components and preliminary biochemical characterization. *Cell Sci* **55,** 199–210 (1982).

Ilavarasi, A., Mubarakali, D., Praveenkumar, R., Baldev, E. & Thajuddin, N. Optimization of Various Growth Media to Freshwater Microalgae for Biomass Production. *Biotechnology* **10,** 540–545 (2011).

Inui, H., Ishikawa, T., and Tamoi, M. Wax Ester Fermentation and Its Application for Biofuel Production. *Adv. Exp. Med. Biol.* **979,** 269–283 (2017).

Jarchow-Choy, S. K., Koppisch, A. T. & Fox, D. T. Synthetic Routes to Methylerythritol Phosphate Pathway Intermediates and Downstream Isoprenoids. *Curr. Org. Chem.* **18**, 1050–1072 (2014).

Jameson, P.E. Plant hormones in the algae. *Progress in Phycological Research*. 239–279. (1993).

Jiraskova, D. *et al.* HIGH-THROUGHPUT SCREENING TECHNOLOGY FOR MONITORING PHYTOHORMONE PRODUCTION IN MICROALGAE. *J. Phycol.* **45,** 108–118 (2009).

Kamada-nobusada, T. & Sakakibara, H. Phytochemistry Molecular basis for cytokinin biosynthesis. *Phytochemistry* 70, 444–449 (2009).

Kasahara, H. *et al.* Distinct Isoprenoid Origins of cis- and trans-Zeatin Biosyntheses in Arabidopsis. *J. Biol. Chem.* 279, 14049–14054 (2004).

Keeling, P. J. & Inagaki, Y. A class of eukaryotic GTPase with a punctate distribution suggesting multiple functional replacements of translation elongation factor 1 α. **101,** 15380–15385 (2004).

Kenrick, P. & Crane, P.R. The Origin and Early Evolution of Plants on Land. *Nature.* **389,** 33-39 (1997).

Kieber, J. J. & Schaller, G. E. *Cytokinins*. *American Society of Plant Biologists* (2014).

Kieber, J. J. & Schaller, G. E. Cytokinin signaling in plant development. *Development* **145,** 1–7 (2018).

Kim, D., Filtz, M. R. & Proteau, P. J. The Methylerythritol Phosphate Pathway Contributes to Carotenoid But Not Phytol Biosynthesis in Euglena gracilis. *J. Nat. Prod.* **67,** 1067–1069 (2004).

Kings, A. J., Raj, R. E., Miriam, L. R. M. & Visvanathan, M. A. Growth studies on microalgae Euglena sanguinea in various natural eco-friendly composite media to optimize lipid productivity. *Bioresour. Technol.* **244,** 1349–1357 (2017).

Kisiala, A., Kambhampati, S., Stock, N. L., Aoki, M. & Emery, R. J. N. Quantification of Cytokinins using High-Resolution Accurate-Mass Orbitrap Mass Spectrometry and Parallel Reaction Monitoring (PRM). *Anal. Chem.* 1–12 (2019).

Kisiala, A., Laffont, C., Emery, R. J. N. & Frugier, F. Bioactive Cytokinins Are Selectively Secreted by Sinorhizobium meliloti Nodulating and Nonnodulating Strains. *Am. Phytopathol. Soc.* **26,** 1225–1231 (2013).

Kiseleva, A. A., Tarachovskaya, E. R. & Shishova, M. F. Biosynthesis of phytohormones in algae. *Russ. J. Plant Physiol.* **59,** 595–610 (2012).

Kozlova, T. A., Hardy, B. P., Krishna, P. & Levin, D. B. Effect of phytohormones on growth and accumulation of pigments and fatty acids in the microalgae Scenedesmus quadricauda. *Algal Res.* 27, 325–334 (2017).

Kuiper, D. *et al.* Cytokinin concentration in relation to mineral nutrition and benzyladenine treatment in Plantago major ssp. pleiosperma. *Physiol. Plant.* **75**, 511–517 (1989).

Lee, E., Jalalizadeh, M. & Zhang, Q. Growth kinetic models for microalgae cultivation: A review. *Algal Res.* **12,** 497–512 (2015).

Leedale, G. F. Pellicle structure in Euglena. *Eur. J. Phycol.* **2,** 291–306 (1964).

Leliaert, F. *et al.* Phylogeny and Molecular Evolution of the Green Algae Phylogeny and Molecular Evolution of the Green Algae. *CRC. Crit. Rev. Plant Sci.* **31,** 1–46 (2012).

Lin, S. *Algal Culturing Techniques*. *Journal of Phycology* 41, (2005).

Liu, L., Pohnert, G. & Wei, D. Extracellular Metabolites from Industrial Microalgae and Their Biotechnological Potential. *Mar. Drugs* **14,** 1–19 (2016).

Loftus, S. E. & Johnson, Z. I. Cross-study analysis of factors affecting algae cultivation in recycled medium for biofuel production. *Algal Res.* **24,** 154–166 (2017).

Lomin, S. N., Krivosheev, D. M., Steklov, M. Y. & Arkhipov, D. V. Plant membrane assays with cytokinin receptors underpin the unique role of free cytokinin bases as biologically active ligands. **66,** 1851–1863 (2015).

Lowrey, J., Armenta, R. E. & Brooks, M. S. Nutrient and media recycling in heterotrophic microalgae cultures. *Applied Microbiology and Biotechnology* (2016).

Lu, Y. & Xu, J. Phytohormones in microalgae: a new opportunity for microalgal biotechnology? *Trends Plant Sci.* **20,** 273–282 (2015).

Markou, G., Vandamme, D. & Muylaert, K. Microalgal and cyanobacterial cultivation: The supply of nutrients. *Water Res.* 65, 186–202 (2014).

Martinez, F. & Orus, M. I. Interactions between Glucose and Inorganic Carbon Metabolism in Chlorella vulgaris Strain UAM 1011. **95,** 1150–1155 (1991).

Milano, P. Model for Cell Growth in Batch Bioreactors. (2010).

Mok, M. C., Martin, R. C. & Mok, D. W. S. Cytokinins: Biosynthesis, Metabolism and Perception. *Vitr. Cell. Dev. Biol* 36, 102–107 (2000).

Mooney, P.A., & Van Staden, J. Algae and cytokinins. *J Plant Physiol* **123,** 1–21 (1986).

Morais, M. G. De, Vaz, S., Morais, E. G. De, Alberto, J. & Costa, V. Biologically Active Metabolites Synthesized by Microalgae. *Biomed Res. Int.* 1–16 (2015).

Morrison, E.N., Emery, R.J.N., Saville, B.J. Phytohormone involvement in the Ustilago maydis- Zea mays pathosystem: relationships between abscisic acid and cytokinin levels and strain virulence in infected cob tissue. *PLoS ONE* (2015).

Morrison, E. N., Emery, R. J. N. & Saville, B. J. Fungal derived cytokinins are necessary for normal Ustilago maydis infection of maize. *Plant Pathol.* 66, 726–742 (2017).

Nambara, E. & Marion-poll, A. Abscisic Acid Biosynthesis and Catabolism. *Annu. Rev. Plant Biol.* **56,** 165–185 (2005).

Noble, A., Kisiala, A., Galer, A., Clysdale, D. & Emery, R. J. N. *Euglena gracilis* (Euglenophyceae) produces abscisic acid and cytokinins and responds to their exogenous application singly and in combination with other growth regulators. *Eur. J. Phycol.* **49,** 244–254 (2014).

Ogbonna, J. C. & Tanaka, H. Light requirement and photosynthetic cell cultivation – Development of processes for efficient light utilization in photobioreactors. *J. Appl. Phycol.* **12,** 207–218 (2000).

O'Neill, E. C. *et al.* The transcriptome of *Euglena gracilis* reveals carbohydrate and natural product biochemistry. *R. Soc. Chem.* 1–13 (2015).

Ord, G., Cameron, I., & Fensom, D. The effect of pH and ABA on the hydraulic conductivity of Nitella membranes. *Candian J. Bot.* **55,** 1–4 (1977).

Ordog, V. *et al.* Screening microalgae for some potentially useful agricultural and pharmaceutical secondary metabolites. *J. Appl. Phycol.* **16,** 309–314 (2004).

Pachapur, V. L., Brar, S. K., Le Bihan, Y. & Buelna, G. Alternate green approach of spent media utilization for hydrogen and for lipid production. *Int. J. Hydrogen Energy* **42,** 5832–5839 (2017).

Passarelli, V., Barsanti, L., Evangelista, V., Frassanito, A. M. & Gualtieri, P. *Euglena gracilis* photoreception interpreted by microspectroscopy. *Eur. J. Protistol.* **39,** 404–409 (2003).

Perez-Garcia, O., Escalante, F. M. E., De-Bashan, L. E. & Bashan, Y. Heterotrophic cultures of microalgae: Metabolism and potential products. *Water Research* **45,** 11–36 (2011).

Pils, B., Heyl, A., Pils, B. & Heyl, A. Unraveling the Evolution of Cytokinin Signaling. *Nature.* **151,** 782–791 (2018).

Price, K. & Farag, I. H. Resources Conservation in Microalgae Biodiesel Production. *Int. J. Eng. Tech. Res.* **1,** 49–56 (2014).

Priyadarshani, I. & Rath, B. Commercial and industrial applications of microalgae – A review. *J. Algal Biomass* **3,** 89–100 (2012).

Proust, H. *et al.* Strigolactones regulate protonema branching and act as a quorum sensing-like signal in the moss Physcomitrella patens. *Development* **1539,** 1531–1539 (2011).

Quesnelle, P.E. and Emery, R.J.N. cis-Cytokinins That Predominate in Pisum sativum during Early Embryogenesis will Accelerate Embryo Growth in Vitro. *Canadian Journal of Botany.* 85, 91-103. (2007).

Raleigh, V. S. World population and health in transition. *Br. Med. J.* **319,** 981–984 (1999).Rashid, N., Rehman, M. S. U. & Han, J. I. Recycling and reuse of spent microalgal biomass for sustainable biofuels. *Biochem. Eng. J.* **75,** 101–107 (2013).

Ratzke, C. & Gore, J. Modifying and reacting to the environmental pH can drive bacterial interactions. *PLOS Biol.* **16,** 1–20 (2018).

Razu, M. H. et al. Heterotrophic Growth of Micro Algae. *Recent Adv. Microalgal Biotechnol.*1–20(2016).

Rodolfi, L., Zittelli, G. C., Barsanti, L., Rosati, G. & Tredici, M. R. Growth medium recycling in Nannochloropsis sp. mass cultivation. *Biomol. Eng.* 20, 243–248 (2003).

Rolc, K.I., Hradecka, J.V. and Stirk, W. A. Endogenous cytokinins, auxins and abscisic acid in Ulva fasciata (Chlorophyta) and Dictyota humifusa (Phaeophyta): towards understanding their biosynthesis and homoeostasis. **44,** 231–240 (2009).

Romanenko, Kateryna, Kosakovskaya, I. V. & Romanenko, P. A. Phytohormones of Microalgae: Biological Role and Involvement in the Regulation of Physiological Processes. Pt I. Auxins, Abscisic Acid, Ethylene. *Int. J. Algae* **17,** 275–289 (2015).

Romanov, G. A., Lomin, S. N. & Schmu, T. Biochemical characteristics and ligand-binding properties of Arabidopsis cytokinin receptor AHK3 compared to CRE1 / AHK4 as revealed by a direct binding assay. **57,** 4051–4058 (2006).

Rösch, C., Skarka, J. & Wegerer, N. Materials flow modeling of nutrient recycling in biodiesel production from microalgae. *Bioresour. Technol.* 107, 191–199 (2012).

Sakakibara, H. Cytokinins: Activity, Biosynthesis, and Translocation. *Annu. Rev. Plant Biol.* 57, 431–439 (2006).

Santner, A., Calderon-villalobos, L. I. A. & Estelle, M. Plant hormones are versatile chemical regulators of plant growth. *Nat. Chem. Biol.* 5, 301–307 (2009).

Satiat-Jeunemaitre, B. & Hawes, C. Insights into the secretory pathway and vesicular transport in plant cells. *Biol Cell* **79**, 7–15 (1993).

Schäfer, M. *et al.* The role of cis-zeatin-type cytokinins in plant growth regulation and mediating responses to environmental interactions. *J. Exp. Bot.* **66**, 4873–4884 (2016).

Schmacht, M., Lorenz, E., Stahl, U. & Senz, M. Medium optimization based on yeast 's elemental composition for glutathione production in Saccharomyces cerevisiae. *J. Biosci. Bioeng.* 1–7 (2016).

Schmidt, M. & Wilhelm, C. Green Algae. *Struct. Basis Biol. Energy Gener. Adv. Photosynth. Respir.* **33,** 309–333 (2014).

Schmülling, T. Cytokinin. *Encycl. Biol. Chem.* 1–7 (2004).

Schwartzbach, S. D. Euglenoid flagellates: A multifaceted biotechnology platform. *J. Biotechnol.* 1–11 (2014).

Schwender, J., Gemunden, C. & Lichtenthaler, H. Chlorophyta exclusively uses the 1-deoxyxylulose 5-phosphate/2-C-methylerythritol 4-phosphate pathway for the biosynthesis of isoprenoids. *Planta* **212**, 416–423 (2001).

Seegobin, M. *et al.* Canis familiaris tissues are characterized by different profiles of cytokinins typical of the tRNA degradation pathway. *FASEB* **32,** 1–7 (2018).

Sims, D.A., & Gamon, J.A. Relationships between leaf pigment content and spectral reflectance across a wide range of species, leaf structures, and developmental stages. Remote Sensing of Environment **81**, 337-354 (2002).

Singh, J. & Saxena, R. C. An Introduction to Microalgae: Diversity and Significance. *Elsevier Inc* (2015).

Spíchal, L. Cytokinins - Recent news and views of evolutionally old molecules. *Funct. Plant Biol.* **39**, 267–284 (2012).

Spíchal, L. *et al.* Two Cytokinin Receptors of Arabidopsis thaliana, CRE1 / AHK4 and AHK3, Differ in their Ligand Specificity in a Bacterial Assay. **45,** 1299–1305 (2004).

Srivastave, L. Abscisic Acid. *Plant Growth and Development* 217–232 (2002).

Stirk, W.A, Novak, O., Strnad, M. Staden, J. Cytokinins in macroalgae. **41**, 13–24 (2003).

Stirk, W. A., and Van Staden, J. Flow of cytokinins through the environment. *Plant Growth Regul.* **62**, 101–116 (2010).

Stirk, Wendy. A., et al. Auxin and cytokinin relationships in twenty-four microalgae strains. *Phycol. Soc. Am.* 1–31 (2013).

Takei K, Yamaya T, Sakakibara H. Arabidopsis CYP735A1 and CYP735A2 encode cytokinin hydroxylases that catalyze the biosynthesis of trans-zeatin. J. Biol. Chem. **279**, 41866–72 (2004).

Takezawa, D. & Komatsu, K. ABA in bryophytes : how a universal growth regulator in life became a plant hormone? *J. Plant Res.* **124,** 437–453 (2011).

Tannreuther, George, W. Nutrition and Reproduction in Euglena. *Zool. Lab.* 367–383 (1922).

Tietz, A., Ruttkowski, U., Köhler, R. & Kasprik, W. Further Investigations on the Occurrence and the Effects of Abscisic Acid in Algae. 266, 259–266 (1989).

Tomaz, R. & Marina, D. Cytokinins and their Function in Developing Seeds. *Acta Chim. Solv.* 57, 617–629 (2010).

Tominaga, N., Takahata, M., & Tominaga, H. Effects of NaCl and KNO3 concentrations on the abscisic acid content of Dunaliella sp. (Chlorophyta). *Hydrobiologia.* 267, 163–168 (1993).

Trinh, C. T., Tran, T. H. & Bui, T. V. Effects Of Plant Growth Regulators On The Growth And Lipid Accumulation Of Nannochloropsis oculata (droop) Hibberd. *Int. Conf. Food Eng. Biotechnol.* **20017,** 1–9 (2017).

Valverde, F., Romero-campero, F. J., León, R. & Guerrero, M. G. New challenges in microalgae biotechnology. *Eur. J. Protistol.* **55,** 95–101 (2016).

Vigani, M. *et al.* Food and feed products from micro-algae: Market opportunities and challenges for the EU. *Trends Food Sci. Technol.* **42,** 81–92 (2015).

Willems, P. *et al.* Towards industrial products from microalgae. *Energy Environ. Sci.* 9, 3036–3043 (2016).

Wanless, I. R., Bryniak, N. & Fensom, D. S. The effect of some growth-regulating compounds upon electroosmotic measurements, transcellular water flow, and Na, K, and C1 influx in Nitella flexilis. *Can. J. Bot.* 51, 1055–1070 (1973).

Wasilewska, A., Vlad, F., Sirichandra, C., Redko, Y., Jammes, F., Valon, C., Freidit Frey, N., and Leung, J. An update on abscisic acid signaling in plants and more. *Molecular Plant* 1, 198–217(2008).

Xinyi, E., Crofcheck, C. & Crocker, M. Application of recycled media and algae-based anaerobic digestate in Scenedesmus cultivation. *J. Renew. Sustain. Energy* 8, (2016).

Yanda, Lu., *et al.* Antagonistic roles of abscisic acid and cytokinin during response to nitrogen depletion in oleaginous microalga Nannochloropsis oceanica expand the evolutionary breadth of phytohormone function. *Plant J.* **1,** 52–68 (2014).

Yang, J. *et al.* Life-cycle analysis on biodiesel production from microalgae: Water footprint and nutrients balance. *Bioresour. Technol.* 102, 159–165 (2011).

Yokoya, N. S. *et al.* ENDOGENOUS CYTOKININS, AUXINS, AND ABSCISIC ACID. *J. Phycol* 46, 1198–1205 (2010).

Yonekura-Sakakibara, K, Kojima, M, Yamaya, T., et. al. Molecular Characterization of Cytokinin-Responsive Histidine Kinases in Maize. Differential Ligand Preferences and Response to cis-Zeatin. *Plant Physiology*. **134,** 1654-1661 (2004).

Zaiimalovii, E. & Kaminek, M. Control of cytokinin biosynthesis and metabolism. *Biochem. Mol. Biol. Plant Horm.* 141–160 (1999).

Zhu, J. Salt and Drought Stress Signal Transduction in Plants. *Annu. Rev. Plant. Biol.* 53, 247–273 (2002).

Zhou, J. *et al.* Quorum sensing is a language of chemical signals and plays an ecological role in algal-bacterial interactions. *Rev Plant Sci* **35,** 81–105 (2016).

Zi, E. *et al.* Control of cytokinin and auxin homeostasis in cyanobacteria and algae. *Ann. Bot.* **119,** 151–166 (2017).

Zürcher, E. & Müller, B. Cytokinin Synthesis, Signaling, and Function — Advances and New Insights. *International Review of Cell and Molecular Biology*.1-38 (2016).

Appendix I

Table 1: *Euglena gracilis* grown for five (Cycles 0-4), three-day-long growth cycles. Supernatant and Biomass fractions were collected for wet and dry weight (g) analysis of total dry weight (g) and total product (g) as well as cell counts (10^6) from a 25 mL sample.

Cycle 0	Sample	Wet Weight (g)	Dry Weight (g)	Cell Count (*10^6)	Total Dry Weight (g)	Product (g)
Day 1 - Start	Supernatant	0.97437	1.47164	3.59	0.03064	0.94373
	Biomass	1.11757	1.087		0.00321	0.03057
Day 2	Supernatant	0.99555	1.57416	5.6	0.02916	0.96639
	Biomass	1.14418	1.10252		0.00512	0.04166
Day 3 - End	Supernatant	0.98878	1.53641	6.675	0.02941	0.95937
	Biomass	1.10258	1.07422		0.00468	0.02836
Cycle 1	Sample	Wet Weight (g)	Dry Weight (g)	Cell Count (*10^6)	Total Dry Weight (g)	Product (g)
Day 1 - Start	Supernatant	0.98241	1.48922	5.225	0.02522	0.95719
	Biomass	1.10328	1.07495		0.00515	0.02833
Day 2	Supernatant	0.98992	1.48829	5.96	0.02529	0.96463
	Biomass	1.10638	1.07266		0.00608	0.03372
Day 3 - End	Supernatant	0.98484	1.53946	6.325	0.02346	0.96138
	Biomass	1.13906	1.10388		0.00645	0.03518
Cycle 2	Sample	Wet Weight (g)	Dry Weight (g)	Cell Count (*10^6)	Total Dry Weight (g)	Product (g)
Day 1 - Start	Supernatant	0.98633	1.56579	4.945	0.02279	0.96354
	Biomass	1.10222	1.07261		0.00592	0.02961
Day 2	Supernatant	0.98035	1.53885	5.9	0.02385	0.9565
	Biomass	1.12453	1.07417		0.00418	0.05036
Day 3 - End	Supernatant	0.98408	1.53783	6.15	0.02683	0.95725
	Biomass	1.13676	1.10164		0.0043	0.03512
Cycle 3	Sample	Wet Weight (g)	Dry Weight (g)	Cell Count (*10^6)	Total Dry Weight (g)	Product (g)
Day 1 - Start	Supernatant	0.98516	1.49879	3.065	0.00736	0.9778
	Biomass	1.11619	1.07288		0.00371	0.04331
Day 2	Supernatant	0.9794	1.58281	6.195	0.00926	0.97014
	Biomass	1.12056	1.0892		0.00503	0.03136
Day 3 - End	Supernatant	0.98726	1.63276	7.675	0.00849	0.97877
	Biomass	1.13453	1.10347		0.00619	0.03106
Cycle 4	Sample	Wet Weight (g)	Dry Weight (g)	Cell Count (*10^6)	Total Dry Weight (g)	Product (g)
Day 1 - Start	Supernatant	0.98916	1.59741	4.2645	0.01073	0.97843
	Biomass	1.14492	1.10401		0.00446	0.04091
Day 2	Supernatant	0.9854	1.57948	6.55	0.00843	1.13649
	Biomass	1.14852	1.10545		0.00818	0.04307
Day 3 - End	Supernatant	0.98243	1.5341	7.775	0.00695	0.97548
	Biomass	1.14564	1.09171		0.00597	0.05393

Table 2: *Euglena gracilis* grown for five (Cycles 0-4), four-day-long growth cycles. Supernatant and Biomass fractions were collected for wet and dry weight (g) analysis of total dry weight (g) and total product (g) as well as cell counts (10^6) from a 25 mL sample.

	Sample	Wet Weight (g)	Dry Weight (g)	Cell Count (*10^6)	Total Dry Weight (g)	Product (g)
Day 1 - Start	Supernatant	0.98101	1.5431	4.2	0.0621	0.91891
	Biomass	1.20713	1.08236		0.00636	0.12477
Day 2	Supernatant	0.98522	1.55751	4.415	0.02751	0.95771
	Biomass	1.0845	1.05245		0.00745	0.03205
Day 3	Supernatant	0.98645	1.55704	6.375	0.02504	0.96141
	Biomass	1.136	1.09168		0.00868	0.04432
Day 4 - End	Supernatant	0.99147	1.47042	7.275	0.02542	0.96605
	Biomass	1.12665	1.08278		0.0051	0.04387
Cycle 1	Sample	Wet Weight (g)	Dry Weight (g)	Cell Count (*10^6)	Total Dry Weight (g)	Product (g)
Day 1 - Start	Supernatant	0.9911	1.50367	5.22	0.02767	0.96343
	Biomass	1.12324	1.0725		0.00493	0.05074
Day 2	Supernatant	0.83327	1.5231	7.43	0.0301	0.80317
	Biomass	1.10003	1.0577		0.00195	0.04233
Day 3	Supernatant	0.98531	1.55484	7.475	0.02684	0.95847
	Biomass	1.13526	1.08883		0.00295	0.04643
Day 4 - End	Supernatant	0.99201	1.55632	7.425	0.02832	0.96369
	Biomass	1.15012	1.10498		0.00541	0.04514
Cycle 2	Sample	Wet Weight (g)	Dry Weight (g)	Cell Count (*10^6)	Total Dry Weight (g)	Product (g)
Day 1 - Start	Supernatant	0.99499	1.58436	6.05	0.02736	0.96763
	Biomass	1.07902	1.04858		0.00082	0.03044
Day 2	Supernatant	0.98506	1.5115	6.475	0.0275	0.95756
	Biomass	1.0982	1.05854		0.0036	0.03966
Day 3	Supernatant	0.99109	1.46899	7.3	0.02599	0.9651
	Biomass	1.14222	1.10118		0.00298	0.04104
Day 4 - End	Supernatant	0.98905	1.46973	7.575	0.02573	0.96332
	Biomass	1.11213	1.08038		0.00173	0.03175
Cycle 3	Sample	Wet Weight (g)	Dry Weight (g)	Cell Count (*10^6)	Total Dry Weight (g)	Product (g)
Day 1 - Start	Supernatant	0.99216	1.56807	6.4	0.02707	0.96509
	Biomass	1.1421	1.08595		0.00055	0.05615
Day 2	Supernatant	0.98976	1.52896	7.8	0.02496	0.9648
	Biomass	1.10222	1.06943		0.00097	0.03279
Day 3	Supernatant	0.99554	1.54922	7.05	0.02522	0.97032
	Biomass	1.11644	1.0806		0.00138	0.03584
Day 4 - End	Supernatant	0.99093	1.50684	6.295	0.02684	0.96409
	Biomass	1.10269	1.06824		0.00154	0.03445
Cycle 4	Sample	Wet Weight (g)	Dry Weight (g)	Cell Count (*10^6)	Total Dry Weight (g)	Product (g)
Day 1 - Start	Supernatant	0.99042	1.55482	5.55	0.02382	0.9666
	Biomass	1.12967	1.09974		0.00135	0.02993
Day 2	Supernatant	1.01401	1.50244	6.25	0.02444	0.98957
	Biomass	1.08	1.04737		0.0021	0.03263
Day 3	Supernatant	0.99093	1.57331	6.375	0.02431	0.96662
	Biomass	1.07814	1.05555		0.00251	0.02259
Day 4 - End	Supernatant	0.99017	1.55471	5.925	0.02871	0.96146
	Biomass	1.12865	1.09985		0.00258	0.0288

Table 3: Experimental Parameters tested for best growth culturing techniques and conditions.

	Parameters					
	Volume (mL)	**Shaker Speed (RPM)**	**Temperature (°C)**	**Culture flask Bottom**	**Culture Flask Top**	**Recycle Rate (%)**
Experiment 1	100 250 500 1000	100	29	Flat & Baffled	Closed (Ajar)	0
Experiment 2	500 1000	120	27	Baffled	Vented	0 75
Experiment 3	500	120	27	Baffled	Vented	0 25 75
Experiment 4	500	120	27	Baffled	Vented	0 25 50 75

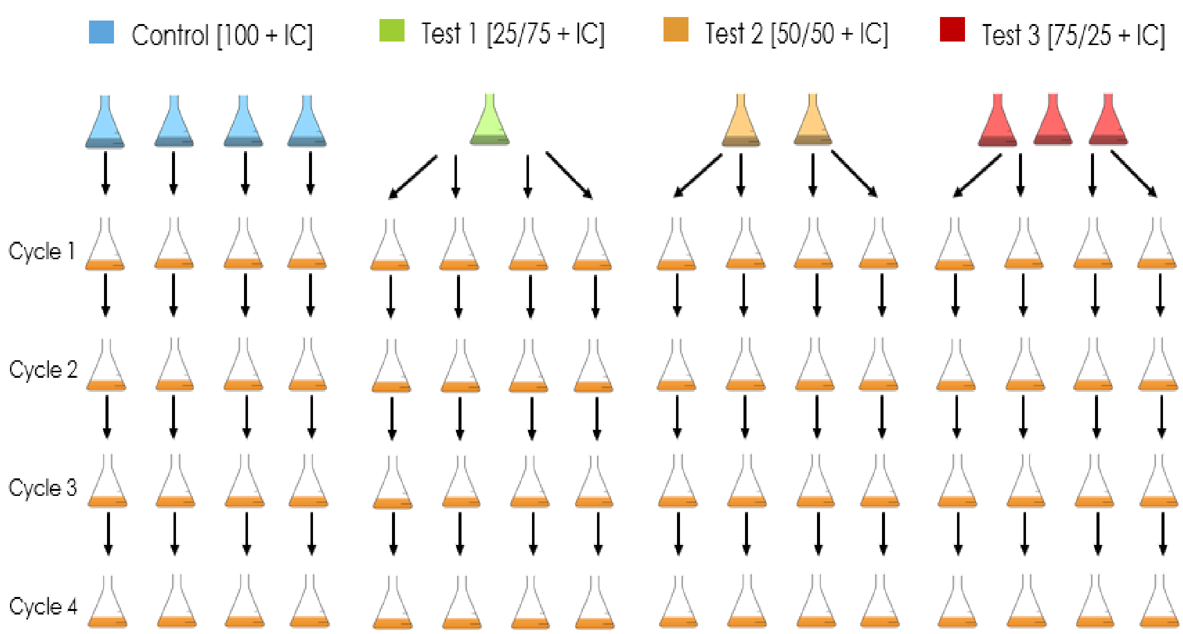

Figure 1: Experiment 4 schematic of 1L flasks with 500 mL working volume needed for 4 cycles, recycle dilutions listed as fractions and inoculated (IC) at $2 \cdot 10^6$ cells/500 mL; Control with 0% recycled medium and 100% fresh media, Test 1 with 25% recycled medium and 75% fresh medium, Test 2 with 50% recycled medium and 50% fresh medium, and Test 3 with 75% recycled medium and 25% fresh medium.

Table 4: Media blank analysis of organic medium for ABA and CKs (FBs, DZ, tZ, cisZ and iP; RBs, DZR, tZR, cisZR and iPR; NUCs, DZNT, tZNT, cisZNT and iPNT; METs, MeSZ, MeSiP, MeSZR and MeSiPA; and GLUCs, DZOG, DZROG, tZROG, cisZROG, DZ9G, tZOG, cisZOG and tZ9G/cisZ9G.

<table>
<tr><th colspan="6">Media Blank</th></tr>
<tr><td colspan="6">Abscisic Acid</td></tr>
<tr><td>ABA</td><td colspan="4">ABA</td><td>Total</td></tr>
<tr><td>(pmol/10mL)</td><td colspan="4">149.47</td><td>149.47</td></tr>
<tr><td colspan="6">Free Bases</td></tr>
<tr><td>CK</td><td>DZ</td><td>tZ</td><td>cisZ</td><td>iP</td><td>Total</td></tr>
<tr><td>(pmol/10mL)</td><td>0.00</td><td>0.00</td><td>25.44</td><td>119.88</td><td>145.32</td></tr>
<tr><td colspan="6">Ribosides</td></tr>
<tr><td>CK</td><td>DZR</td><td>tZR</td><td>cisZR</td><td>iPR</td><td>Total</td></tr>
<tr><td>(pmol/10mL)</td><td>17.35</td><td>5.35</td><td>7.09</td><td>279.34</td><td>309.13</td></tr>
<tr><td colspan="6">Nucleotides</td></tr>
<tr><td>CK</td><td>DZNT</td><td>tZNT</td><td>cisZNT</td><td>iPNT</td><td>Total</td></tr>
<tr><td>(pmol/10mL)</td><td>32.83</td><td>0.00</td><td>0.00</td><td>1673.19</td><td>1706.02</td></tr>
<tr><td colspan="6">Methyl-thiols</td></tr>
<tr><td>CK</td><td>MeSZ</td><td>MeSiP</td><td>MeSZR</td><td>MeSiPA</td><td>Total</td></tr>
<tr><td>(pmol/10mL)</td><td>16.16</td><td>1.02</td><td>0.57</td><td>0.34</td><td>18.09</td></tr>
<tr><td colspan="6">Glucosides</td></tr>
<tr><td>CK</td><td>DZOG</td><td>DZROG</td><td>tZROG</td><td>cisZROG</td><td rowspan="3">Total</td></tr>
<tr><td>(pmol/10mL)</td><td>8.47</td><td>1.79</td><td>0.00</td><td>30.01</td></tr>
<tr><td>CK</td><td>DZ9G</td><td>tZOG</td><td>cisZOG</td><td>tZ9G/cisZ9G</td></tr>
<tr><td>(pmol/10mL)</td><td>0.00</td><td>11.69</td><td>17.84</td><td>0.00</td><td>69.79</td></tr>
<tr><td colspan="6">CK Types</td></tr>
<tr><td>CK</td><td>tZ type</td><td>cZ type</td><td>DZ type</td><td>iP type</td><td>Total</td></tr>
<tr><td>(pmol/10mL)</td><td>17.03</td><td>80.37</td><td>60.44</td><td>2072.41</td><td>2230.25</td></tr>
</table>

Table 5: Two-Way ANOVA of experimental parameters tested, cycle, day and percent and combinations of these parameters to determine best statistical data representation. Significant values: *P<0.05; **P<0.01; ***P <0.001

		ABA	Free Bases				Ribosides			Nucleotides			Methylthiols		Glucosides							Types				Totals					
Source	*df*	ABA	DZ	tZ	cisZ	iP	tZR	cisZR	iPR	DZNT	tZNT	cisZNT	MeSZR	MeSiPA	DZOG	cisZROG	DZ9G	tZOG	cisZOG	tZ9G	CisZ9G	tZ type	cZ type	DZ type	iP type	FB	RB	NT	Met	Glucs	Total
Cycle	1	-	-	-	-	-	*** +	-	*** +	*** +	-	-	** +	** +	-	-	-	-	* +	-	-	-	-	** +	** +	-	** +	*** +	** +	-	*** +
Day	1	* +	-	* +	-	-	*** +	*** +	*** +	-	-	-	-	* +	-	-	-	-	* +	-	-	* +	** +	-	*** +	-	-	-	* +	-	-
%	3	-	-	** +	-	-	-	*** +	-	-	* +	-	*** +	-	** +	* +	*** +	-	-	-	-	-	-	-	-	-	*** +	-	*** +	*** +	-
Cycle*Day	1	* +	-	-	*** +	-	*** +	*** +	*** +	-	-	-	-	-	* +	-	** +	-	*** +	-	** +	-	*** +	* +	** +	-	-	-	-	*** +	-
Cycle*%	3	-	-	-	-	-	-	** +	-	-	* +	-	-	-	-	-	** +	-	* +	-	-	-	-	-	-	-	-	-	-	* +	-
Day*%	3	-	-	-	-	-	-	** +	-	-	-	-	-	-	*+	-	-	-	-	-	-	-	-	-	-	-	-	-	-	-	-
Cycle*Day *%	3	-	-	* +	-	-	-	** +	-	-	-	-	* +	-	-	-	* +	-	-	-	-	-	-	-	-	-	* +	-	* +	* +	-

Significant values: *P < 0.05; **P < 0.01; ***P < 0.001

Table 6: Post-Hoc analysis of extracted hormones from supernatant fractions. Statistically significant differences were calculated between the beginning and end of each cycle, per recycling rate (in red) and statistical differences between cycles 1 and 4 (bolded). Significant values: **P*<0.05.

Fraction	%	B/E	DZ Type											
			DZ		DZR		DZNT		DZOG		DZ9G		DZROG	
			Cycle 1	Cycle 4	Cycle 1	Cycle 4	Cycle 1	Cycle 4	Cycle 1	Cycle 4	Cycle 1	Cycle 4	Cycle 1	Cycle 4
SUP	0	B	0.00±0.00b	85.15±69.53a	230.35±32.81bcd	207.55±69.65b	66.87±21.27d	68.67±30.12c	N.D.		1659.03±64.71c	1622.40±342.55bc	N.D.	
		E	0.00±0.00b	22.87±18.67a	79.92±30.17d	129.85±24.16b	97.80±41.69d	55.74±27.31c			**1607.42±353.42c**	**946.16±101.74c**		
	25	B	0.00±0.00b	59.70±32.95a	256.13±46.68bc	352.03±129.07ab	276.14±30.44bcd	442.34±214.32ab			**2903.76±193.11bc**	**1580.05±98.25bc**		
		E	25.79±21.07b	28.70±14.76a	199.47±30.53cd	126.70±21.33b	239.52±67.08cd	51.94±17.19c			2872.81±1462.59bc	925.76±119.04c		
	50	B	0.00±0.00b	35.96±29.36a	331.39±71.81bc	332.73±67.66ab	478.32±109.89ab	305.07±134.46bc			8167.62±3368.95a	3879.76±1317.72b		
		E	11.40±9.31b	14.22±11.61a	308.83±68.17bc	505.49±39.91a	330.09±100.18bc	574.51±43.30ab			6365.61±826.56ab	3029.74±514.20bc		
	75	B	91.26±18.30a	25.39±20.73a	**389.46±1.56b**	**579.24±33.25a**	603.06±16.72a	766.81±51.19a			**0.00±0.00c**	7969.48±1260.07a		
		E	32.96±26.91b	45.84±18.86a	557.29±44.43a	365.09±97.53ab	671.85±17.05a	683.13±47.47a			**3457.62±1368.26bc**	**782.32±54.10c**		

Fraction	%	B/E	tZ Type											
			tZ		tZR		tZNT		tZOG		tZ9G		tZROG	
			Cycle 1	Cycle 4	Cycle 1	Cycle 4	Cycle 1	Cycle 4	Cycle 1	Cycle 4	Cycle 1	Cycle 4	Cycle 1	Cycle 4
SUP	0	B	0.00±0.00b	0.00±0.00b	N.D.		77.38±10.33a	73.60±15.47a	0.00±0.00a	132.93±60.23a	55.58±9.97a	21.37±10.95a	N.D.	
		E	23.41±19.11b	13.07±10.67b			33.82±3.41bc	37.26±3.05bc	718.80±520.26a	72.30±59.03a	**14.08±1.31a**	**0.00±0.00a**		
	25	B	43.67±18.06b	0.00±0.00b			60.34±8.98ab	53.03±6.85ab	**0.00±0.00a**	**237.71±24.89a**	41.14±17.34a	23.61±14.22a		
		E	33.83±13.89b	46.48±2.95ab			**39.25±0.45bc**	**21.18±0.95c**	16.77±8.43a	0.00±0.00a	11.93±4.95a	13.35±6.25a		
	50	B	49.67±70.24b	130.23±55.58a			53.28±7.67abc	26.85±6.26bc	0.00±0.00a	223.74±145.62a	16.91±16.89a	10.21±4.18a		
		E	89.05±36.43b	149.77±30.43a			30.41±5.52c	40.07±2.24bc	11.76±9.60a	172.98±108.72a	33.93±13.89a	37.29±20.19a		
	75	B	0.00±0.00b	128.23±32.12a			**40.40±0.95bc**	**42.72±4.01bc**	0.00±0.00a	60.47±35.91a	44.92±5.57a	17.09±6.98a		
		E	220.12±33.79a	80.54±37.57ab			52.46±10.80abc	39.68±3.19bc	271.53±117.20a	141.68±115.68a	16.91±8.50a	29.34±8.40a		

Fraction	%	B/E	cisZ Type											
			cisZ		cisZR		cisZNT		cisZOG		cisZ9G		cisZROG	
			Cycle 1	Cycle 4	Cycle 1	Cycle 4	Cycle 1	Cycle 4	Cycle 1	Cycle 4	Cycle 1	Cycle 4	Cycle 1	Cycle 4
SUP	0	B	**240.36±196.25d**	**1600.24±296.89ab**	0.00±0.00c	0.00±0.00b	89.92±13.36b	76.71±14.46c	0.00±0.00c	590.59±157.90abc	0.00±0.00a	1.73±1.42b	**142.32±116.21cd**	**661.22±256.53abc**
		E	291.04±84.25cd	552.97±148.46b	74.44±28.18bc	18.99±3.36b	68.72±7.65b	66.88±2.61c	899.21±296.02ab	137.30±76.18c	3.16±1.44a	0.00±0.00b	38.35±31.32d	282.78±62.39c
	25	B	539.99±83.64bcd	1959.34±671.54a	86.81±21.72bc	29.15±19.83b	92.51±9.71b	80.59±17.73c	**0.00±0.00c**	**1267.82±178.76a**	0.00±0.00a	1.41±1.15b	143.57±47.71cd	446.07±117.88bc
		E	**1004.14±279.31bc**	**257.76±66.32b**	**78.86±1.75bc**	**37.62±9.84b**	86.42±10.95b	53.27±5.434c	367.56±19.47bc	324.10±123.76bc	9.40±4.03a	0.54±0.44b	**165.80±40.82cd**	**583.74±64.87abc**
	50	B	717.14±310.15bcd	990.68±170.34ab	147.49±57.89b	173.59±56.03ab	92.28±28.33b	58.10±14.19c	**0.00±0.00c**	**1121.69±91.89ab**	8.96±8.22a	5.82±1.98ab	365.24±281.97bcd	542.57±75.64abc
		E	1163.08±146.19b	1083.38±320.59ab	147.50±32.33b	304.74±34.42a	94.58±14.71b	143.46±4.66b	396.98±64.43bc	834.10±353.14abc	5.65±3.19a	3.44±2.81ab	701.00±170.91ab	800.51±74.02ab
	75	B	612.52±105.87bcd	938.19±389.90ab	**121.81±3.40b**	**304.82±13.17a**	92.39±0.66b	191.03±8.35a	**0.00±0.00c**	**664.46±131.58abc**	**0.00±0.00a**	**9.38±1.70a**	**517.65±25.63abc**	**1020.62±91.88a**
		E	**1853.12±222.57a**	**489.14±33.52b**	297.89±21.89a	331.84±138.46a	165.28±10.84a	227.62±20.80a	1095.97±305.62a	488.62±398.96abc	4.34±3.55a	1.49±1.21b	947.58±119.49a	693.27±102.17abc

Table 6 (continued): Post-Hoc analysis of extracted hormones from supernatant fractions. Statistically significant differences were calculated between the beginning and end of each cycle, per recycling rate (in red) and statistical differences between cycles 1 and 4 (bolded). Significant values: *P<0.05.

Fraction	%	B/E	iP Type					
			iP		iPR		iPNT	
			Cycle 1	Cycle 4	Cycle 1	Cycle 4	Cycle 1	Cycle 4
SUP	0	B	N.D.d	49.79±40.65b	3934.70±703.55bc	3699.73±326.00abc	0.00±0.00b	0.00±0.00b
		E	2.92±2.38d	92.43±75.47b	1446.29±297.07d	1565.21±188.80bc	0.00±0.00b	0.00±0.00b
	25	B	447.71±139.27bcd	919.16±462.15ab	5181.62±497.91abc	3883.14±1994.70abc	0.00±0.00b	0.00±0.00b
		E	206.88±26.18cd	ND	**3115.14±436.88cd**	**545.82±97.43c**	0.00±0.00b	0.00±0.00b
	50	B	894.16±364.40ab	614.37±267.57ab	5121.99±967.99abc	3820.37±847.42abc	**8021.56±1688.92a**	**0.00±0.00b**
		E	554.24±227.40bc	857.43±203.56ab	3447.73±900.06cd	5069.34±281.77ab	2624.55±2057.93ab	873.31±625.11ab
	75	B	1123.03±40.48a	1229.42±54.55a	5934.24±98.43ab	7056.04±611.69a	4687.93±3314.87ab	7712.53±3150.92a
		E	1358.09±39.66a	1029.39±304.89a	6962.65±452.50a	4368.42±1210.95ab	2822.39±2304.47ab	5055.89±4128.11ab

Fraction	%	B/E	Methyl-thiols								ABA	
			MeSZ		MeSiP		MeSZR		MeSiPA		ABA	
			Cycle 1	Cycle 4	Cycle 1	Cycle 4	Cycle 1	Cycle 4	Cycle 1	Cycle 4	Cycle 1	Cycle 4
SUP	0	B	0.00±0.00d	888.24±505.64a	4.43±1.81bc	187.76±74.26a	39.52±12.66c	42.01±9.50b	0.00±0.00e	0.00±0.00c	242.41±154.49bc	0.00±0.00b
		E	0.55±0.45d	96.35±43.29a	0.63±0.51c	9.8326.24±9.83b	42.66±6.20bc	70.06±14.36ab	13.78±1.24cd	11.12±0.93b	0.00±0.00c	362.06±285.70b
	25	B	**6.85±5.59d**	**443.71±101.26a**	**10.37±4.82abc**	**173.05±44.75ab**	51.59±6.53bc	103.70±22.78ab	10.28±1.01d	9.62±3.02bc	**570.922±91.47abc**	**0.00±0.00b**
		E	**67.91±22.91bd**	**452.78±16.06a**	0.00±0.00c	28.49±21.04b	81.30±7.99bc	106.36±23.82ab	20.68±1.47bc	11.22±4.71b	227.51±185.76bc	271.83±221.95b
	50	B	206.80±176.93ab	373.09±113.88a	16.01±2.63a	52.87±33.49ab	59.95±21.26bc	265.11±116.68a	19.18±3.16bcd	19.71±1.84ab	1318.74±365.69ab	843.99±380.84b
		E	279.06±71.81a	438.07±119.69a	0.00±0.00c	63.39±44.23ab	104.43±16.57b	236.59±59.90ab	24.41±3.95b	24.52±2.08a	0.00±0.00c	30.53±24.93b
	75	B	190.89±17.35abd	245.66±44.84a	**2.42±1.71bc**	**19.95±2.51b**	70.98±1.13a	253.36±41.89a	23.92±1.05b	22.91±2.27a	1770.41±14.33a	1876.96±110.09a
		E	321.41±35.99a	377.80±22.57a	12.13±4.66ab	37.31±29.29ab	210.70±31.49bc	166.82±15.06ab	**42.32±3.98a**	**22.93±3.33a**	1316.6±773.05ab	799.47±351.99b

Fraction	%	B/E	Fractions											
			FB		RB		NT		Met		Glucs		Total	
			Cycle 1	Cycle 4	Cycle 1	Cycle 4	Cycle 1	Cycle 4	Cycle 1	Cycle 4	Cycle 1	Cycle 4	Cycle 1	Cycle 4
SUP	0	B	**240.35±196.25c**	**1735.18±354.51ab**	4165.05±727.76bc	3907.28±391.85abc	234.17±4.07d	218.97±53.49cd	43.95±10.94c	229.78±81.21a	1856.94±68.53d	3030.24±817.10bcd	6540.46±860.72de	10009.69±2098.37bc
		E	317.36±101.53c	681.34±222.33b	1600.65±321.33d	1714.05±191.75bc	200.34±52.20d	159.88±28.15cd	57.07±7.85bc	107.42±23.54a	**3281.02±457.40bcd**	**1438.54±37.70d**	5456.99±764.18e	4197.58±393.78c
	25	B	1031.36±165.61bc	2938.20±1157.10a	5524.56±523.11abc	4264.32±2142.55abc	428.98±18.20cd	575.96±236.51abc	72.25±11.99bc	286.37±70.14a	3088.48±186.63bcd	3556.67±404.26bcd	10152.48±615.70cde	12065.22±3587.35bc
		E	**1270.65±261.55b**	**332.96±78.57b**	**3393.47±466.29cd**	**710.13±83.56c**	365.19±77.79cd	126.40±18.82d	101.98±9.32bc	146.08±46.72a	3444.28±1489.71bcd	1847.49±49.47cd	8643.48±1827.13cde	3615.84±118.68c
	50	B	1660.97±368.45b	1771.26±482.20ab	5600.89±1020.10abc	4326.69±987.60abc	623.88±145.69bc	390.02±154.90bcd	95.14±25.77bc	337.69±115.49a	8558.73±3085.56a	5783.78±1189.27b	**24767.96±3491.12a**	**12982.53±2454.69bc**
		E	1817.78±366.09b	2104.81±506.08ab	3904.06±1000.28cd	5879.57±308.94a	455.08±119.79cd	758.04±49.67ab	128.84±20.45b	324.50±105.09a	**7514.92±671.51ab**	**4878.07±244.29bc**	16724.27±2364.03abc	15256.36±1692.98b
	75	B	1826.81±128.06b	2321.24±380.53ab	6445.50±100.27ab	7940.10±648.55a	735.85±16.43ab	1000.56±61.59a	97.32±3.90bc	296.23±41.92a	**562.57±20.06d**	**9770.24±1493.06a**	**14546.88±3317.78bcd**	**29286.56±1259.01a**
		E	**3464.30±238.82a**	**1644.90±354.07ab**	7817.83±510.91a	5065.35±1387.29ab	889.59±21.94a	950.44±70.88a	265.15±39.18a	227.06±10.99a	5793.95±1559.07abc	2136.72±471.83cd	21374.62±3316.79ab	15458.15±4507.51b

Table 7: Post-Hoc analysis of extracted hormones from pellet fractions. Statistically significant differences were calculated between the beginning and end of each cycle, per recycling rate (in red) and statistical differences between cycles 1 and 4 (bolded). Significant values: *P<0.05.

Fraction	%	B/E	DZ Type											
			DZ		DZR		DZNT		DZOG		DZ9G		DZROG	
			Cycle 1	Cycle 4	Cycle 1	Cycle 4	Cycle 1	Cycle 4	Cycle 1	Cycle 4	Cycle 1	Cycle 4	Cycle 1	Cycle 4
PEL	0	B	0.40±0.08ab	0.61±0.18a	5.88±1.21a	4.00±0.19ab	12.41±4.29ab	10.28±3.24b	N.D		N.D.		0.07±0.06a	N.D.
		E	0.51±0.17ab	0.33±0.11a	3.15±0.92a	2.50±0.22b	9.03±2.40ab	7.59±0.86b					0.09±0.01a	0.03±.0.03a
	25	B	0.21±0.02b	0.96±0.31a	3.80±0.40a	6.04±1.52ab	7.65±0.31b	15.24±2.92ab					0.00±0.00a	0.04±0.03a
		E	0.31±0.02ab	0.79±0.23a	4.27±1.26a	5.48±0.85ab	9.09±0.91ab	13.36±2.35ab					0.02±0.02a	0.04±0.03a
	50	B	**0.21±0.04ab**	**1.10±0.20a**	**3.80±0.34a**	**6.43±0.68a**	**8.43±0.84ab**	**13.81±0.42ab**					0.04±0.03a	0.03±0.03a
		E	0.72±0.04a	1.48±0.66a	5.38±0.89a	6.38±0.17a	15.20±2.15ab	20.36±1.65a					0.04±0.03a	0.00±0.00a
	75	B	0.33±0.02ab	0.70±0.35a	3.48±0.11a	5.08±0.45ab	7.50±0.85b	13.68±1.24ab					0.04±0.04a	0.04±0.03a
		E	0.62±0.18ab	0.87±0.16a	6.65±1.10a	4.20±1.64ab	17.11±1.64a	16.04±3.55ab					0.05±0.04a	N.D.

Fraction	%	B/E	tZ Type											
			tZ		tZR		tZNT		tZOG		tZ9G		tZROG	
			Cycle 1	Cycle 4	Cycle 1	Cycle 4	Cycle 1	Cycle 4	Cycle 1	Cycle 4	Cycle 1	Cycle 4	Cycle 1	Cycle 4
PEL	0	B	N.D.		2.20±0.10ab	1.39±0.28ab	18.35±6.00a	13.42±4.01a	1..86±0.78a	1.33±0.73a	N.D.		0.24±0.12a	0.00±0.00b
		E			2.19±0.24ab	1.97±0.11ab	5.03±1.77c	6.61±0.63a	0.83±0.68a	1.12±0.12a			1.17±0.22a	0.45±0.19ab
	25	B			1.44±0.38ab	2.68±1.23a	7.64±0.87bc	16.91±6.02a	1.57±0.23a	0.82±0.35a			0.29±0.14a	0.09±0.04ab
		E			2.49±0.46a	2.49±0.33a	4.13±0.43c	9.08±2.25a	2.00±0.04a	0.85±0.38a			**0.87±0.11a**	**0.17±0.14ab**
	50	B			1.15±0.15b	1.49±0.15ab	7.39±1.11bc	13.52±2.64a	0.54±0.15a	0.61±0.39a			0.07±0.06a	0.12±0.06ab
		E			1.73±0.03ab	1.75±0.12ab	**6.77±0.15bc**	**8.92±0.25a**	0.06±0.05a	2.57±1.06a			1.09±0.45a	0.74±0.31a
	75	B			1.25±0.10b	0.87±0.20ab	**3.96±0.18c**	**10.07±0.80a**	1.99±0.46a	1.63±0.45a			0.07±0.07a	0.21±0.12ab
		E			**1.89±0.28ab**	**0.47±0.18b**	16.39±2.57ab	9.05±0.59a	1.71±0.67a	1.58±0.66a			1.08±0.48a	0.44±0.20ab

Fraction	%	B/E	cisZ Type											
			cisZ		cisZR		cisZNT		cisZOG		cisZ9G		cisZROG	
			Cycle 1	Cycle 4	Cycle 1	Cycle 4	Cycle 1	Cycle 4	Cycle 1	Cycle 4	Cycle 1	Cycle 4	Cycle 1	Cycle 4
PEL	0	B	**98.18±18.28c**	**27.62±4.16bc**	1.31±0.12b	1.11±0.16a	14.05±2.28cd	20.63±1.02b	3.10±1.09ab	2.04±0.65a	N.D.		7.20±0.77ab	6.63±1.70a
		E	**219.39±24.56a**	**77.57±8.81a**	1.21±0.38b	1.19±0.18a	27.51±4.02bc	23.81±0.63b	1.38±0.39ab	1.93±0.06a			4.30±1.25b	4.15±0.12a
	25	B	85.75±2.71c	54.26±16.92abc	1.14±0.15b	3.49±1.75a	11.93±1.17d	23.37±3.87b	1.00±0.24b	2.29±0.70a			4.90±0.14ab	6.49±1.34a
		E	134.10±10.78bc	61.32±25.24ab	1.99±0.64b	2.78±0.41a	26.49±0.92bcd	27.73±3.82b	**1.73±0.21ab**	**3.11±0.33a**			4.00±0.65b	6.01±0.81a
	50	B	**96.11±11.84c**	**31.40±3.39bc**	**1.87±0.18b**	**3.55±0.26a**	12.91±2.30cd	22.72±2.82b	1.73±0.17ab	4.05±0.58a			5.61±0.98ab	7.48±0.24a
		E	57.64±34.72c	20.49±1.75bc	3.50±0.67b	4.51±0.39a	35.31±1.72b	35.68±1.12b	3.36±0.72a	4.36±0.69a			7.37±1.39ab	8.76±0.60a
	75	B	**198.22±22.68ab**	**24.43±2.02bc**	2.17±0.11b	3.77±0.36a	**12.97±0.97cd**	**32.74±0.35b**	1.60±0.06ab	3.10±0.93a			**4.94±0.41ab**	**7.68±0.32a**
		E	47.05±22.41c	13.99±1.85c	6.74±1.18a	3.95±1.49a	58.74±7.87a	51.89±10.21a	3.19±0.30ab	4.05±1.04a			8.61±1.43a	7.75±2.22a

Table 7 (continued): Post-Hoc anlaysis of extracted hormones from pellet fractions. Statisitcally significant differences were calculated between the beginning and end of each cycle, per recycling rate (in red) and statistitcal differences between cycles 1 and 4 (bolded). Significant values: *P<0.05.

Fraction	%	B/E	iP Type					
			iP		iPR		iPNT	
			Cycle 1	Cycle 4	Cycle 1	Cycle 4	Cycle 1	Cycle 4
PEL	0	B	56.68±8.59ab	65.36±17.87ab	112.24±20.69ab	87.30±11.33a	373.46±78.21b	602.02±120.38ab
		E	37.40±8.95b	34.68±2.39b	44.86±14.46c	39.47±0.79a	703.17±183.19ab	528.55±17.70b
	25	B	88.07±26.16ab	83.66±10.23ab	64.88±7.08abc	89.06±21.99a	478.90±18.17ab	489.97±104.93b
		E	75.88±39.02ab	54.58±8.67ab	42.75±7.08c	72.76±9.75a	582.36±55.60ab	608.52±74.02ab
	50	B	49.40±6.77b	89.59±23.95ab	**64.48±4.68abc**	**106.48±8.10a**	455.06±66.37ab	459.12±148.61b
		E	75.06±13.96ab	108.74±23.07a	97.37±20.68abc	101.97±6.18a	**794.96±55.93a**	**997.69±16.86a**
	75	B	238.33±101.10a	64.76±7.24ab	55.25±0.48bc	94.52±10.75a	494.27±30.68ab	718.98±89.86ab
		E	71.82±7.88ab	85.37±6.91ab	125.44±20.31a	91.43±34.75a	722.64±74.02ab	992.33±166.73a

Fraction	%	B/E	Methyl-thiols								ABA	
			MeSZ		MeSiP		MeSZR		MeSiPA		ABA	
			Cycle 1	Cycle 4	Cycle 1	Cycle 4	Cycle 1	Cycle 4	Cycle 1	Cycle 4	Cycle 1	Cycle 4
PEL	0	B	20.96±2.80a	16.27±2.65bc	48.41±8.30a	46.76±13.75bc	3.91±0.48c	5.21±1.88b	1.12±0.38a	0.15±0.12b	N.D.	
		E	10.72±1.41c	9.24±0.14b	24.71±2.30b	24.51±0.76c	2.88±0.89c	3.62±0.29b	0.24±0.20a	0.62±0.29b		
	25	B	18.88±1.49abc	19.95±3.03ab	49.86±7.26a	46.35±7.59bc	4.45±0.67c	5.71±1.27b	0.41±0.17a	0.00±0.00b		
		E	12.33±1.69bc	15.48±3.38bc	**26.46±1.78b**	**122.72±9.78b**	**3.36±0.38c**	**8.33±0.78b**	0.31±0.25a	0.83±0.68b		
	50	B	19.28±2.82ab	13.98±1.13bc	39.42±3.98ab	34.54±3.39bc	**3.13±0.56c**	**6.88±0.62b**	1.42±0.94a	0.66±0.54b		
		E	**15.18±0.47abc**	**21.44±1.55ab**	**38.78±5.00ab**	**234.44±56.41a**	**7.44±0.34b**	**42.21±9.24a**	0.64±0.52a	3.77±1.59a		
	75	B	16.24±0.38abc	15.97±0.97bc	**29.67±0.73ab**	**44.07±0.92bc**	**3.50±0.58c**	**11.65±0.97b**	0.20±0.20a	0.75±0.61b		
		E	21.01±2.63a	24.55±1.57a	**48.46±3.19a**	**208.35±28.19a**	**12.16±0.75a**	**44.82±4.24a**	0.51±0.42a	0.00±0.00b		

Fraction	%	B/E	Fractions											
					RB		NT		Met		Glucs		Total	
			Cycle 1	Cycle 4	Cycle 1	Cycle 4	Cycle 1	Cycle 4	Cycle 1	Cycle 4	Cycle 1	Cycle 4	Cycle 1	Cycle 4
PEL	0	B	155.27±26.93b	93.58±18.56a	121.64±22.04ab	93.81±11.94a	418.27±83.91b	646.35±123.07b	74.39±10.22ab	68.39±18.17b	12.48±2.31a	10.00±3.07ab	782.05±116.13a	912.13±156.05b
		E	**257.30±32.65ab**	**112.57±11.17a**	51.41±15.95c	45.13±1.18a	744.74±191.30ab	566.55±15.75b	38.56±4.31c	38.00±0.98b	8.26±2.78a	7.69±0.17b	1100.26±246.00a	769.95±4.19b
	25	B	174.03±28.37b	138.88±26.58a	71.27±7.91bc	101.28±26.46a	506.12±18.59ab	545.49±102.89b	73.61±8.97ab	72.02±11.46b	7.79±0.28a	9.74±1.80ab	832.82±16.15a	867.40±116.33b
		E	210.29±45.99ab	116.69±32.60a	51.51±9.06c	83.51±11.26a	622.08±57.25ab	658.69±75.72ab	**42.47±3.45c**	**147.37±11.57b**	8.63±0.95a	10.17±1.24ab	934.98±114.49a	1016.43±126.01b
	50	B	145.72±18.49b	122.09±27.46a	**71.30±5.29bc**	**117.95±9.01a**	483.80±70.52ab	509.17±146.14b	63.25±6.05abc	56.07±4.59b	8.11±1.32a	12.30±0.98ab	772.17±94.33a	817.57±172.44b
		E	133.42±44.19b	130.71±21.57a	107.98±22.18abc	114.62±6.82a	852.24±59.65a	1062.66±18.16a	**62.04±4.99abc**	**301.86±68.05a**	11.91±2.46a	16.43±2.02a	1167.60±121.03a	1626.28±73.08a
	75	B	436.88±123.80a	89.89±6.28a	62.14±0.79bc	104.24±11.62a	518.69±30.38ab	775.46±90.72ab	**49.61±1.13bc**	**72.43±2.41b**	8.63±0.77a	12.66±1.33ab	1075.97±154.60a	1054.68±89.42b
		E	119.49±27.21b	100.23±8.48a	140.72±22.84a	100.05±38.05a	814.88±85.81a	1069.30±160.27a	**84.14±6.60a**	**277.71±29.55a**	14.65±2.70a	13.82±3.11ab	1171.87±140.61a	1561.12±228.84a

Table 8: Abscisic Acid (ABA) and Cytokinin (CK) levels of *Euglena gracilis* in both supernatant and pellet fractions for the beginning (B) and end (E) cycle 1 under recycled conditions 0, 25, 50 and 75% of recycled medium to fresh medium in 500 mL culture flasks represented in a heat map. Colours were assigned as blue (lowest), red (highest) and white (not detected). All remaining values were assigned a colour per value with three different shades of both blue and red. Panel A displays the supernatant fraction and B, the pellet fraction. CK forms as Free Bases (FBs), Ribosides (RBs), Nucleotide (NUCs), Methyl-thiol (METs), and Glucosides (GLUCs) and CK Types as transCKs, cisCKs, FBs (DHZ + tZ + cisZ + iP), RBs (DZR, tZR, cisZR, IPR), NUCs (DZNT + tZNT + cisZNT + iPNT), METs (MeSZ + MeSiP + MeSZR + MeSiPA) and GLUCs (DZOG + DZROG + tZROG + cisZROG + DZ9G tZOG + cisZOG + tZ9G + cZ9G).

	SUPERNATANT		ABA			FBs				RBs				NTs				METs							GLUCs			
Cycle	Stage	Percent	ABA	DZ	tZ	cisZ	iP	DZR	tZR	cisZR	iPR	DZNT	tZNT	cisZNT	iPNT	MeSZ	MeSiP	MeSZR	MeSiPA	DZOG	DZROG	tZROG	cisZROG	DZ9G	tZOG	cisZOG	tZ9G	cisZ9G
1	B	0%	242.4139	N.D	N.D	240.3546	N.D	230.3458	N.D	N.D	3934.702	66.87001	77.37648	89.92082	N.D	N.D	4.430716	39.5166	N.D	N.D	N.D	N.D	142.325	1659.034	N.D	N.D	55.58466	N.D
		25%	570.9222	N.D	43.66913	539.9838	447.7108	256.1255	N.D	86.80792	5181.624	276.1352	60.33784	92.50719	N.D	6.84983	10.36955	51.59275	10.28274	N.D	N.D	N.D	143.5734	2903.764	N.D	N.D	41.14123	N.D
		50%	1318.741	N.D	49.66793	717.1413	894.1572	331.3946	N.D	147.4997	5121.997	478.3218	53.2754	92.27987	8021.556	206.802	16.00925	59.9526	19.17575	N.D	N.D	N.D	365.2361	8167.624	N.D	N.D	16.90964	8.962186
		75%	1770.406	91.25638	N.D	612.5222	1123.032	389.4565	N.D	121.8086	5934.24	603.063	40.40026	92.38926	4687.933	190.8882	2.419361	70.97747	23.92093	N.D	N.D	N.D	517.6531	N.D	N.D	N.D	44.91787	N.D
	E	0%	N.D	N.D	23.40259	291.0362	2.918669	79.92027	N.D	74.44367	1446.288	97.80071	33.81548	68.72411	N.D	0.553437	0.625343	42.65607	13.78416	N.D	N.D	N.D	38.35642	1607.422	718.7952	899.2146	14.08008	3.156073
		25%	227.5056	25.79968	33.82859	1004.142	206.8849	199.472	N.D	78.85622	3115.141	239.517	39.25287	86.41922	N.D	67.90726	N.D	81.29598	20.68068	N.D	N.D	N.D	165.8015	2872.808	16.77379	367.5614	11.93316	9.401985
		50%	N.D	11.40365	89.04558	1163.084	554.243	308.8312	N.D	147.5009	3447.726	330.0864	30.40913	94.57974	2624.545	279.0565	N.D	104.4313	24.40971	N.D	N.D	N.D	700.9954	6365.61	11.76243	396.9791	33.9258	5.647881
		75%	1316.601	32.96292	220.1233	1853.118	1358.094	557.2994	N.D	297.8854	6962.648	671.8542	52.45575	165.2792	2822.39	321.407	12.129	210.7	42.32158	N.D	N.D	N.D	947.5805	3457.619	271.5277	1095.966	16.91062	4.343653

	PELLET		ABA			FBs				RBs				NTs				**METs**							GLUCs			
Cycle	Stage	Percent	ABA	DZ	tZ	cisZ	iP	DZR	tZR	cisZR	iPR	DZNT	tZNT	cisZNT	iPNT	MeSZ	MeSiP	MeSZR	MeSiPA	DZOG	DZROG	tZROG	cisZROG	DZ9G	tZOG	cisZOG	tZ9G	cisZ9G
1	B	0%	N.D	0.404871	N.D	98.18104	56.68399	5.884314	2.203398	1.308563	112.242	12.41349	18.34697	14.04777	373.4583	20.95544	48.40673	3.913597	1.116043	N.D	0.073978	0.244333	7.202793	N.D	1.858189	3.101456	N.D	N.D
		25%	N.D	0.208174	N.D	85.75105	88.07368	3.802527	1.444327	1.13953	64.88461	7.647875	7.636216	11.93281	478.8985	18.88052	49.86433	4.449888	0.412681	0.035775	N.D	0.285171	4.896522	N.D	1.568106	1.003785	N.D	N.D
		50%	N.D	0.214294	N.D	96.10528	49.39867	3.800591	1.150623	1.869788	64.4798	8.433776	7.389941	12.91418	455.0577	19.27978	39.4184	3.128237	1.422571	0.123765	0.0395	0.071844	5.607558	N.D	0.538899	1.725673	N.D	N.D
		75%	N.D	0.32707	N.D	198.2207	238.3334	3.477452	1.247245	2.173469	55.24674	7.498765	3.958469	12.96565	494.2715	16.23997	29.67395	3.495784	0.203983	N.D	0.04231	0.065304	4.93598	N.D	1.987362	1.604023	N.D	N.D
	E	0%	N.D	0.510547	N.D	219.3887	37.39609	3.152233	2.190803	1.206938	44.85888	9.031004	5.026217	27.5091	703.171	10.72436	24.71415	2.878736	0.239808	0.490854	0.091101	1.16614	4.296526	N.D	0.834232	1.380346	N.D	N.D
		25%	N.D	0.311331	N.D	134.0963	75.88393	4.273523	2.490518	1.994174	42.75158	9.094355	4.126083	26.49454	582.3637	12.33483	26.46213	3.361488	0.308533	N.D	0.02354	0.870817	4.002498	N.D	2.001729	1.730889	N.D	N.D
		50%	N.D	0.715632	N.D	57.63598	75.06457	5.38337	1.727608	3.504766	97.36743	15.20216	6.772014	35.30881	794.9597	15.18388	38.77744	7.442483	0.639915	N.D	0.037288	1.088429	7.371711	N.D	0.057079	3.355815	N.D	N.D
		75%	N.D	0.617268	N.D	47.05165	71.81903	6.649515	1.893837	6.742022	125.4374	17.11064	16.38679	58.73533	722.6439	21.01373	48.45843	12.15754	0.508656	N.D	0.053868	1.084634	8.612294	N.D	1.708635	3.189777	N.D	N.D

	SUPERNATANT		ABA			FBs				RBs				NTs				METs							GLUCs			
Cycle	Stage	Percent	ABA	DZ	tZ	cisZ	iP	DZR	tZR	cisZR	iPR	DZNT	tZNT	cisZNT	iPNT	MeSZ	MeSiP	MeSZR	MeSiPA	DZOG	DZROG	tZROG	cisZROG	DZ9G	tZOG	cisZOG	tZ9G	cisZ9G
4	B	0%	N.D	85.15119	N.D	1600.239	49.79183	207.5507	N.D	0.000000	3699.727	68.66613	73.59841	76.70644	N.D	888.2406	187.7644	42.01264	N.D	N.D	N.D	N.D	661.222	1622.397	132.9303	590.5859	21.36852	1.733911
		25%	N.D	59.70443	N.D	1959.342	919.1551	352.0349	N.D	29.14975	3883.138	442.3378	53.02745	80.59379	N.D	443.7068	173.0514	103.6963	9.620399	N.D	N.D	N.D	446.0724	1580.049	237.7061	1267.821	23.60538	1.408654
		50%	843.9922	35.95945	130.2475	990.6808	614.3683	332.7342	N.D	173.5862	3820.366	305.0737	26.85192	58.09845	N.D	373.0948	52.86647	265.1125	19.70822	N.D	N.D	N.D	542.5659	3879.756	223.7434	1121.689	10.20898	5.817463
		75%	1876.957	25.39142	128.2259	938.1981	1229.424	579.241	N.D	304.8182	7056.043	766.8106	42.72091	191.0279	7712.53	245.6623	19.95016	253.3606	22.91444	28.7412	N.D	N.D	1020.618	7969.483	60.46685	664.4574	17.09	9.383562
	E	0%	362.0591	22.86778	13.06908	552.9724	92.4298	129.8487	N.D	18.99576	1565.208	55.73785	37.26026	66.88348	N.D	96.352	26.24159	70.0583	11.11735	N.D	N.D	N.D	282.7834	946.1574	72.29913	137.2964	N.D	N.D
		25%	271.8284	28.70352	46.47873	257.7759	N.D	126.6971	N.D	37.62033	545.8157	51.94409	21.18162	53.27453	N.D	452.7825	28.49267	106.3634	11.2233	N.D	N.D	N.D	583.7442	925.7611	N.D	324.0978	13.34587	0.540954
		50%	30.53159	14.22405	149.7715	1083.383	857.4318	505.4906	N.D	304.7421	5069.336	574.5069	40.06937	143.4629	873.3084	438.0705	63.38881	236.5893	24.52101	N.D	N.D	N.D	800.5109	3029.74	172.9822	834.1028	37.28666	3.44527
		75%	799.4735	45.83721	80.54187	489.1355	1029.389	365.0905	N.D	331.8353	4368.424	683.1331	39.68269	227.6226	5055.887	377.8	37.30715	166.8206	22.93105	N.D	N.D	N.D	693.2696	782.3219	141.6772	488.6235	29.33557	1.487494

	PELLET		ABA			FBs				RBs				NTs				METs							GLUCs			
Cycle	Stage	Percent	ABA	DZ	tZ	cisZ	iP	DZR	tZR	cisZR	iPR	DZNT	tZNT	cisZNT	iPNT	MeSZ	MeSiP	MeSZR	MeSiPA	DZOG	DZROG	tZROG	cisZROG	DZ9G	tZOG	cisZOG	tZ9G	cisZ9G
4	B	0%	N.D	0.605346	N.D	27.61616	65.35706	4.002569	1.392647	1.112467	87.30383	10.27971	13.41819	20.62866	602.0224	16.27222	46.75742	5.213599	0.148723	N.D	N.D	N.D	6.630897	N.D	1.32561	2.043553	N.D	N.D
		25%	N.D	0.961304	N.D	54.25661	83.65715	6.042477	2.678911	3.494982	89.06037	15.23953	16.90624	23.37031	489.9748	19.95248	46.35159	5.712811	N.D	N.D	0.041845	0.090742	6.492114	N.D	0.821933	2.291144	N.D	N.D
		50%	N.D	1.100429	N.D	31.39722	89.59308	6.425504	1.493374	3.553199	106.4822	13.81254	13.51646	22.71551	459.1217	13.98141	34.54452	6.88431	0.655772	N.D	0.034039	0.124739	7.476549	N.D	0.610158	4.050048	N.D	N.D
		75%	N.D	0.704162	N.D	24.43032	64.75853	5.076675	0.869264	3.770823	94.52122	13.676	10.06554	32.73509	718.9849	15.9664	44.06635	11.65024	0.747174	N.D	0.040508	0.212027	7.678178	N.D	1.627997	3.099481	N.D	N.D
	E	0%	N.D	0.327116	N.D	77.56725	34.67925	2.502128	1.969637	1.188061	39.4698	7.587252	6.607588	23.80506	528.5547	9.244236	24.51256	3.622575	0.62309	N.D	0.03303	0.448809	4.154249	N.D	1.122913	1.932955	N.D	N.D
		25%	N.D	0.787149	N.D	61.32251	54.58457	5.483334	2.489596	2.780993	72.7553	13.36093	9.080709	27.7268	608.5178	15.48438	122.7227	8.327965	0.832293	N.D	0.041108	0.170942	6.005847	N.D	0.846371	3.105798	N.D	N.D
		50%	N.D	1.478024	N.D	20.49106	108.7391	6.381771	1.749622	4.51455	101.9706	20.36491	8.920569	35.68017	997.6928	21.43791	234.4362	42.21194	3.774514	N.D	N.D	0.744145	8.75561	N.D	2.570236	4.361882	N.D	N.D
		75%	N.D	0.865141	N.D	13.99133	85.37407	4.19842	0.470435	3.951272	91.43381	16.03633	9.045828	51.885	992.3343	24.54896	208.348	44.81588	N.D	N.D	N.D	0.438454	7.753106	N.D	1.581547	4.045293	N.D	N.D

Table 9: *Euglena gracilis* grown for three-day-long growth cycles for cycles 1 and 2. Supernatant and Biomass fractions were collected for wet and dry weight (g), pH and glucose readings as well as cell counts (10^6) from a 25 mL sample. Continuation of data collection in Table 5.

Treatment	Recycle Rate	Fresh Weight (g)	Dry Weight (g)	pH	Glucose	Cell Count (10^6)	Treatment	Recycle Rate	Fresh Weight (g)	Dry Weight (g)	pH	Glucose	Cell Count (10^6)
Supernatant													
	0	0.985	0.018	3.268	0.733	1.33		0	0.9820	0.0111	3.283	0.403	1.46
	0	0.985	0.012	3.272	0.683	1.18		0	0.988	0.012	3.293	0.453	1.41
	0	0.988	0.019	3.266	0.771	1.28		0	0.986	0.010	3.279	0.435	1.51
	25	0.988	0.021	3.329	0.677	1.26		25	0.984	0.012	3.325	0.403	1.45
	25	0.987	0.019	3.337	0.667	1.34		25	0.984	0.010	3.334	0.405	1.63
Cycle 1 DPI	25	0.979	0.012	3.347	0.696	1.38	Cycle 2 DPI	25	0.986	0.008	3.329	0.440	1.51
0	50	0.991	0.024	3.367	0.600	1.48	0	50	0.990	0.012	3.459	0.357	1.48
	50	0.978	0.015	3.372	0.555	1.39		50	0.985	0.012	3.47	0.427	1.55
	50	0.989	0.013	3.363	0.597	1.62		50	0.986	0.009	3.468	0.432	1.77
	75	0.986	0.019	3.43	0.528	1.94		75	0.978	0.011	3.69	0.384	1.8
	75	1.002	0.023	3.434	0.509	2.03		75	0.987	0.010	3.708	0.400	1.9
								75	0.983	0.010	3.71	0.395	1.74
	0	0.989	0.016	3.293	0.469	2.21		0	0.991	0.011	3.281	0.536	2.49
	0	0.986	0.020	3.306	0.451	2.49		0	0.985	0.008	3.276	0.517	2.37
	0	0.986	0.015	3.314	0.563	1.97		0	0.987	0.013	3.3	0.499	2.1
	25	0.987	0.012	3.504	0.475	2.24		25	0.989	0.010	3.429	0.461	2.02
	25	0.992	0.023	3.553	0.469	2.07		25	0.988	0.012	3.447	0.459	1.91
Cycle 1 DPI	25	0.993	0.019	3.547	0.523	1.78	Cycle 2 DPI	25	0.991	0.016	3.434	0.451	1.99
2	50	0.987	0.012	3.706	0.453	1.99	2	50	0.990	0.005	3.75	0.395	1.95
	50	0.992	0.016	3.715	0.467	2		50	0.986	0.009	3.761	0.387	1.79
	50	0.984	0.013	3.709	0.464	1.48		50	0.984	0.009	3.752	0.395	1.85
	75	0.986	0.015	3.842	0.368	1.72		75	0.990	0.009	4.147	0.328	2.19
	75	0.987	0.011	3.877	0.384	1.68		75	0.991	0.009	4.183	0.344	2.05
	75	0.984	0.013	3.848	0.379			75	0.985	0.008	4.18	0.312	1.9
Pellet													
	0	0.037	0.010	3.268	0.733	1.33		0	0.033	0.004	3.283	0.403	1.46
	0	0.034	0.004	3.272	0.683	1.18		0	0.039	0.004	3.293	0.453	1.41
	0	0.043	0.008	3.266	0.771	1.28		0	0.038	0.002	3.279	0.435	1.51
	25	0.030	0.005	3.329	0.677	1.26		25	0.032	0.004	3.325	0.403	1.45
	25	0.044	0.007	3.337	0.667	1.34		25	0.045	0.003	3.334	0.405	1.63
Cycle 2 DPI	25	0.039	0.006	3.347	0.696	1.38	Cycle 2 DPI	25	0.044	0.005	3.329	0.440	1.51
0	50	0.054	0.007	3.367	0.600	1.48	0	50	0.040	0.005	3.459	0.357	1.48
	50	0.043	0.009	3.372	0.555	1.39		50	0.041	0.004	3.47	0.427	1.55
	50	0.031	0.005	3.363	0.597	1.62		50	0.037	0.005	3.468	0.432	1.77
	75	0.049	0.009	3.43	0.528	1.94		75	0.050	0.005	3.69	0.384	1.8
	75	0.052	0.005	3.434	0.509	2.03		75	0.052	0.004	3.708	0.400	1.9
								75	0.050	0.004	3.71	0.395	1.74
	0	0.077	0.020	3.293	0.469	2.12		0	0.064	0.013	3.281	0.536	2.49
	0	0.095	0.011	3.306	0.451	2.21		0	0.077	0.013	3.276	0.517	2.37
	0	0.066	0.016	3.314	0.563	2.49		0	0.084	0.013	3.3	0.499	2.1
	25	0.061	0.020	3.504	0.475	1.97		25	0.047	0.009	3.429	0.461	2.02
	25	0.084	0.017	3.553	0.469	2.24		25	0.060	0.009	3.447	0.459	1.91
Cycle 2 DPI	25	0.059	0.014	3.547	0.523	2.07	Cycle 2 DPI	25	0.075	0.011	3.434	0.451	1.99
2	50	0.053	0.009	3.706	0.453	1.78	2	50	0.069	0.008	3.75	0.395	1.95
	50	0.060	0.007	3.715	0.467	1.99		50	0.072	0.007	3.761	0.387	1.79
	50	0.055	0.010	3.709	0.464	2		50	0.052	0.007	3.752	0.395	1.85
	75	0.052	0.006	3.842	0.368	1.48		75	0.059	0.009	4.147	0.328	2.19
	75	0.046	0.007	3.877	0.384	1.72		75	0.045	0.006	4.183	0.344	2.05
	75	0.038	0.005	3.848	0.379	1.68		75	0.048	0.006	4.18	0.312	1.9

Table 9 (continued): *Euglena gracilis* grown for three-day-long growth cycles for cycles 3 and 4. Supernatant and Biomass fractions were collected for wet and dry weight (g), pH and glucose readings as well as cell counts (10^6) from a 25 mL sample.

Supernatant

Treatment	Recycle Rate	Fresh Weight (g)	Dry Weight (g)	pH	Glucose	Cell Count (10^6)	Treatment	Recycle Rate	Fresh Weight (g)	Dry Weight (g)	pH	Glucose	Cell Count (10^6)
	0	0.983	0.017	3.275	0.483	1.38		0	0.979	0.035	3.228	0.496	1.42
	0	0.981	0.011	3.26	0.493	1.27		0	0.981	0.012	3.212	0.605	1.21
	0	0.984	0.016	3.268	0.467	1.2		0	0.982	0.012	3.216	0.547	1.4
	25	0.984	0.016	3.332	0.437	1.35		25	0.974	0.004	3.321	0.504	1.52
	25	0.985	0.010	3.34	0.416	1.19		25	0.979	0.009	3.336	0.507	1.3
Cycle 3 DPI 0	25	0.980	0.013	3.351	0.443	1.31	Cycle 4 DPI 0	25	0.991	0.017	3.308	0.512	1.25
	50	0.988	0.010	3.515	0.379	1.52		50	0.981	0.006	3.522	0.435	1.48
	50	0.983	0.006	3.529	0.384	1.55		50	0.979	0.007	3.524	0.429	1.7
	50	0.984	0.013	3.533	0.392	1.47		50	0.984	0.009	3.531	0.413	1.63
	75	0.984	0.010	3.897	0.355	1.65		75	0.976	0.008	4.018	0.291	1.67
	75	0.986	0.012	3.865	0.339	1.52		75	0.975	0.004	4.042	0.293	1.51
	75	0.978	0.014	3.881	0.349	1.73		75	0.969	0.004	4.049	0.280	1.74
	0	0.984	0.007	3.316	0.645	2.04		0	0.982	0.014	3.243	0.320	2.05
	0	0.985	0.009	3.285	0.669	1.89		0	0.983	0.012	3.254	0.344	1.95
	0	0.986	0.008	3.32	0.656	1.94		0	0.986	0.014	3.261	0.296	2.19
	25	0.991	0.008	3.561	0.597	1.99		25	0.977	0.007	3.41	0.339	1.91
	25	0.987	0.010	3.569	0.600	2.06		25	0.982	0.007	3.442	0.283	1.995
Cycle 3 DPI 2	25	0.986	0.007	3.58	0.608	2.02	Cycle 4 DPI 2	25	0.984	0.008	3.438	0.277	2.01
	50	0.985	0.008	3.903	0.501	1.88		50	0.979	0.007	3.832	0.224	1.85
	50	0.987	0.008	3.922	0.451	1.91		50	0.995	0.011	3.81	0.237	1.96
	50	0.986	0.008	3.917	0.432	1.94		50	0.981	0.009	3.795	0.288	1.89
	75	0.990	0.008	4.381	0.320	2.26		75	0.976	0.008	4.65	0.125	2.27
	75	0.990	0.010	4.398	0.328	2.04		75	0.969	0.006	4.641	0.120	2.15
	75	0.985	0.011	4.403	0.317	1.98		75	0.978	0.009	4.634	0.157	1.97
Pellet													
	0	0.033	0.005	3.275	0.483	1.38		0	0.051	0.005	3.228	0.496	1.42
	0	0.040	0.003	3.26	0.493	1.27		0	0.025	0.004	3.212	0.605	1.21
	0	0.044	0.003	3.268	0.467	1.2		0	0.052	0.005	3.216	0.547	1.4
	25	0.052	0.006	3.332	0.437	1.35		25	0.030	0.003	3.321	0.504	1.52
	25	0.042	0.003	3.34	0.416	1.19		25	0.036	0.006	3.336	0.507	1.3
Cycle 4 DPI 0 0%	25	0.050	0.004	3.351	0.443	1.31	Cycle 4 DPI 0 0%	25	0.050	0.003	3.308	0.512	1.25
	50	0.045	0.004	3.515	0.379	1.52		50	0.062	0.003	3.522	0.435	1.48
	50	0.056	0.004	3.529	0.384	1.55		50	0.054	0.004	3.524	0.429	1.7
	50	0.042	0.009	3.533	0.392	1.47		50	0.041	0.003	3.531	0.413	1.63
	75	0.048	0.004	3.897	0.355	1.65		75	0.051	0.005	4.018	0.291	1.67
	75	0.047	0.003	3.865	0.339	1.52		75	0.061	0.002	4.042	0.293	1.51
	75	0.053	0.006	3.881	0.349	1.73		75	0.048	0.004	4.049	0.280	1.74
	0	0.056	0.011	3.316	0.645	2.04		0	0.072	0.011	3.243	0.320	2.05
	0	0.073	0.013	3.285	0.669	1.89		0	0.072	0.010	3.254	0.344	1.95
	0	0.078	0.016	3.32	0.656	1.94		0	0.080	0.010	3.261	0.296	2.19
	25	0.054	0.009	3.561	0.597	1.99		25	0.087	0.009	3.41	0.339	1.91
	25	0.063	0.010	3.569	0.600	2.06		25	0.067	0.008	3.442	0.283	1.995
Cycle 4 DPI 2 0%	25	0.064	0.008	3.58	0.608	2.02	Cycle 4 DPI 2 0%	25	0.061	0.007	3.438	0.277	2.01
	50	0.045	0.006	3.903	0.501	1.88		50	0.057	0.005	3.832	0.224	1.85
	50	0.062	0.008	3.922	0.451	1.91		50	0.051	0.014	3.81	0.237	1.96
	50	0.047	0.012	3.917	0.432	1.94		50	0.055	0.006	3.795	0.288	1.89
	75	0.065	0.006	4.381	0.320	2.26		75	0.070	0.005	4.65	0.125	2.27
	75	0.057	0.006	4.398	0.328	2.04		75	0.052	0.005	4.641	0.120	2.15
	75	0.053	0.005	4.403	0.317	1.98		75	0.062	0.005	4.634	0.157	1.97

Appendix II

Waste Accumulation Analysis - Organic Media Based Recipe

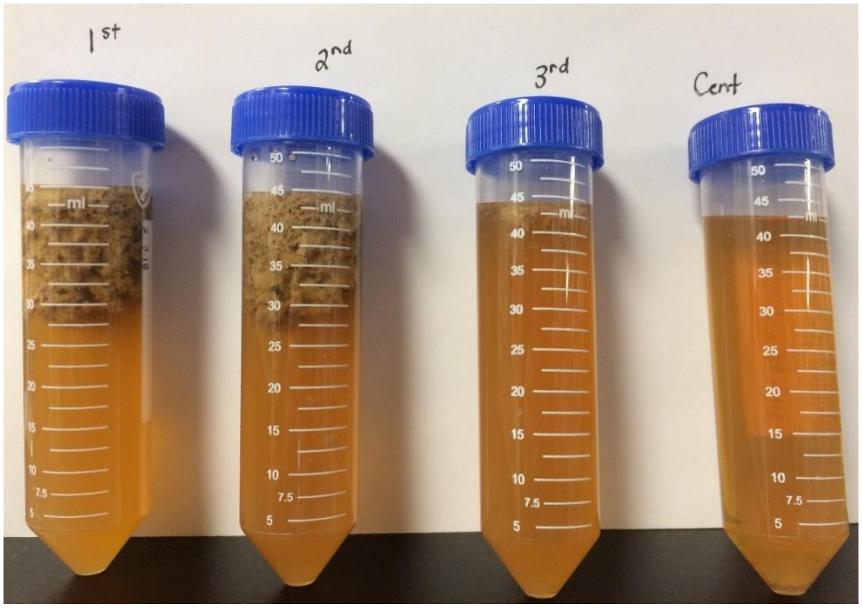

1st – First hand pour-off of 50% recycled culture medium.

2nd – Second hand pour-off of 50% recycled culture medium.

3rd – Third hand pour-off 50% recycled culture medium.

Cent – Centrifuged 50% recycled medium culture (2400 x *g*, 5 minutes)

Figure 1: Waste accumulation product formed from a supernatant fraction of 500mL *Euglena gracilis* culture in 50% recycled, organic NOM media. The first three tubes are consecutive pour-offs by hand and the fourth tube as a centrifuged fraction from the same culture supernatant.

Waste accumulation on the surface of the *Euglena gracilis* cultures, media autoclaving effects, and pour-off filtering effects were analyzed by POS-Bio-Sciences (Analytical Services, POS-Bio-Sciences). Analysis of 6 fractions of 50% recycled medium included: filtered medium using fibre filter circles, 4.25cm (Fisherbrand, Fisher Scientific Company, Ottawa, ON, Canada); vacuum filtered medium using 4.25cm, with 22 μm pore size; medium that was poured off by hand; centrifuged medium (Thermo Scientific Sorvall ST 16 centrifuge; 2400 x *g*, 5 minutes); a cell concentrate ($73 \cdot 10^6$ cells/mL); 2 samples of freshly made media was portioned to be autoclaved and some was not, all provided in 50 mL aliquots. All eight samples were tested for Proximate Analysis Package (ash, moisture and volatiles, and protein (N x6.25) content), and additionally, three samples (cell concentrate, pre- and post-autoclaved media) were analyzed for amino acid 18 primary amino acids) and sugar profile by high-pressure liquid chromatography (HPLC) (Figure 12).

POS BIO-SCIENCES

OUR PEOPLE.
YOUR OPPORTUNITIES.
BRILLIANT SOLUTIONS.

POS BIO-SCIENCES
118 Veterinary Road
Saskatoon SK
Canada S7N 2R4

MAIN • 1-306-978-2800
TOLL FREE • 1-800-230-2751
FAX • 1-306-975-3766

To: Trent University
2140 East Bank Drive
Peterborough, ON
K9L 1Z8
Neil Emeru

Project No: 905
Report Date: 2/8/2018
Lab Group ID: 180129006
Lab Number: AA82338

ANALYTICAL REPORT

Sample Description: Filtered Media - 26.09.17

PO#:

Analysis Results:

Analyte	Result	Units	Analysis Reference
Ash	0.17	%	AOCS Bc 5-49
Moisture and Volatiles	99.4	%	AOCS Ba 2a-38
Protein (N x 6.25)	0.58	%	AOCS Ba 4e-93

This is a final report of analysis performed by POS Bio-Sciences.

These results have been approved for release by

Angie Johnson
Analytical Services
POS Bio-Sciences

POS BIO-SCIENCES

OUR PEOPLE.
YOUR OPPORTUNITIES.
BRILLIANT SOLUTIONS.

POS BIO-SCIENCES
118 Veterinary Road
Saskatoon SK
Canada S7N 2R4

MAIN • 1-306-978-2800
TOLL FREE • 1-800-230-2751
FAX • 1-306-975-3766

To: Trent University
2140 East Bank Drive
Peterborough, ON
K9L 1Z8
Neil Emeru

Project No: 905
Report Date: 2/8/2018
Lab Group ID: 180129006
Lab Number: AA82339

ANALYTICAL REPORT

Sample Description: Vacuum Filtered Supernatant - 26.09.17

PO#:

Analysis Results:

Analyte	Result	Units	Analysis Reference
Ash	0.24	%	AOCS Bc 5-49
Moisture and Volatiles	77.2	%	AOCS Ba 2a-38
Protein (N x 6.25)	1.86	%	AOCS Ba 4e-93

This is a final report of analysis performed by POS Bio-Sciences.

These results have been approved for release by

Angie Johnson
Analytical Services
POS Bio-Sciences

POS
BIO-SCIENCES

OUR PEOPLE.
YOUR OPPORTUNITIES.
BRILLIANT SOLUTIONS.

POS BIO-SCIENCES
118 Veterinary Road
Saskatoon SK
Canada S7N 2R4

MAIN • 1-306-978-2800
TOLL FREE • 1-800-230-2751
FAX • 1-306-975-3766

To: Trent University
2140 East Bank Drive
Peterborough, ON
K9L 1Z8
Neil Emeru

Project No: 905
Report Date: 2/8/2018
Lab Group ID: 180129006
Lab Number: AA82340

ANALYTICAL REPORT

Sample Description: Recycled Supernatant - 1st Pour Off - 22.9.17

PO#:

Analysis Results:

Analyte	Result	Units	Analysis Reference
Ash	0.16	%	AOCS Bc 5-49
Moisture and Volatiles	98.2	%	AOCS Ba 2a-38
Protein (N x 6.25)	0.77	%	AOCS Ba 4e-93

This is a final report of analysis performed by POS Bio-Sciences.

These results have been approved for release by

Angie Johnson
Analytical Services
POS Bio-Sciences

POS BIO-SCIENCES

OUR PEOPLE.
YOUR OPPORTUNITIES.
BRILLIANT SOLUTIONS.

POS BIO-SCIENCES
118 Veterinary Road
Saskatoon SK
Canada S7N 2R4

MAIN • 1-306-978-2800
TOLL FREE • 1-800-230-2751
FAX • 1-306-975-3766

To: Trent University
2140 East Bank Drive
Peterborough, ON
K9L 1Z8
Neil Emery

Project No: 905
Report Date: 2/8/2018
Lab Group ID: 180129006
Lab Number: AA82341

ANALYTICAL REPORT

Sample Description: Recycled Supernatant - 2nd Pour Off - 22.9.17

PO#:

Analysis Results:

Analyte	Result	Units	Analysis Reference
Ash	0.16	%	AOCS Bc 5-49
Moisture and Volatiles	99.1	%	AOCS Ba 2a-38
Protein (N x 6.25)	0.76	%	AOCS Ba 4e-93

This is a final report of analysis performed by POS Bio-Sciences.

These results have been approved for release by

Angie Johnson
Analytical Services
POS Bio-Sciences

BIO-SCIENCES

OUR PEOPLE.
YOUR OPPORTUNITIES.
BRILLIANT SOLUTIONS.

POS BIO-SCIENCES
118 Veterinary Road
Saskatoon SK
Canada S7N 2R4

MAIN • 1-306-978-2800
TOLL FREE • 1-800-230-2751
FAX • 1-306-975-3766

To: Trent University
2140 East Bank Drive
Peterborough, ON
K9L 1Z8
Neil Emery

Project No: 905
Report Date: 2/8/2018
Lab Group ID: 180129006
Lab Number: AA82342

ANALYTICAL REPORT

Sample Description: Recycled Supernatant - 3rd Centrifuged Pour Off - 22.9.17

PO#:

Analysis Results:

Analyte	Result	Units	Analysis Reference
Ash	0.16	%	AOCS Bc 5-49
Moisture and Volatiles	99.2	%	AOCS Ba 2a-38
Protein (N x 6.25)	0.70	%	AOCS Ba 4e-93

This is a final report of analysis performed by POS Bio-Sciences.

These results have been approved for release by

Angie Johnson
Analytical Services
POS Bio-Sciences

FM-LS-80 (05)

BIO-SCIENCES

OUR PEOPLE.
YOUR OPPORTUNITIES.
BRILLIANT SOLUTIONS.

POS BIO-SCIENCES
118 Veterinary Road
Saskatoon SK
Canada S7N 2R4

MAIN + 1-306-978-2800
TOLL FREE + 1-800-230-2751
FAX + 1-306-975-3766

To: Trent University
2140 East Bank Drive
Peterborough, ON
K9L 1Z8
Neil Emeru

Project No: 905
Report Date: 2/8/2018
Lab Group ID: 180129006
Lab Number: AA82343

ANALYTICAL REPORT

Sample Description: Cell Concentrate - 73x10^6 cells/mL - 22.9.17

PO#:

Analysis Results:

Analyte	Result	Units	Analysis Reference
Amino Acid Profile - 18 primary			
Aspartic Acid	0.15	%	Waters Pico-Tag
Glutamic Acid	0.23	%	Waters Pico-Tag
Serine	0.09	%	Waters Pico-Tag
Glycine	0.08	%	Waters Pico-Tag
Histidine	0.09	%	Waters Pico-Tag
Arginine	0.20	%	Waters Pico-Tag
Threonine	0.07	%	Waters Pico-Tag
Alanine	0.12	%	Waters Pico-Tag
Proline	0.11	%	Waters Pico-Tag
Tyrosine	0.07	%	Waters Pico-Tag
Valine	0.14	%	Waters Pico-Tag
Methionine	0.04	%	Waters Pico-Tag
Cystine	0.04	%	Waters Pico-Tag
Isoleucine	0.08	%	Waters Pico-Tag
Leucine	0.15	%	Waters Pico-Tag
Phenylalanine	0.08	%	Waters Pico-Tag
Lysine	0.14	%	Waters Pico-Tag
Tryptophan	0.02	%	Waters Pico-Tag
Total Amino Acids	1.87	%	Waters Pico-Tag
Ash	0.38	%	AOCS Bc 5-49
Moisture and Volatiles	95.0	%	AOCS Ba 2a-38
Protein (N x 6.25)	2.44	%	AOCS Ba 4e-93
Sugar Profile by HPLC			
Ribose	<0.01	%	Internal Method
Xylose	<0.01	%	Internal Method
Fructose	0.04	%	Internal Method

POS
BIO-SCIENCES

OUR PEOPLE.
YOUR OPPORTUNITIES.
BRILLIANT SOLUTIONS.

POS BIO-SCIENCES
118 Veterinary Road
Saskatoon SK
Canada S7N 2R4

MAIN • 1-306-978-2800
TOLL FREE • 1-800-230-2751
FAX • 1-306-975-3766

To: Trent University
2140 East Bank Drive
Peterborough, ON
K9L 1Z8
Neil Emeru

Project No: 905
Report Date: 2/8/2018
Lab Group ID: 180129006
Lab Number: AA82343

ANALYTICAL REPORT

Sample Description: Cell Concentrate - 73x10^6 cells/mL - 22.9.17

PO#:

Analysis Results:

Analyte	Result	Units	Analysis Reference
Glucose	0.10	%	Internal Method
Sucrose	0.02	%	Internal Method
Maltose	<0.01	%	Internal Method
Lactose	0.02	%	Internal Method

This is a final report of analysis performed by POS Bio-Sciences.

These results have been approved for release by

Angie Johnson
Analytical Services
POS Bio-Sciences

FM-LS-80 (05)

POS
BIO-SCIENCES

OUR PEOPLE.
YOUR OPPORTUNITIES.
BRILLIANT SOLUTIONS.

POS BIO-SCIENCES
118 Veterinary Road
Saskatoon SK
Canada S7N 2R4

MAIN • 1-306-978-2800
TOLL FREE • 1-800-230-2751
FAX • 1-306-975-3766

To: Trent University
2140 East Bank Drive
Peterborough, ON
K9L 1Z8
Neil Emeru

Project No: 905
Report Date: 2/8/2018
Lab Group ID: 180129006
Lab Number: AA82344

ANALYTICAL REPORT

Sample Description: Post-Autoclaved Media - 26.9.17

PO#:

Analysis Results:

Analyte	Result	Units	Analysis Reference
Amino Acid Profile - 18 primary			
Aspartic Acid	0.03	%	Waters Pico-Tag
Glutamic Acid	0.06	%	Waters Pico-Tag
Serine	0.02	%	Waters Pico-Tag
Glycine	0.01	%	Waters Pico-Tag
Histidine	0.01	%	Waters Pico-Tag
Arginine	0.02	%	Waters Pico-Tag
Threonine	0.01	%	Waters Pico-Tag
Alanine	0.02	%	Waters Pico-Tag
Proline	0.02	%	Waters Pico-Tag
Tyrosine	0.01	%	Waters Pico-Tag
Valine	0.02	%	Waters Pico-Tag
Methionine	0.01	%	Waters Pico-Tag
Cystine	0.01	%	Waters Pico-Tag
Isoleucine	0.02	%	Waters Pico-Tag
Leucine	0.02	%	Waters Pico-Tag
Phenylalanine	0.01	%	Waters Pico-Tag
Lysine	0.02	%	Waters Pico-Tag
Tryptophan	0.00	%	Waters Pico-Tag
Total Amino Acids	0.31	%	Waters Pico-Tag
Ash	0.16	%	AOCS Bc 5-49
Moisture and Volatiles	99.1	%	AOCS Ba 2a-38
Protein (N x 6.25)	0.73	%	AOCS Ba 4e-93
Sugar Profile by HPLC			
Ribose	<0.01	%	Internal Method
Xylose	<0.01	%	Internal Method
Fructose	0.08	%	Internal Method

BIO-SCIENCES

OUR PEOPLE.
YOUR OPPORTUNITIES.
BRILLIANT SOLUTIONS.

POS BIO-SCIENCES
118 Veterinary Road
Saskatoon SK
Canada S7N 2R4

MAIN + 1-306-978-2800
TOLL FREE + 1-800-230-2751
FAX + 1-306-975-3766

To: Trent University
2140 East Bank Drive
Peterborough, ON
K9L 1Z8
Neil Emeru

Project No: 905
Report Date: 2/8/2018
Lab Group ID: 180129006
Lab Number: AA82344

ANALYTICAL REPORT

Sample Description: Post-Autoclaved Media - 26.9.17

PO#:

Analysis Results:

Analyte	Result	Units	Analysis Reference
Glucose	0.08	%	Internal Method
Sucrose	0.01	%	Internal Method
Maltose	<0.01	%	Internal Method
Lactose	0.02	%	Internal Method

This is a final report of analysis performed by POS Bio-Sciences.

These results have been approved for release by

Angie Johnson
Analytical Services
POS Bio-Sciences

POS BIO-SCIENCES

OUR PEOPLE.
YOUR OPPORTUNITIES.
BRILLIANT SOLUTIONS.

POS BIO-SCIENCES
118 Veterinary Road
Saskatoon SK
Canada S7N 2R4

MAIN • 1-306-978-2800
TOLL FREE • 1-800-230-2751
FAX • 1-306-975-3766

To: Trent University
2140 East Bank Drive
Peterborough, ON
K9L 1Z8
Neil Emery

Project No: 905
Report Date: 2/8/2018
Lab Group ID: 180129006
Lab Number: AA82345

ANALYTICAL REPORT

Sample Description: Pre-Autoclaved Media - 25.9.17

PO#:

Analysis Results:

Analyte	Result	Units	Analysis Reference
Amino Acid Profile - 18 primary			
Aspartic Acid	0.04	%	Waters Pico-Tag
Glutamic Acid	0.06	%	Waters Pico-Tag
Serine	0.02	%	Waters Pico-Tag
Glycine	0.01	%	Waters Pico-Tag
Histidine	0.01	%	Waters Pico-Tag
Arginine	0.02	%	Waters Pico-Tag
Threonine	0.01	%	Waters Pico-Tag
Alanine	0.02	%	Waters Pico-Tag
Proline	0.02	%	Waters Pico-Tag
Tyrosine	0.01	%	Waters Pico-Tag
Valine	0.02	%	Waters Pico-Tag
Methionine	0.01	%	Waters Pico-Tag
Cystine	0.01	%	Waters Pico-Tag
Isoleucine	0.02	%	Waters Pico-Tag
Leucine	0.02	%	Waters Pico-Tag
Phenylalanine	0.01	%	Waters Pico-Tag
Lysine	0.02	%	Waters Pico-Tag
Tryptophan	0.00	%	Waters Pico-Tag
Total Amino Acids	0.31	%	Waters Pico-Tag
Ash	0.13	%	AOCS Bc 5-49
Moisture and Volatiles	99.0	%	AOCS Ba 2a-38
Protein (N x 6.25)	0.78	%	AOCS Ba 4e-93
Sugar Profile by HPLC			
Ribose	<0.01	%	Internal Method
Xylose	<0.01	%	Internal Method
Fructose	0.04	%	Internal Method

FM-LS-80 (05)

OUR PEOPLE.
YOUR OPPORTUNITIES.
BRILLIANT SOLUTIONS.

POS BIO-SCIENCES
118 Veterinary Road
Saskatoon SK
Canada S7N 2R4

MAIN • 1-306-978-2800
TOLL FREE • 1-800-230-2751
FAX • 1-306-975-3766

To: Trent University
2140 East Bank Drive
Peterborough, ON
K9L 1Z8
Neil Emeru

Project No: 905
Report Date: 2/8/2018
Lab Group ID: 180129006
Lab Number: AA82345

ANALYTICAL REPORT

Sample Description: Pre-Autoclaved Media - 25.9.17

PO#:

Analysis Results:

Analyte	Result	Units	Analysis Reference
Glucose	0.04	%	Internal Method
Sucrose	0.12	%	Internal Method
Maltose	<0.01	%	Internal Method
Lactose	0.02	%	Internal Method

This is a final report of analysis performed by POS Bio-Sciences.

These results have been approved for release by

Angie Johnson
Analytical Services
POS Bio-Sciences